Inorganic carbon acquisition in *Palmaria palmata* (Rhodophyta)

Gregg Hill

University of London

Acknowledgements

I wish to acknowledge the help and support of my supervisor Brenda Thake, my examiners, Dr. Ford and Prof. Dring, and Dr. Mo Brindley and Dr. Vickie Gallon. Also special gratitude to Hannah, for her help and encouragement.

Abstract

DIC acquisition mechanisms and the use of DIC in photosynthesis were examined in the temperate red macroalga, *Palmaria palmata* (Linnaeus) O. Kuntze. Photosynthetic O_2 evolution was unsaturated at the ambient DIC concentration in seawater. Experiments with inhibitors of the mammalian HCO_3^-/Cl^- anion exchanger AE1, and the HCO_3^--hydroxylating enzyme carbonic anhydrase (CA), showed that HCO_3^- uptake is mediated mainly by a bicarbonate transporter protein. Photosynthesis measured at small increments of DIC addition showed biphasic kinetics, with a hiatus located at 0.625 mM DIC. Inhibitor experiments indicated that extracellular CA is active at low DIC, therefore the biphasic kinetics of photosynthesis may have been caused by the presence of two DIC acquisition mechanisms. Culturing thalli for 6 d in artificial seawater containing 8 mM DIC induced a bicarbonate transporter in the CA-user *Chondrus crispus*, but no change in activity was detected in *P. palmata*.

Presence of a bicarbonate transporter mechanism was also confirmed by using the polymerase chain reaction. Primers based on the mammalian AE1 gene sequence were used to amplify a 1500bp fragment of bicarbonate transporter gene from genomic DNA extracted from *P. palmata* and the calcifying microalga, *Emiliania huxleyi*. Comparison of the algal and mammalian sequences revealed a high amino acid sequence homology, indicating that they encoded structurally and functionally similar proteins.

F.F. Blackman's precept, which implies that carbon limitation does not occur at subsaturating light, was investigated by measuring induced chlorophyll fluorescence at different DIC concentrations and irradiances. Photosynthetic electron transport rate was was stimulated at saturating light, but only slightly at subsaturating light. Thus, Blackman's theory was upheld.

Photosynthesis and bicarbonate transporter activity was monitored in *P. palmata* growing at St. Margaret's Bay, Kent, UK. Distinct peaks in photosynthesis occurred in March and October, and coincided with equinoctial tides. Bicarbonate transporter activity was maximal in spring, and decreased during summer. Although it was not possible to show what determined the seasonal patterns of photosynthesis and bicarbonate transporter activity, the possibility that exposure to springwater containing high concentrations of DIC and nitrate is discussed.

Table of Contents

Acknowledgements 2

Abstract 3

Table of Contents 5

List of Figures 8

List of Tables 15

Abbreviations 18

Chapter 1 19

Introduction

1.1 Carbon Chemistry in Seawater 23

1.2 Primary productivity in the sea 31

1.3 Inorganic carbon acquisition by marine macroalgae 33

1.4 Aims 39

Chapter 2 40

Materials and Methods

2.1 Organisms 41

2.2 Media 42

2.3 Measurement of Photosynthesis and Respiration 44

2.3.1 Clark-Type O_2 Electrodes 44

2.3.2 Induced Chlorophyll Fluorescence 52

2.4 Inhibitors of Bicarbonate Acquisition Mechanisms 57

2.5 Analysis of nitrate and DIC concentrations in solution 57

2.6 Total Alkalinity Determinations 58

2.7 Molecular Biology Methods 59

2.7.1 Preservation of nucleic acids in tissue 59

2.7.2 Genomic DNA extraction 60

2.7.3 Polymerase Chain Reaction 61

2.7.4 Primer Design 62

2.7.5 pGEM® -T Easy Cloning of PCR Products 63

2.7.6 Isolation of plasmid DNA and Restriction digest of DNA 65

Chapter 3 66

Mechanisms and Kinetics of DIC Uptake in *Palmaria palmata*

3.1 Introduction 67

3.1.2 Carbonic Anhydrase 67

3.1.3 Anion exchangers 71

3.1.4 Use of CA and AE in algae 77

3.2 Aims 82

3.3 Materials and Methods 83

3.3.1 Photosynthesis versus irradiance (PI) curves 83

3.3.2 Primer Design for PCR 83

3.3.3 Curve-fitting 85

3.4 Results 85

3.5 Discussion 98

Chapter 4 107

Regulation of DIC Acquisition Mechanisms in *Palmaria palmata*

4.1 Introduction 108

4.2 Aims 116

4.3 Materials and Methods 117

4.3.1 Culture of *P. palmata* and *C. crispus* at different DIC concentrations 117

4.3.2 Short-term incubation of *P. palmata* at different DIC and $NaNO_3$ concentrations 118

4.4 Results 119

4.5 Discussion 128

Chapter 5 134

The effect of light and DIC concentration on photosynthesis in *Palmaria palmata*

5.1.1 Introduction 135

5.1.2 A brief overview of photosynthesis 137

5.2 Aims 142

5.3 Materials and Methods 143

5.4 Results 146

5.4.1 The effect of light and DIC concentration on photosynthesis 146

5.5 Discussion and Conclusions 156

Chapter 6 **160**

Seasonal variations of DIC uptake in *Palmaria palmata*

Introduction **161**

6.1.2 Seasonal patterns of productivity in algae. **164**

6.2 Aims **168**

6.3 Materials and Methods **169**

6.4 Results **170**

6.5 Discussion **178**

Chapter 7 **183**

Discussion and Conclusions

References 190

List of Figures

P 20 **Figure 1.1** A. Morphology of a typical tetrasporangial plant of *Palmaria palmata*, B. Trans-section of the thallus of a tetrasporangial plant, C. A morphologically distinct plant of *Palmaria palmata* (var. sarniensis). From Irvine & Farnham (1983).

P 21 **Figure 1.2** The sexual life cycle of *Palmaria palmata*. From van der Meer & Todd, 1980.

P 31 **Figure 1.3** The concentrations of CO_2, HCO_3^-, and $CO_3^=$ in seawater as a function of pH (from Zeebe & Gattuso, 2006).

P 46 **Figure 2.1** Schematic diagram of a Clark-type oxygen electrode, similar to the model used in the present study.

P 48 **Figure 2.2** Schematic diagram of a thallus disc inside the electrode chamber, supported by a panel of acetate.

P 51 **Figure 2.3** Rates of photosynthesis in pieces of thalli of different weights, cut from the thallus of *Palmaria palmata* (*n*=6).

P 52 **Figure 2.4** Schematic diagram of the Hansatech fluorescence monitoring system used in the present study.

P 55 **Figure 2.5** Schematic illustration of primary energy conversion in photosynthesis, which governs *in vivo* chlorophyll fluorescence yield. Variable fluorescence originates almost entirely from PSII. LHC = light harvesting complex,

and represent additional forms of chlorophyll a (Chl_a*) and accessory pigments, increase the spectral range of light energy that can be absorbed. From Schreiber *et al.* 1994.

P 56 **Figure 2.6** Induced chlorophyll fluorescence in a disc cut from the thallus of *Palmaria palmata*, measured using a Hansatech fluorescence monitoring system.

P 71 **Figure 3.1** The chemical structure of acetazolamide (*N*-(5-sulphamoyl-1,3,4-thiadiazol-2-yl) acetamide) From Ch'En *et al.* (2008).

P 73 **Figure 3.2** Topological model for Human AE1. Numbers indicate the residue number in erythrocyte AE1. The boxed numbers show the trans membrane segment number. This figure is reproduced from Cordat & Casey, (2009), where it was adapted from Zhu *et* al, (2003).

P 75 **Figure 3.3** The chemical structures of two stilbene disulphonate anion exchange inhibitors, DIDS and SITS. From Fan *et al*. (2001).

P 76 **Figure 3.4** A schematic representation of the bicarbonate transporter metabolon thought to exist in human erythrocytes. From Sterling *et al*. (2001). AE = anion exchanger, CAII = carbonic anhydrase II.

P 87 **Figure 3.5** NPS in *P. palmata* as a function of irradiance. NPS was measured in individual samples whilst altering the irradiance in increments from either high-low PFDs, or low-high PFDs. Data points are means of +/- SE. *n*=6

P 88 **Figure 3.6** (A) NPS in *P. palmata* as a function of DIC concentration, with and without the addition of 1 mM SITS. (B) A double reciprocal plot of the data shown in (A). Data points are means of +/- SE (*n*=4).

P 90 **Figure 3.7** The dose response curves of the AE1 inhibitors DIDS (A), and SITS (B), on NPS in *P. palmata* photosynthesising at 2 mM DIC. Data points are means +/-SE (*n*=5).

P 92 **Figure 3.8** Translated amino acid sequences for the amplified *R. norvegicus* AE1 gene fragment aligned against (A) the amplified *P. palmata* gene fragment, and (B) the amplified *E. huxleyi* fragment. Amino acids connected by verticle lines are identical, amino acids connected by dots are non-identical but functionally very similar. Dissimilar amino acids are not connected.

P 93 **Figure 3.9** The effect of 100 uM AZ, and 500 µM DIDS, on rates of net photosynthesis in *Palmaria palmata*, *Chondrus crispus*, and *Laminaria digitata.* Data points are means +/- SE (*n*=4).

P 94 **Figure 3.10** The effect of external DIC concentration on net photosynthesis (NPS) in *P. palmata*, *C. crispus*, and *L. digitata*. Data points are means +/- SE (*n*=6).

P 96 **Figure 3.11** The effect of different DIC concentrations on NPS in *P. palmata*. Data points are means +/- SE (*n*=6).

P 104 **Figure 3.12** Part of the human AE1 amino acid sequence, showing the location of the degenerate primers F1, R1 and R2. The transmembrane domains are shown in boxes, and the cytoplasmic and extracellular domains are labelled “C” and “E” respectively.

P 109 **Figure 4.1** The carbon-fixation reaction catalysed by Rubisco.

P 113 **Figure 4.2** Inorganic carbon transport and CO_2 accumulation processes in eukaryotic algal cells. Active transport is shown by the shaded bases. From Girodano *et al*. (2005).

P 119 **Figure 4.3** Percentage inhibition of NPS in *P. palmata* incubated for 2h in seawater containing no added DIC, with and without the addition of 50 μM $NaNO_3$ or 50 μM NH_4Cl. Date are +/-SE (*n*=3).

P 120 **Figure 4.4** Percentage inhibition of net photosynthesis (NPS) by 50μM AZ addition, in *Palmaria palmata* incubated for 2 h in ASW containing 50μM $NaNO_3$ and DIC concentrations of 0.25mM, 0.5mM and 2mM. Data are means +/-SE (*n*=3)

P 121 **Figure 4.5** Respiration and net photosynthesis of *Palmaria palmata* cultured for 6 days in ASW with 8mM, 2mM, and 0mM added DIC, before and after the addition of 1mM DIDS. Measurements were made in buffered ASW containing 2mM DIC. Data are means +/-SE (*n*=6).

P 123 **Figure 4.6** Photosynthesis of *Palmaria palmata* that had been cultured in ASW with 0mM, 2mM and 8mM DIC, measured in buffered ASW with 0mM DIC addition. Data are means +/- SE (*n*=4).

P 124 **Figure 4.7** Photosynthesis of *P. palmata* that had been cultured at 2mM and 8mM DIC, measured in buffered ASW containing 0mM DIC, after being submersed briefly in 1M HCl solution. Data are means +/- SE (*n*=4).

P 125 **Figure 4.8** Photosynthesis of *C. crispus,* cultured at 2mM and 8mM DIC, before and after the addition of 500μM DIDS. Measurements were made in buffered ASW containing 2mM DIC. Data are means +/-SE (*n*=11-16).

P 126 **Figure 4.9** Inhibition of net photosynthesis in *Chondrus crispus* cultured at 2mM and 8mM DIC, after 500 μM DIDS addition. Measurements were made in buffered ASW containing 2mM DIC. Data are means +/-SE (*n*=11-16).

P 127 **Figure 4.10** Net photosynthesis of *Chondrus crispus* cultured for 6 days in seawater containing 2 mM and 8 mM DIC, which was measured in buffered ASW containing, 2 mM DIC, Photosynthesis was measured before and after the addition of 100uM AZ, and after AZ was added and photosynthesis had been measured, 500μM DIDS was added. Data are means +/- SE (*n*=6).

P 136 **Figure 5.1** Schematic representation of PI curves that represent models proposed by (**A)** Blackman (1905), and (**B)** Bose (1924). *PS* = photosynthetic rate, C_i = inorganic carbon concentration.

P 138 **Figure 5.2** The z-scheme of photosynthesis in plants, reproduced from Allen (2004).

P 141 **Figure 5.3** The basic parameters of a PI curve.

P 147 **Figure 5.4** The effect of irradiance (PFD) on relative ETR in *Palmaria palmata*, measured in buffered natural seawater containing no added DIC and 6mM added DIC. **A** shows measurements made at PFD 0-1020 μmol m^{-2} s^{-1}, **B** shows measurements between 0-75 μmol m^{-2} s^{-1}. Data are means +/- SE (*n*=6).

P 148 **Figure 5.5** The effect of irradiance (PFD) on relative ETR in *Alaria esculenta*, measured in buffered natural seawater containing no added DIC and 6mM added DIC. **A** shows measurements made at PFD 0-1020 μmol m^{-2} s^{-1}, **B** shows measurements between 0-75 μmol m^{-2} s^{-1}. Data are means +/- SE (*n*=6).

P 149 **Figure 5.6** The effect of irradiance (PFD) on relative ETR in *Laminaria digitata*, measured in buffered natural seawater containing no added DIC and 6mM added DIC. **A** shows measurements made at PFD 0-2000 μmol m^{-2} s^{-1}, **B** shows measurements between 0-75 μmol m^{-2} s^{-1}. Data are means +/- SE (*n*=6).

P 153 **Figure 5.7** The effect of irradiance (PFD) on relative ETR in *Palmaria palmata*, measured in aritificial seawater containing 1-8 mM DIC. **A** shows measurements made at PFD 0-1020 μmol m^{-2} s^{-1}, **B** shows measurements between 0-75 μmol m^{-2} s^{-1}. Data are means +/- SE (*n*=5).

P 155 **Figure 5.8** The effect of irradiance (PFD) on Relative ETR in *Palmaria palmata*, measured in artificial seawater containing 1 and 8mM DIC at PFD 4-34 μmol m^{-2} s^{-1}. Data are means +/- SE (*n*=5).

P 163 **Figure 6.1** (a) penetration of light into water; irradiance (I) as a percentage of that at the surface as a function of depth (Z); (b) rate of photosynthesis (P) as a percentage of the maximum as a function of depth under dull and bright conditions. Reproduced from Fogg & Thake (1987).

P 170 **Figure 6.2** Dark respiration rates and net photosynthesis (NPS) of *P. palmata* collected from St. Margaret's Bay at monthly intervals during 2003, measured in artificial seawater medium containing 2mM DIC, 8mM DIC, and 2mM DIC + 1mM SITS. Data points are means SE +/- *n*=6-8.

P 173 **Figure 6.3** Net photosynthesis of *Palmaria palmata* in artificial seawater containing **A** 2mM DIC and **B** 8mM DIC, in high shore and low shore plants. Means are +/- SE *n*=(6-8)

P 175 **Figure 6.4** Net photosynthesis of *Palmaria palmata* in artificial seawater containing (A) 2mM DIC , and (B) 8 mM DIC, measured in plants collected from St. Margaret's Bay during 2003 and 2004. Means are +/- SE (*n*=6-8)

P 177 **Figure 6.5** Measurements of temperature (°C), salinity (‰), and nitrate concentrations (µmol) concentrations of water collected directly from springs at St. Margaret's Bay, and the mean fresh weight of 9mm discs of thalli used in experiments.

List of Tables

P 24 **Table 1.1** Concentrations of the major constituents in seawater of 34.32‰ salinity, and their salinity ratios (taken from Dring, M.J., (1982), adapted from Pytkowicz, R.M., Atlas, E. and Culberson, C.H. (1977))

.

P 26 **Table 1.2** Concentrations of the major gases in the atmosphere and in seawater, 35 ppt salinity, 15°C, equilibrated with air, and their K_H values at 0°C and 24°C. Gas concentrations taken from Dring, 1982, calculated from Riley & Chester, R. (1971), K_H values from Broecker & Peng (1982). * The atmospheric CO_2 concentration has increased since the time of publication to 0.384 ml l^{-1}.

P 43 **Table 2.1** Chemical compositions of stock solutions used to create artificial seawater media used in experiments.

P 78 **Table 3.1** Evidence of bicarbonate transporter activity in marine macroalgae and microalgae. In column 2, the method of detection and the inhibitor used is given. Rhodophytes and Chlorophytes are highlighted in red and green respectively.

P 84 **Table 3.2** The AE1 sequences from different organisms that were used to identify conserved domains of the AE1 gene. The “accession number” assigned to each sequence on the NCBI data base is shown.

P 84 **Table 3.3** Primer sequences designed from the amino acid and nucleic acid alignments of AE1 genes in different organisms, and the corresponding non-degenerate nucleic acid sequences in *Rattus norvegicus*.

P 86 **Table 3.4** 2-way ANOVA statistical test for the effect of the direction of changing irradiance from high to low PFDs and low to high PFDs.

P 89 **Table 3.5** 2-way ANOVA for the effect of DIC and SITS inhibition of NPS in *P. palmata.*

P 95 **Table 3.6** Values of $K_{1/2}$ DIC, and V_{max} of net photosynthesis, for three macroalgae. Values were obtained using three linear plots of the data displayed in Fig 3.10

P 122 **Table 4.1** 1-way ANOVA to analyse the effect of DIC concentration in the culture medium on rates of respiration.

P 122 **Table 4.2** 2-way ANOVA to analyse the effect of DIC concentration in culture medium on the NPS with out without DIDS addition in *P. palmata*.

P 150 **Table 5.1** 2-way ANOVA for the effect of PFD and DIC concentration on photosynthetic ETR between PFD 13-1020 umol m^{-2} s^{-1} in *Palmaria palmata*.

P 150 **Table 5.2** 2-way ANOVA for the effect of PFD and DIC concentration on photosynthetic ETR between PFD 13-1020 umol m^{-2} s^{-1} in *Alaria esculenta.*

P 150 **Table 5.3** 2-way ANOVA for the effect of PFD and DIC concentration on photosynthetic ETR between PFD 13-1020 umol m^{-2} s^{-1} in *Laminaria digitata..*

P 151 **Table 5.4** 2-way ANOVA for the effect of PFD and DIC concentration on photosynthetic ETR between PFD 13-38 umol m^{-2} s^{-1}in *Palmaria palmata*.

P 151 **Table 5.5** 2-way ANOVA for the effect of PFD and DIC concentration on photosynthetic ETR between PFD 13-38 umol m^{-2} s^{-1}in *Alaria esculenta*.

P 151 **Table 5.6** 2-way ANOVA for the effect of PFD and DIC concentration on photosynthetic ETR between PFD 13-38 umol m^{-2} s^{-1}in *Laminaria digitata*.

P 154 **Table 5.7** 2-way ANOVA for the effect of PFD and DIC concentration on photosynthetic ETR between PFD 4-1020 umol m^{-2} s^{-1} in *Palmaria palmata*.

P 154 **Table 5.8** 2-way ANOVA for the effect of PFD and DIC concentration on photosynthetic ETR between PFD 4-34 umol m^{-2} s^{-1} in *Palmaria palmata*.

P 171 **Table 6.1** 2-way ANOVA for the effect of DIC stimulation on photosynthesis from February to December in *P. palmata* growing at St. Margaret's Bay.

P 171 **Table 6.2** 2-way ANOVA for the effect of SITS on photosynthesis from February to December in *P. palmata* growing at St. Margaret's Bay.

P 174 **Table 6.3** 2-way ANOVA for the effect of month of measurement and height on shore on photoynthesis in *P. palmata* at 2mM DIC.

P 174 **Table 6.4** 2-way ANOVA for the effect of month of measurement and height on shore on photoynthesis in *P. palmata* at 8mM DIC.

P 176 **Table 6.5** 2-way ANOVA for rates of photosynthesis in *P. palmata* at 2mM DIC, measured from February-April during 2003 and 2004.

P 176 **Table 6.6** 2-way ANOVA for rates of photosynthesis in *P. palmata* at 8mM DIC, measured from February-April during 2003 and 2004.

List of Abbreviations

AE1	Anion exchanger 1
ASW	Artificial seawater
AZ	Acetazolamide
CA	Carbonic anhydrase
DIC	Dissolved inorganic carbon
DIDS	4,4- Diisothiocyanatostilbene- 2,2'-disuphonic acid
ETR	Electron transport rate
FMS	Fluorescence monitoring system
NPS	Net photosynthesis
NSW	Natural seawater
PFD	Photon flux density
SITS	4-Acetamido-4'-isothiocyanato-2,2'-stilbenedisulphonic acid

Chapter 1

Introduction

Palmaria palmata (Linnaeus) O. Kuntze (1981) is a temperate red seaweed that inhabits the intertidal and shallow subtidal zones at depths of up to 20 m on both sheltered and unsheltered shores. Its species name, after the Latin "*palma*", describes the thallus shape of mature plants which resembles a human hand (Figure 1.1). Growth is distributed throughout the British Isles and the northern coasts of the Atlantic and Pacific oceans (Irvine & Farnham, 1983). In northern Europe it is traditionally used as a food source for human and animal consumption (Guiry & Blunden 1991), and is therefore of interest as a species suitable for mass cultivation (Martinez *et al.* 2006; Pang & Lüning, 2006; Matos *et al.* 2005).

Figure 1.1 **A**. Morphology of a typical tetrasporangial plant of *Palmaria palmata*, **B**. Trans-section of the thallus of a tetrasporangial plant, **C.** A morphologically distinct plant of *Palmaria palmata* (var. sarniensis). From Irvine & Farnham (1983).

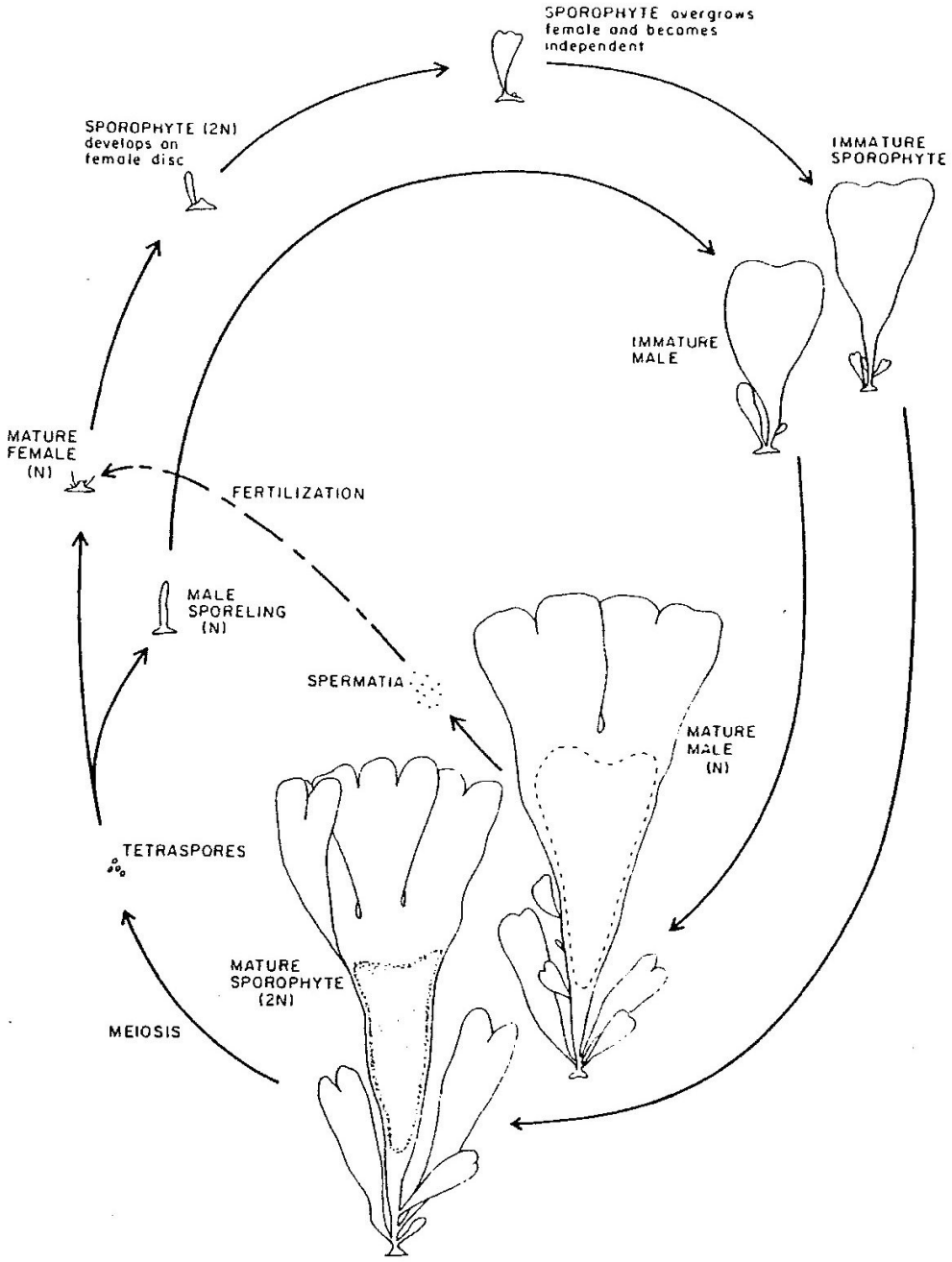

Figure 1.2 The sexual life cycle of *Palmaria palmata*. From van der Meer & Todd, 1980.

The life history of *P. palmata* has been described by van de Meer & Todd (1980), and is shown in Figure 1.2. Tetraspores are produced meiotically by mature diploid sporophytic plants, and give rise to male and female haploid

plants. The female gametophytes, which are very small, become sexually mature after about 4 days, and produce trichogynes. These are fertilised by mature male plants from previous gametangial generations, since they require up to a year's vegetative growth before they produce spermatia. After fertilisation, diploid tetrasporangial plants develop on the female plants and grow over them, forming holdfast attachments to the substrate. Mature sporophytes then produce tetraspores meiotically. Previously it had been difficult to observe the development of the tetrasporangial phase because of the small size of the female gametophytes, but this was facilitated by using a recessive mutation resulting in green frond colour, designed to produce red diploid tissue on green females after fertilisation.

P. palmata is often used as an experimental organism for algal research, and has been well-characterised in regards to its nutrient acquisition (Martinez & Rico 2008, 2004), chemical composition (Barrow & Shahidi, 2007; Dawczynski *et al.* 2007; Hagen Rødde *et al.* 2004) and molecular phylogeny (Provan *et al*. 2005). Its carbon acquisition strategy, however, which, although having been examined rather extensively, is not yet fully understood. Some studies have indicated that it may be atypical, but the precise mechanisms of carbon uptake have not been identified (Larsson & axelsson 1999; Dong, 1993; Dong *et al*. 1991; Maberly, 1990; Colman & Cook 1985).

P. palmata was chosen for the present investigation because preliminary experiments in the algal laboratory at QMUL showed that it possesses an unusual carbon uptake mechanism. Moreover, although dissolved inorganic

carbon (DIC) is not generally considered to be an important limiting factor in the ocean (Redfield, 1958), DIC addition to seawater was found to substantially increase photosynthetic O_2 production in this species, at both saturating and subsaturating irradiances. Against this background, the general aims of this study are to identify how DIC is taken up by *P. palmata*, and to examine the interactions between photosynthesis, DIC concentration and light. Seasonal variations in carbon acquisition, which had not been examined in this alga prior to this study, were measured also.

1.1 Carbon Chemistry in Seawater

Seawater has an average dissolved salt content, or salinity, of about 35 parts per thousand (ppt), 99.7% of which is made up by 11 elements, often termed the 'major constituents' (Dring, 1982). At river mouths and near melting glaciers, where seawater mixes with freshwater, salinities are often substantially lower than average, whereas high salinities are found where there are high rates of evaporation with little rainfall and river inflow (Lobban & Harrison, 1997). Regardless of salinity, however, the individual concentrations of the major constituents relative to the salinity of seawater, their 'salinity ratios', vary by only 1-12%, with the exception of boron and fluoride, among the least abundant of these elements, which vary by 19% and 43% respectively (Table 1.1).

Constituent	Concentration mg-at l^{-1}	mg l^{-1}	Salinity ratio mg $l^{-1}(‰)^{-1}$	Range
Chloride, Cl^-	536.000	18971.000	552.800	-
Sodium, Na^+	459.100	10555.000	307.500	306.1-308.7
Magnesium, Mg^{++}	52.860	1268.000	36.950	36.8-37.3
Sulphate, $SO_4^=$	27.670	2657.000	77.420	7.2-77.8
Calcium, Ca^{++}	10.070	403.900	11.770	11.7-11.9
Potassium, K^+	10.000	391.000	11.390	11.2-11.6
Bicarbonate, HCO_3^-	2.330	142.000	4.138	3.91-4.38
Bromide, Br^-	0.825	65.900	1.920	1.9-1.94
Boron, B	0.421	4.480	0.131	0.123-0.146
Strontium, Sr^{++}	0.088	7.700	0.224	0.210-0.244
Fluoride, F^-	0.067	1.300	0.038	0.035-0.050

Table 1.1 Concentrations of the major constituents in seawater of 34.32‰ salinity, and their salinity ratios (taken from Dring, M.J., (1982), adapted from Pytkowicz, R.M., Atlas, E. and Culberson, C.H. (1977)).

The stability of the relative composition of the major constituents indicates that salts are added to and removed from seawater at similar rates, which are slow enough to enable the mixing of oceans to distribute them evenly. Some of the salts are acquired inland from the weathering of rocks, soils and mineral deposits, and are transported via rivers to the ocean, where they are retained and concentrated by the process of evaporation. Others originate from reactions between seawater and the basalt rocks that form the ocean bed, particularly at hot springs along mid-ocean ridges, which introduce mineral-rich magma from below the Earth's crust. Precipitation of salts out of solution occurs when hot hydrothermal fluids from these springs mix with cold seawater, when salts become concentrated by evaporation, and because of certain biological processes such as the formation of $CaCO_3$ by calcifying algae (Pinet, 1996).

As well as dissolved salts, seawater contains various dissolved gases which are acquired principally from the atmosphere, the major ones being N_2, O_2, Ar and CO_2, which account for 98% of all gases in surface waters (Kennish, 2000). Absorption of gases from the atmosphere is subject to Henry's Law, which states: *At a constant temperature, the amount of a given gas dissolved in a given type and volume of liquid is directly proportional to the partial pressure of that gas in equilibrium with that liquid.*

This is described by the equation:-

$$Sg = k_H P_g$$

where S*g* is the solubility of a gas in a liquid (in this case seawater), P_g is its partial pressure of the gas above the liquid, and k_H is a constant with the dimensions of pressure divided by concentration. Because K_H varies between atmospheric gases, the relative concentrations of the dissolved gases in seawater do not necessarily reflect the atmospheric concentrations. For example, the atmospheric N_2 concentration of 780.9 ml l^{-1} is almost four times greater than the atmospheric O_2 concentration of 209.5ml l^{-1}. This compares to a seawater N_2 concentration of 10.57 ml l^{-1}, which is only double the seawater O_2 concentration of of 5.65 ml l^{-1}. The marked contrast in the atmospheric and seawater N_2:O_2 ratios is created by a substantial difference in their solubility, ie. the K_H of N_2 in seawater of 0.8 x 10^{-3} mol kg^{-1} is much lower than the K_H of O_2, which is 1.69 x 10^{-3} mol kg^{-1} (Table 1.2).

Gas	Atmospheric conc / ml l^{-1}	Seawater conc / ml l^{-1}	K_H (0°C) 10^{-3} mol/kg	K_H (24°C) 10^{-3} mol/kg
N_2	780.80	10.57	0.8	0.51
O_2	209.50	5.65	1.69	1.03
Ar	9.30	0.28	1.83	1.13
CO_2	0.33*	0.27	63	29

Table 1.2 Concentrations of the major gases in the atmosphere and in seawater, 35 ppt salinity, 15°C, equilibrated with air, and their K_H values at 0°C and 24°C. Gas concentrations taken from Dring, 1982, calculated from Riley & Chester, R. (1971), K_H values from Broecker & Peng (1982). * The atmospheric CO_2 concentration has increased since the time of publication to 0.384 ml l^{-1}.

Whereas N_2 varies in concentration by no more than about 10% in seawater, the O_2 concentration varies greatly because of its involvement in photosynthesis and respiration (Kennish, 2000). Since oxygen is produced by photosynthesis and consumed by respiration, the relative magnitude of these processes can affect the dissolved O_2 concentration in waters containing a sufficient number of living organisms. In surface waters containing large numbers of phytoplankton, for example, photosynthetic O_2 production during the day in summer often greatly exceeds respiratory O_2 consumption. At the lower limit of the photic zone, where respiratory O_2 consumption exceeds photosynthetic O_2 production, there will be a decrease in the seawater O_2 concentration (Fogg & Thake, 1987).

The relationship between the atmospheric and seawater concentration of CO_2 is more complex, because when dissolved in seawater, it hydrates to yield carbonic acid (H_2CO_3), which dissociates to form hydrated protons (H^+) and bicarbonate ions (HCO_3^-). The subsequent dissociation of HCO_3^- then forms

carbonate ions (CO_3^{2-}). Being a weak acid, H_2CO_3 only partially dissociates, and there is an equilibrium between the acid and its conjugate base, HCO_3^-. Similarly an equilibrium exists between HCO_3^- and its conjugate base, CO_3^{2-}. Together these reactions form a dynamic CO_2-carbonate equilibrium, shown in equation 1.1.

$$H_2O + CO_2 \leftrightarrow H_2CO_3 \leftrightarrow H^+ + HCO_3^- \leftrightarrow 2H^+ + CO_3^{2-} \qquad \textbf{Equation 1.1}$$

The propensity of an acid to dissociate from its conjugate base can be expressed quantitatively as an acid dissociation constant, K_a, which is calculated using equation 1.2:-

$$K_a = \frac{[H^+][A^-]}{[HA]} \qquad \textbf{Equation 1.2}$$

where HA represents the generic acid, which dissociates to form a proton, H^+, and a conjugate base, A^-.

The concentrations of each of the carbon species in the CO_2-carbonate equilibrium are determined by the dissociation constants for each of the reversible reactions, which are calculated using equations 1.3 and 1.4:-

$$K_{a1} = \frac{[H^+][HCO_3^-]}{[H_2CO_3]} \qquad \textbf{Equation 1.3}$$

$$K_{a2} = \frac{[H^+][CO_3^{=}]}{[HCO_3^-]} \qquad \textbf{Equation 1.4}$$

Because the K_a values of different acids can vary by many orders of magnitude, $-\log_{10} K_a$, or pK_a is often used instead. The larger the pK_a, the smaller the extent of dissociation, therefore, the weaker the acid. Weak acids have pK_a values in the approximate range −2 to 12 in water, whereas acids with pK_a values less than about −2 are said to be strong acids. The value of pK_a varies with temperature and salinity, as both affect the tendency of an acid to dissociate (Atkins & de Paula, 2006). In seawater at 25°C and 35ppt salinity, the values for pK_{a1} and pK_{a2} are 5.94 and 9.13 respectively.

Once the dissociation constants are known, the concentrations of each of the components of the CO_2-carbonate equilibrium can be determined from any two of the following measurements:-

I) Carbonate alkalinity

II) pH

III) Total CO_2

IV) The partial pressure of CO_2 in the air which is in equilibrium with seawater (Kennish, 2000; Stumm & Morgan, 1996).

The alkalinity of seawater is a measure of its capacity to neutralise acids to the equivalence point of HCO_3^- and CO_3^{2-}, and its total alkalinity (A_T) can be determined by potentiometric titration against a strong acid solution. The amount of acid used is proportional to the total amount of protons required to neutralise the negative charges of the solution (Dickson, 1981). In the absence of bicarbonate, a net positive charge in seawater is conferred by the total charge of the major cations and anions shown in Table 1.1. This excess

positive charge is neutralised by the formation of negatively charged inorganic carbon species, ie. HCO_3^- and CO_3^{2-} subsequent to the absorption of CO_2 from the atmosphere. Thus, the greater the positive charge imbalance, the greater the solubility of CO_2. As well as inorganic carbon, borate ions, $B(OH)_4^-$ also contribute towards the total alkalinity in seawater. Since the concentration of boron in the ocean is over 30 times smaller than bicarbonate, however, (Table 1.2), it is mainly the negatively-charged carbon species and the resultant carbonate alkalinity which neutralise the excess of positive ions in seawater.

The occurrence of photosynthesis and respiration in seawater, and the resultant removal and addition of CO_2 does not affect alkalinity, because the net reaction in the CO_2-carbonate system produces the same number of positively-charged species (ie. H^+) as negatively charged species (HCO_3^- and CO_3^{2-}). For example, when CO_2 is produced by respiration, it reacts with water to create HCO_3^- and H^+, as shown in equation 1.5.

$$CO_2 + H_2O \rightarrow HCO_3^- + H^+ \qquad \textbf{Equation 1.5}$$

The resultant increase in H^+ ions, which would otherwise cause a reduction in ambient pH, is offset by their reaction with CO_3^{-2}, as shown in equation 1.6.

$$CO_3^{2-} + H^+ \rightarrow HCO_3^- \qquad \textbf{Equation 1.6}$$

As a result of these reactions, there has been no net change in the total negative charge of the system, therefore the carbonate alkalinity is unaffected. Because the overall DIC concentration is a factor which influences the balance of the CO_2-carbonate equilibrium, the slight increase in DIC as a result of respiration will lead to a decrease in pH. However, since the CO_2-carbonate system acts as a buffer for both dissolved CO_2 and for pH, this effect is minimised (Stumm & Morgan, 1996).

The pH of seawater has a substantial effect on the equilibria between CO_2, HCO_3- and $CO_3^{=}$ (Fig. 1.3). At low pH, the high concentration of H^+ ions promotes the production of HCO_3^- from CO_3^{2-}, and CO_2 from HCO_3^-. The reverse is true of high pH. At present, at the ambient seawater pH of 8.2, 90% of the total DIC is HCO_3^-, 9% is $CO_3^{=}$, and less than 1% is CO_2, but, with increasing concentrations of atmospheric CO_2, these proportions are likely to change (Stumm & Morgan, 1996)

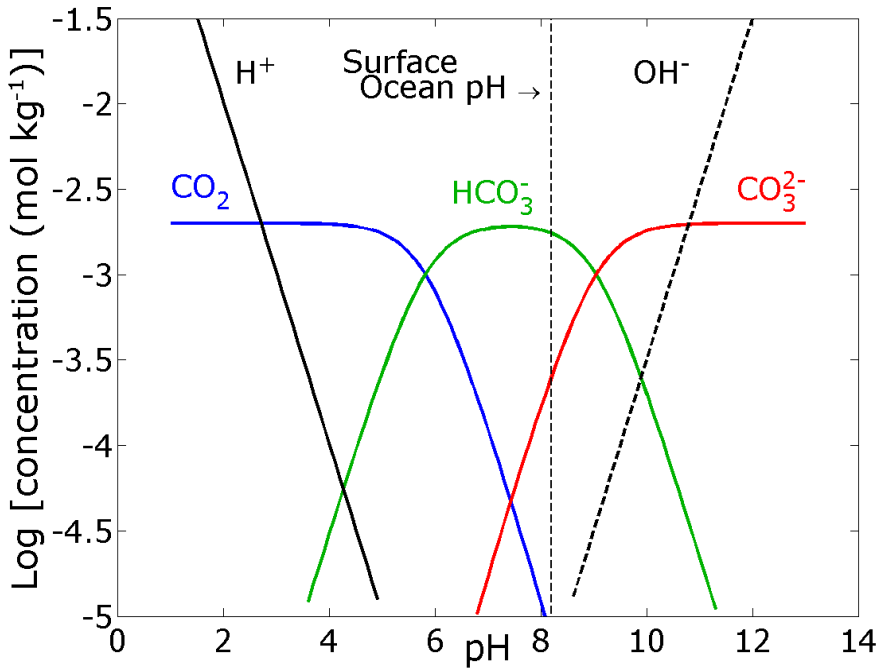

Figure 1.3 The concentrations of CO_2, HCO_3^-, and $CO_3^=$ in seawater as a function of pH (from Zeebe & Gattuso, 2006).

1.2 Primary productivity in the sea

Estimates of global net primary production (NPP), based on satellite indices of solar radiation absorbed and reflected by land-surface vegetation and sea-surface chlorophyll, suggest that around 104.9 Pg of carbon are fixed by photoautotrophic organisms each year. Of this total, 56.4 Pg are the product of terrestrial production, and 48.5 Pg are accountable to oceanic production (Geider *et al.* 2001, Field *et al*. 1998). The vast majority of carbon fixation in the ocean is achieved by phytoplankton, whereas macroalgae only contribute

about 1 Pg C y^{-1} (Field *et al.* 1998), although Dring (1982) has suggested that the rates of primary production in benthic communities are much greater compared to phytoplankton populations.

In both terrestrial and marine organisms, the enzyme ribulose-1,5-bisphosphate carboxylase/oxygenase (Rubisco) catalyses the first major step in the Calvin cycle, and uses CO_2 alone as a substrate for carbon fixation (Tcherkez *et al* 2006). The prevalent form of inorganic carbon in seawater, however, is bicarbonate (HCO_3^-), and although the respective atmospheric and oceanic CO_2 concentrations of 12μM and 14μM are very similar, the total dissolved inorganic carbon concentration in seawater of 2.2 mM is much greater. .

Over the last 250 years, industrialisation and the growth of the human population has led to an increase in the rate of fossil fuel combustion and deforestation. Consequently, the atmospheric CO_2 concentration ($[CO_2]_{atm}$) has risen dramatically (Falkowski & Raven, 1999). 2000 years before the industrial revolution, $[CO_2]_{atm}$ was 280 μmol mol^{-1}, and has now increased to 387 μmol mol^{-1} (Whorf & Keeling 2005), leading to an elevated surface seawater CO_2 partial pressure (Caldeira & Wickett 2003). A doubling of the atmospheric CO_2 concentration is predicted during the next century, and will represent the highest level recorded in the last 24 million years (Gattuso & Buddemeier, 2000). It is expected to lead to the acidification of seawater and an increase the concentrations of both CO_2 and HCO_3^- (Orr *et al*. 2005)

Although the changes in seawater chemistry that will be caused by the rise in atmospheric CO_2 are easy to predict, there is great uncertainty associated with the effects that it will have on global primary production. This is partly because the diversity and complexity of responses of different organisms make it difficult to form general predictions (Vézina & Hoegh-Guldberg, 2008). There is evidence that photosynthesis and growth of both microalgae and macroalgae are enhanced at elevated concentrations of atmospheric CO_2 (Wu *et al*. 2008, Riebesell *et al.* 1993), and several studies have shown that DIC addition to seawater increases rates of photosynthesis in some macroalgae (Andria *et al.* 2001, Mecardo *et al*. 1998, Holbrook *et al*. 1988). Although these findings indicate that increasing atmospheric CO_2 may have a fertilising effect in the ocean, according to a relatively recent textbook written by two leading authorities in the field of aquatic photosynthesis (Falkowski & Raven 1997), DIC limitation is not common among marine algae. To establish this, it is necessary to examine the physiology of a larger number of species at above-ambient concentrations of DIC. Thus, in the present study, the effect of DIC addition on photosynthesis and carbon acquisition mechanisms was explored in several seaweeds.

1.3 Inorganic carbon acquisition by marine macroalgae

Terrestrial plants are entirely dependent on atmospheric CO_2 as a source of inorganic carbon for photosynthesis, whereas marine plants are also exposed to HCO_3^- and CO_3^{2-}. Assuming that marine plants are also entirely dependent on

CO_2, the rate that it could be transported into cells would be subject to both the rate of CO_2 diffusion in seawater and the rate of CO_2 formation from the spontaneous dehydration of HCO_3^- . Since CO_2 in seawater diffuses *c.* 10^4 times slower compared to the atmosphere, and the spontaneous dehydration of HCO_3^- occurs more slowly than many of the reactions involved in inorganic carbon assimilation (Falkowski & Raven, 1997). It has been suggested that seaweeds which rely exclusively on the diffusive entry of CO_2 are likely to be carbon-limited (Giordano *et al*. 2005).

Several studies have demonstrated that the rate that CO_2 diffuses into cells is too slow to support the observed rates of photosynthesis in some macroalgae (Zou *et al*. 2004; Andria *et al,* 2001; Dong *et al*. 1991; Cook *et al.* 1986), and that numerous seaweeds can photosynthesise at high pH, when HCO_3^- and CO_3^{2-} are the only available forms of DIC (Maberly, 1990). This indicates that either they are using internal stores of inorganic carbon, which is characteristic of C_4 carbon fixation, or they are able to use the ionic forms of DIC as well as CO_2. Since C_4 metabolism is seldom found in macroalgae (Douglas *et al*. 2003; Falkoski & Raven, 1997), it is likely that ionic forms of DIC are being used. Because plasma membranes are permeable to small uncharged molecules, but impermeable to charged molecules, CO_2 rapidly diffuses freely in and out of cells, whereas the transport of HCO_3^- and CO_3^{2-} must be facilitated. Also, because Rubisco only uses CO_2 as its carbon substrate, this means that if HCO_3^- and/or CO_3^{2-} are used as sources of inorganic carbon by algae, they must possess mechanisms that convert them into CO_2.

The enzyme carbonic anhydrase (CA), is a well-characterised carbon transport mechanism in animal systems (Sterling *et al*. 2002), and has also been isolated in plants (Moroney *et al*. 2001). After it was discovered that some algae may be capable of using HCO_3^-, evidence of CA activity was sought.

Carbonic anhydrases are a family of zinc-containing metalloenzymes which catalyse the reversible hydration of CO_2, as shown in equation 1.7.

$$CO_2 + H_2O \leftrightarrow HCO_3^- + H^+$$ **Equation 1.7**

Catalytic rates of the different forms of this enzyme range between 10^4 and 10^6 reactions per second, which is among the fastest of all enzymes, and typically limited by the rate of diffusion of its substrate (Lindskog, 1997).

Carbonic anhydrases are particularly well-characterised in animal systems, where they are involved in numerous physiological processes, including renal and male reproductive tract acidification, respiration, gluconeogenesis, signal transduction, and formation of gastric acid (Sly & Hu, 1995). They have a major role in the removal of respiratory CO_2, and operate in conjunction with another major carbon transport mechanism, anion exchanger 1 (AE1), which facilitates the exchange of HCO_3^- and Cl^- ions across erythrocyte plasma membranes. Like CA, AE1 is well-characterised in animals. It is the most

abundant protein in erythrocytes and constitutes 55% of the integral cell membrane proteins, and around 25% of the total cellular protein (Sterling & Casey, 2002). The human AE1 gene has been sequenced (Tanner *et al.* 1988) and expressed in yeast cells (Groves *et al*. 1996), but unlike CA, there is little evidence for AE1 occurring in plants.

The function of CA and AE1 in erythrocytes is as follows: respiratory CO_2 is transported out of respiring cells, into the blood plasma then across the erythrocyte cell membrane via passive diffusion. Because blood plasma has a pH of about 7.4, it rapidly becomes saturated with CO_2, thus by converting it into the more soluble form of HCO_3^-, this allows more inorganic carbon to be transported. This reaction occurs in the cytoplasm of erythrocytes, and is catalysed by CA. The resultant HCO_3^- ions are then transported across the cell membrane into the blood plasma by AE1, in exchange for Cl^- ions This mechanism operates independently of ATP, and since both ions carry a negative change, there is no net loss or gain of electrons. Once HCO_3^- dissolves in the plasma it is transported into capillaries adjacent to alveolar membranes in the lungs, where AE1 and CA operate in reverse, ie. AE1 transports HCO_3^- in the blood plasma back into the cytoplasm of erythrocytes, and CA catalyses the conversion of HCO_3^- into CO_2. This CO_2 is then transported across the erythrocyte, capillary and alveolar membranes via passive diffusion, and enters the gaseous phase of the lung tissue (Jensen, 2004).

The extensive examination of DIC transport in animals has led to the

development of specific inhibitors which have been used to demonstrate that HCO_3^- acquisition mechanisms in some algae may be similar to those present in erythrocytes. Acetazolamide (AZ) for example, is a membrane-impermeable, specific inhibitor of external CA which decreases rates of photosynthesis in numerous seaweeds (Zou *et al*. 2004; Mercado *et al*. 1998; Giordano & Maberly, 1989) and microalgae (Colman *et al*. 2002). The AE1 inhibitors SITS (4-Acetamido-4'-isothiocyanato-2,2'-stilbenedisulfonic acid) and DIDS (4,4-Diisothiocyanatostilbene-2,2'-disulfonic acid) also decrease photosynthesis in some seaweeds and microalgae (Herfort *et al*. 2002; Larsson & Axelsson 1999; Mercado *et al*. 1998; Nimer *et al.* 1998; Axelsson *et al.* 1995; Beer, 1995), although at the present time, relatively few species have been tested.

Inhibitors do not provide infallible evidence for the presence of CA and AE1 in algae however, as they may have non-specific effects. For example, they can affect transporters that are not directly involved in DIC acquisition (Cabantchik & Gregor, 1992). At present, molecular evidence for the presence of CA in macroalgae is relatively scarce. There is genetic evidence of CA in microalgae however; for example, CA genes have been cloned from the red microalga *Porphyridium purpureum* (Mitsuhashi & Miyachi, 1996) and the coccolithophore *Emiliania huxleyi* (Soto *et al.* 2006), and eight CAs have been identified in *Chlamydomonas reinhardtii* (Mitra *et al.* 2005). Bicarbonate transporter genes have not been cloned prior to the present study, although Sharkia *et al* (1994), have shown that antibodies raised against human AE1 reacted with a similar-sized protein extracted from the cell membrane of *Ulva* sp.

Although the precise mechanism of uptake in *P. palmata* had remained unidentified, previous research has established that HCO_3^- is its major source of DIC (Maberly, 1990; Colman & Cook, 1985). There are reports that this alga lacks external CA activity (Larsson & Axelsson, 1999, Dong *et al*. 1991; Colman & Cook, 1985), and Kübler & Raven (1995) have speculated that a mechanism of direct bicarbonate uptake may be used instead. Larsson & Axelsson (1999) have sought inhibitor evidence of bicarbonate transport, by exposing actively photosynthesising tissue to 200uM of DIDS, but they recorded no rate change on inhibitor addition.

Research in the algal laboratory at QMUL by Dong (1993) indicates that *Palmaria palmata* uses a bicarbonate transporter mechanism which operates in the absence of external CA activity. This was established by demonstrating that photosynthetic O_2 evolution is reduced by the addition of the AE1 inhibitors SITS and DIDS, but not by the CA inhibitor acetazolamide. In the present study, both biochemical and molecular methods were used to identify and characterise inorganic carbon uptake mechanisms in *P. palmata*. Particular emphasis was placed on examining the adaptation of the carbon uptake strategy in this species in response to DIC concentration, the interaction between light and DIC supply, and changes in carbon uptake in response to seasonal changes experienced by plants growing on the shore.

1.4 Aims

Against this background, the following questions were examined:-

What mechanisms are used by *P. palmata* at the ambient DIC concentration in seawater?

Is photosynthesis in *P. palmata* saturated at the ambient DIC concentration in seawater?

How do the kinetics of DIC uptake in *P. palmata* compare with species that use extracellular carbonic anhydrase?

Are carbon acquisition mechanisms in *P. palmata* regulated by the DIC concentration in seawater?

Is the rate of photosynthesis in *P. palmata* influenced by DIC concentration at both saturating and subsaturating light?

Are there seasonal variations of DIC uptake in plants of *P. palmata* growing on a shore?

Chapter 2

Materials and Methods

2.1 Organisms

Plants were collected from two sites in the UK: St. Margaret's Bay near Dover (Latitude = 51.1507N, Longitude = 1.3872E), and a shore at Dale Fort in Milford Haven, Pembrokeshire (Latitude = 51.7034N, Longitude = -5.1514E).

Plants from St. Margaret's Bay were collected from the highest position that they grew on the shore, at 1.5m above chart datum. Upon collection, they were stored in plastic bags with a small quantity of seawater. Plants were transported to the lab in an insulated box containing freezer blocks, to prevent increases in temperature during transit. Time of transport between collection and arrival at the lab was approximately two hours.

Immediately on arrival at QMUL, plants were sorted manually, to ensure that unhealthy plants and epiphytes were discarded. Healthy plants were then placed in plastic tanks containing 5L simple artificial seawater medium (as described in 2.2), which had been adjusted to pH 8.2, and stored overnight at 15^{o}C. The seawater was vigorously aerated with airlines, and received about 10-15 µmol m^{-2} s^{-1} incident photon flux density (PFD), in 12:12 h light:dark photoperiods. Plants were used in experiments within 7 days, but normally within 2 days after collection. In the seasonal experiments described in Chapter 5, experiments were carried out within 12 hours of their collection from the shore.

Plants collected from Dale Fort taken to the lab within 15 minutes, and immediately placed in outdoor tanks containing natural seawater, and were aerated with airlines. Plants were used in experiments within 12 hours.

Axenic cultures of *Emiliania huxleyi* (Lohnmann) Hay & Mohler calcifying strain PCC.B11 were obtained from the Marine Biological Association Culture Collection (Plymouth, UK). Cultures were grown in 100 mL conical flasks containing 100 mL of Harrison's aritificial seawater medium (Harrison et al. 1980), prepared as described in 2.2 (below). To sterilise the glassware and medium, they were autoclaved for 20 min at 120^{o}C. Cultures were maintained at 15^{o}C on a rotating shaker at 100 rpm, under white fluorescent lights providing a continuous downwelling photon flux density of 120 µmol m^{-2} s^{-1}.

2.2 Media

Two types of artificial seawater media were made according to the method of Harrison *et al* (1980). A complex “full Harrison's” medium was used in long-term cultures of *P. palmata* and *C. crispus*, as described in Chapter 4, and for the culture of *E. huxleyi* in Chapter 3. For axenic culture of *E. huxleyi*, initially stock solution were made, which included two salt stock solutions and a trace metal stock solution (Table 2.1). After being autoclaved and allowed to cool, stocks 1 and 2 were combined in a 1:1 ratio, 10 ml/l of the trace metal stock was then added, and pH was adjusted to 8.2 using concentrated solutions of NaOH and HCl. For the culture of *E. huxleyi*, 100mL of the complete medium was dispensed into conical flasks, which were then autoclaved and allowed to cool.

Table 2.1 Chemical compositions of stock solutions used to create artificial seawater media used in experiments.

Stock Solution 1 (anhydrous salts)

Compound	g/L	mmol/L*[1]
NaCl	41.52	362.66
Na_2SO_4	6.95	24.99
KCl	1.17	8.04
$NaHCO_3$	0.34	2.07
KBr	0.17	7.25×10^{-1}
H_3BO_3	0.045	3.72×10^{-1}
NaF	0.0054	6.570×10^{-2}

Stock Solution 2 (hydrous salts)

Compound	g/L	mmol/L*[1]
$MgCl_2.6H_2O$	18.79	47.18
$CaCl_2.2H_2O$	2.63	9.14
$SrCl_2.6H_2O$	0.04	8.200×10^{-2}

Nutrients and trace metal solution

Compound	g/L	mmol/L*[2]
$NaNO_3$	4.67	549.09
$Na_2SiO_3.9H_2O$	3	105.6
Na_2glycerolPO_4	0.67	21.79
Na_2EDTA	0.55	14.86
H_3BO_3	0.38	61.46
$Fe(NH_4)_2(SO_4)2.6H_2O$	0.234	5.97
$FeCl_3.6H_2O$	0.016	5.92×10^{-1}
$MnSO_4.4H_2O$	0.054	2.42
$ZnSO_4.7H_2O$	0.0073	2.54×10^{-1}
$CoSO_4.7H_2O$	0.0016	5.69×10^{-2}

*[1] Final mmol/L in combined Sol. 1 & 2 mixture
*[2] Final umol/L in complete medium

For macroalgal culture, which did not require a sterile medium, all of the salts in stocks 1 and 2 were dissolved together, followed by the addition of the trace metal solution.

A simplified Harrison's seawater medium, which did not contain many of the trace elements in seawater, was used in all short-term experiments, ie. oxygen electrode chambers, and incubation experiments that did not exceed 24 hours. It contained 355.6mM NaCl, 24.4mM Na_2SO_2, 7.9mM KCl, 46.2mM $MgCl_2.6H_2O$, 8.6mM $CaCl_2.2H_2O$, and 2mM $NaHCO_3$. When buffering was required, 25mM of N,N-bis [2-Hydroxyethyl] glycine (Bicine) was added. All solutions were made with deionised water. Seawater pH was measured using a 420A Orion pH meter calibrated with pH 7.0 and 9.22 buffers, and adjusted to 8.2 using 1M solutions of NaOH and HCl.

2.3 Measurement of Photosynthesis and Respiration

2.3.1 Clark-Type O_2 Electrodes

Respiration and net oxygen production was measured using Clark-type oxygen electrodes (Hansatech, Norfolk, UK). A diagram of an oxygen electrode, similar to the model used in this study, is shown in Figure 2.1.

This electrode is known as "Clark Type" after its inventor, Dr. Leland Clark. It

comprises a silver anode and a platinum cathode that are submersed in an electrolyte solution (KCl), and in the presence of a polarising voltage, molecular oxygen is reduced. This involves two separate chemical reactions:

Firstly, at the surface of the anode, silver is oxidised to produce four electrons (Equation 2.1).

$$4Ag + 4Cl^- \rightarrow 4AgCl + 4e^- \qquad \textbf{Equation 2.1}$$

The electrons flow through the electrolyte solution, and are involved in the reduction of molecular oxygen at the surface of the cathode (Equation 2.2).

$$O_2 + 4H^+ + 4e^- \rightarrow 2H_2O \qquad \textbf{Equation 2.2}$$

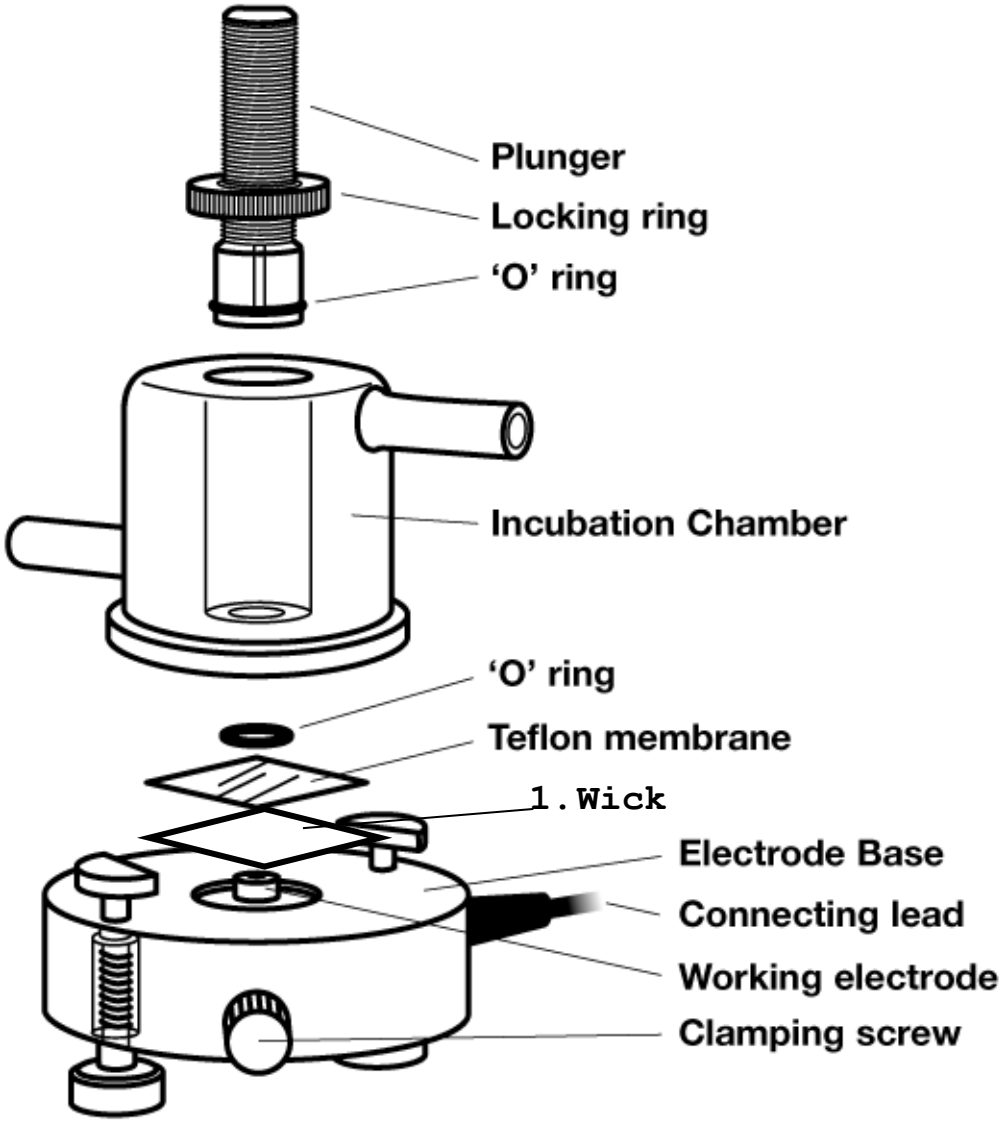

Figure 2.1 Schematic diagram of a Clark-type oxygen electrode, similar to the model used in the present study.

The electrode measures the flow of electrons from the cathode to the anode at a constant polarising voltage, which is directly proportional to the amount of oxygen in the electrode chamber that diffuses across the teflon membrane to the surface of the anode. In this way, oxygen concentrations in the incubation

chamber, which are changed by photosynthesis and respiration, can be measured over time to obtain a rate net oxygen production. This was recorded automatically using computer software that was supplied with the electrodes.

The electrode discs were prepared as follows: firstly, the anode is cleaned with a mild abrasive solvent to remove silver oxide deposits, which would otherwise reduce the electrode sensitivity. The well surrounding the silver anode was filled with a 0.5M solution of KCl, and a drop of this solution was then placed onto the platinum cathode. Approximately 2 cm^2 of fine cigarette paper was then placed on top of the cathode, as recommended by the Hansatech manual. This acts as a wick for the KCl solution, to ensure that KCl is constantly in contact with the anode. No particular brand was recommended by the manual, and Rizla green paper (approximately 50μM thickness) was used. On top of the cigarette paper, a slightly larger square of teflon membrane was placed. Care was taken not to allow grease from fingers to be deposited onto the teflon membrane, as this may have affected its permeability to oxygen. An 'O' ring was used to secure the teflon membrane and cigarette paper to the electrode disc, which created a thin layer of electrolyte between the cathode and the teflon membrane. The prepared electrode discs were attached to the incubation chamber, which was then filled with the incubation medium, circulated by an automated magnetic stirrer. The electrodes were normally allowed to operate for about 20-30 min before calibration.

Discs of thalli, 9 mm in diameter, were cut with a cork borer immediately before experiments. They were supported inside the incubation chamber with a panel

of acetate into which two slots were cut. The upper and lower edge of the thallus discs were inserted into these slots, and held in place (Figure 2.2). Because the thalli were not positioned immediately against the acetate panel surface, the seawater medium was able to flow freely around them.

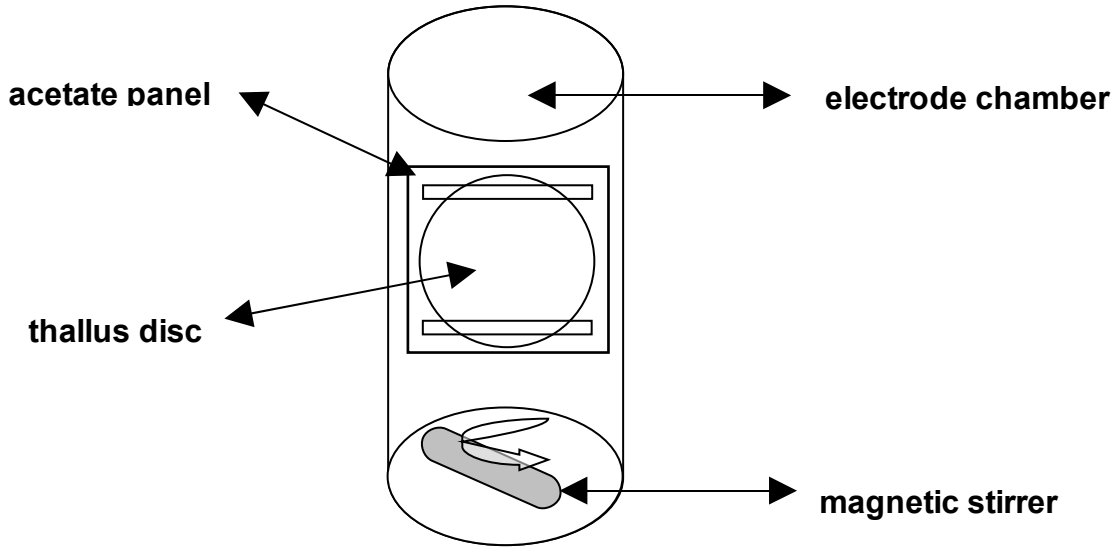

Figure 2.2 Schematic diagram of a thallus disc inside the electrode chamber, supported by a panel of acetate.

The solution inside the electrode chamber was sealed from the air with a plunger and a rubber 'O' ring, which prevented any exchange of oxygen between the incubation medium and the atmosphere. Solutions of inhibitors and DIC were injected into the incubation chamber with microlitre syringes, via a thin capillary tube in the plunger.

The incubation chamber was surrounded by flowing deionised water maintained at 15^{o}C by a waterbath, and light was supplied by projector lamps containing halogen lightbulbs. The incident photon flux density (PFD) was determined using a Hansatech Quantitherm light meter with a submersible probe

(Hansatech, Norfolk, UK). The probe was inserted into the electrode chamber, and positioned at the same level as the thallus discs.

The electrodes were calibrated with air-saturated seawater and seawater containing no oxygen. The air saturated measurement was acquired from unsealed electrode chambers which contained 1mL of simplified artificial seawater medium. The seawater was left in the chamber for approximately 10 minutes to allow it to reach the temperature set by the water bath, usually 15°C, and the stirrer bar was activated. It was ensured that the oxygen measurement over time was stable, and the calibration was set by the computer software. To obtain a zero oxygen measurement, a few crystals of sodium dithionite were added to the same seawater used to set the air-saturated oxygen value. Since sodium dithionite is a powerful reductant, gaseous oxygen was removed from the medium, which could be observed on the trace of oxygen measurement over time recorded by the computer software. Once this stabilised, the "zero oxygen" calibration was set on the computer. The electrode chamber was then flushed several with deionised water, followed by three to four changes of artificial seawater.

To measure photosynthesis using the oxygen electrodes, 1mL of simplified artificial seawater was placed in the electrode chamber, and left for 5-10 min to allow it to reach the required temperature. A thallus disc attached to an acetate support was then inserted into the electrode chamber, as shown in Figure 2.2. The electrode plunger was inserted into the top of the electrode chamber, and carefully pushed into place. Often a small air bubble would become trapped directly under the plunger. To remove this, the plunger was inserted slightly

further, which caused some of the seawater to move into a small capillary tube which runs vertically from the centre of the top of the plunger to the bottom. The plunger was then returned to its original position. Because the base of the plunger was fitted with a rubber 'O'-ring, this sealed the seawater in the chamber from the air.

The thallus discs were left in the electrode chamber for about 5 min before the start of experiments, during which time they consumed oxygen. This was observed on the oxygen vs time trace displayed on the computer software, and experiments began once the rate of respiration stabilised. The projector lamps were then switched on to illuminate the chamber, and photosynthesis was allowed to procede until the rate of oxygen production had stabilised, after which, photosynthesis was measured for about 5 min. Respiration was then measured by switching off the lamps, and covering the electrode chambers with foil to obscure light. Once the rate of respiration had stabilised, it was measured for about 5 min.

In inhibitor experiments, after respiration was measured, the electrode chambers were uncovered and illuminated by the projector lamps. Again, once the rate of photosynthesis had stabilised, it was measured for about five minutes. Solutions of inhibitors that had been prepared previously (2.4) were added to the seawater in the electrode chamber using 100μL and 50μL syringes, after the syringe needle was inserted into the fine capillary in the electrode stopper. Once inhibitors were added, photosynthesis was allowed to proceed for 10-15 min. Inhibition usually occurred about 30 seconds after inhibitors were added.

One thallus disc was used for each experiment, after which they were discarded. Between experiments the electrode chambers were flushed with several changes of deionised water followed by three changes of fresh artificial seawater.

To ensure that oxygen evolution measurements were biomass-independent, photosynthesis was measured in different-sized pieces of tissue cut from thalli. The results of one of these experiments is shown in Figure 2.3, and indicates that the rate of photosynthesis double when the thallus weight was increased from 5 mg to 10 mg, but increased disproportionately between 10mg and 20mg. The 9mm discs of thalli used in experiments weighed between 6-10mg, therefore biomass-dependant rates of photosynthesis were avoided.

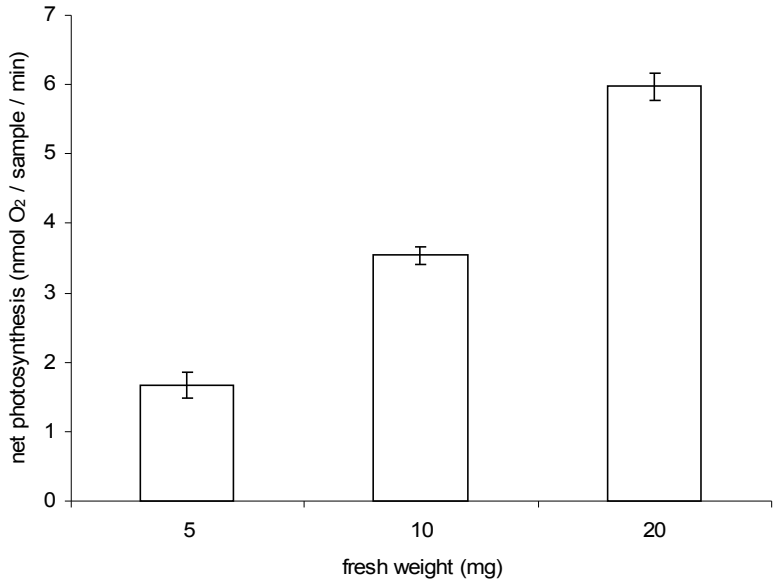

Figure 2.3 Rates of photosynthesis in pieces of thalli of different weights, cut from the thallus of *Palmaria palmata* (*n*=6).

2.3.2 Induced Chlorophyll Fluorescence

Induced chlorophyll fluorescence was measured with an FMS1 fluorescence monitoring system (Hansatech, Norfolk, UK). This model uses the pulse-modulated technique to measure chlorophyll fluorescence emissions from samples under ambient illumination. A schematic representation of the FMS experimental setup is shown in Figure 2.4

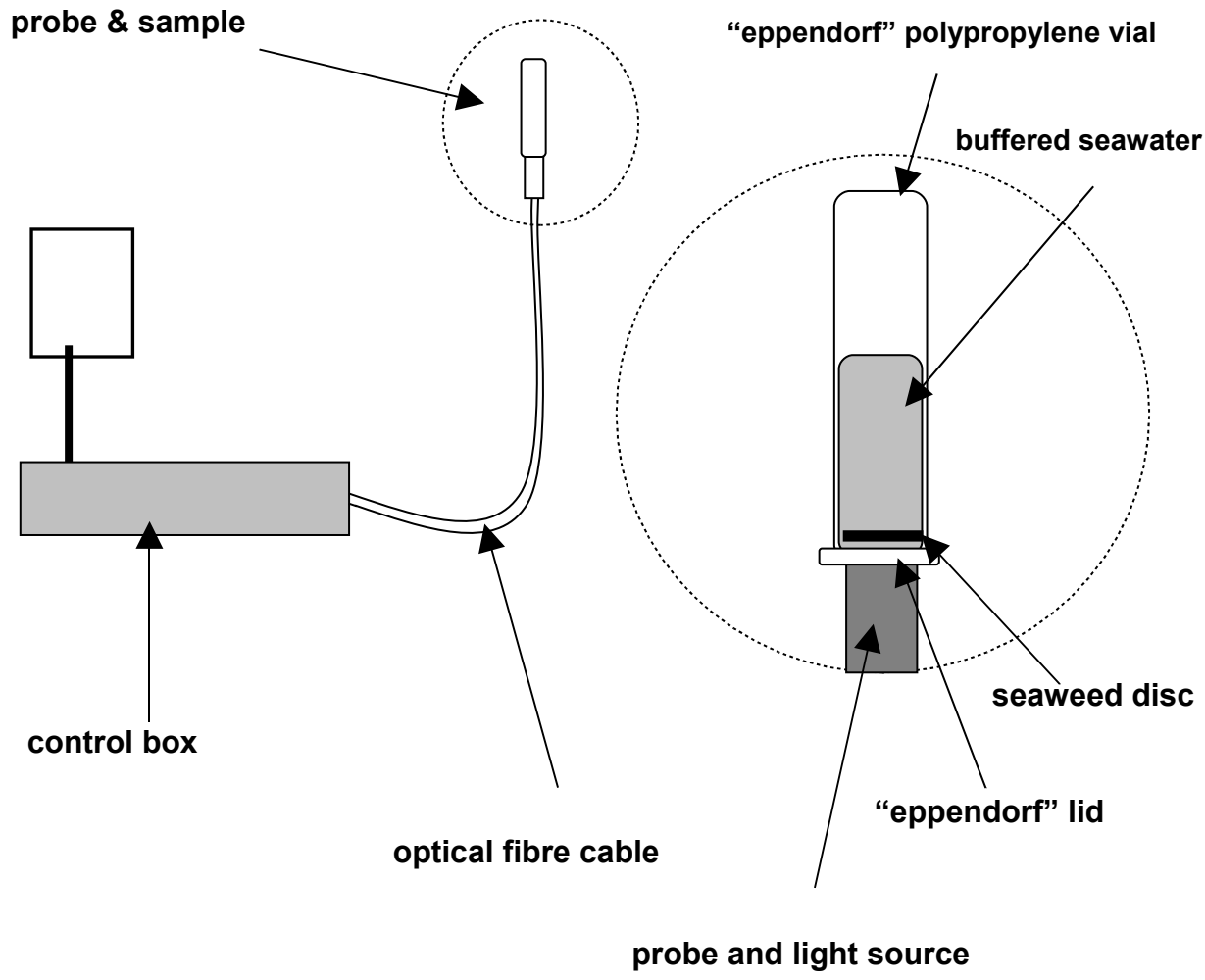

Figure 2.4 Schematic diagram of the Hansatech fluorescence monitoring system used in the present study.

The apparatus consisted of a control box containing a halogen lamp, which provided an actinic light source via a cable containing optical fibres. This was directed towards the incubation chamber, which consisted of a 1 mL polypropylene “eppendorf” vial, containing 1 mL of buffered artificial seawater.

The technique works on the principle that in plants at room temperature, the reaction centre of PSII is the main source of variable fluorescence and that any change in fluorescence is related to a modification of the state of PSII. Photons absorbed by chlorophyll molecules can trigger either photochemical or non-photochemical processes. The former uses the absorbed energy for photochemical reactions, whereas non-photochemical processes dissipate energy and do not drive photosynthesis (Schreiber *et al.* 1994). Instead, energy is either quenched as infrared radiation, or as red/far-red radiation (chlorophyll fluorescence). An increasing in non-photochemical quenching is attributed with a diminution in photosynthetic activity. A schematic illustration of primary energy conversion in photosynthesis is shown in Figure 2.5.

The FMS provides two sorts of primary fluorescence parameters: dark and light-adapted ones. The fluorescence origin, known as Fo, represents the minimum fluorescence yield in dark-adapted tissue; i.e. when the primary electron acceptor, Q_A, is fully oxidised (Schreiber *et al.* 1994). This is measured in dark-adapted tissue. The maximum fluorescence yield, known as Fm, is measured after exposing dark-adapted tissue to a short, intense beam of saturating light, which corresponds to the fully reduced state of Q_A. Variable fluorescence, or Fv, is calculated as shown in equation 2.3.

$$Fv = Fm - Fo$$ **Equation 2.3**

Since Fv is the difference between Fm and Fo, it is an estimation of the maximum capacity for photochemical quenching. The most important dark-adapted fluorescence parameter is the ratio of the variable to maximum fluorescence (Fv/Fm), which is directly proportional to the maximum quantum efficiency of PSII. Fv/Fm is biomass independent, and widely used to determine plant health, as a healthy terrestrial plant will have an Fv/Fm of around 0.8, and anything less than this indicates stress and the presence of a quenching mechanism (Papageorgiou & Govindjee, 2004) .

The light-adapted equivalent of Fv/Fm is ΦPSII, and is measured after exposing a sample to a beam of actinic light, of known photon flux density (PFD). The ΦPSII calculation incorporates Fs, the steady state fluorescence yield, and Fm', which correspond to Fo and Fm respectively. ΦPSII is calculated as follows:-

$$\Phi PSII = (Fm' - Fs) / Fm'$$ **Equation 2.4**

When excess light energy is absorbed by chlorophylls and accessory pigments (which constitute the light harvesting pigments, or LHC), electrons can be transferred to other components of the photosystem, and may be damaging. This is prevented by mechanisms that redirect this excess energy, which is referred to as non-photochemical quenching.

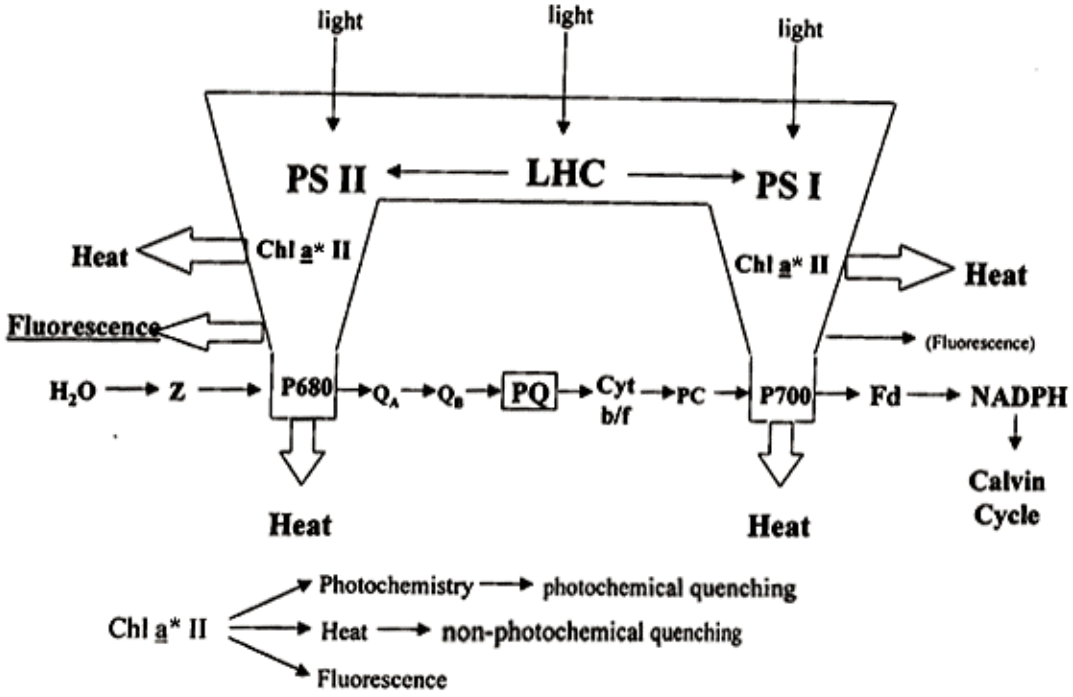

Figure 2.5 Schematic illustration of primary energy conversion in photosynthesis, which governs *in vivo* chlorophyll fluorescence yield. Variable fluorescence originates almost entirely from PSII. LHC = light harvesting complex, and represent additional forms of chlorophyll a (Chl_a*) and accessory pigments, increase the spectral range of light energy that can be absorbed. From Schreiber *et al.* 1994.

Chlorophyll fluorescence was measured over time on a computer, by using the custom software which was supplied with the FMS1. A typical trace of fluorescence measurement over time in a 9 mm disc cut from a thallus of *Palmaria palmata,* is shown in Figure 2.6

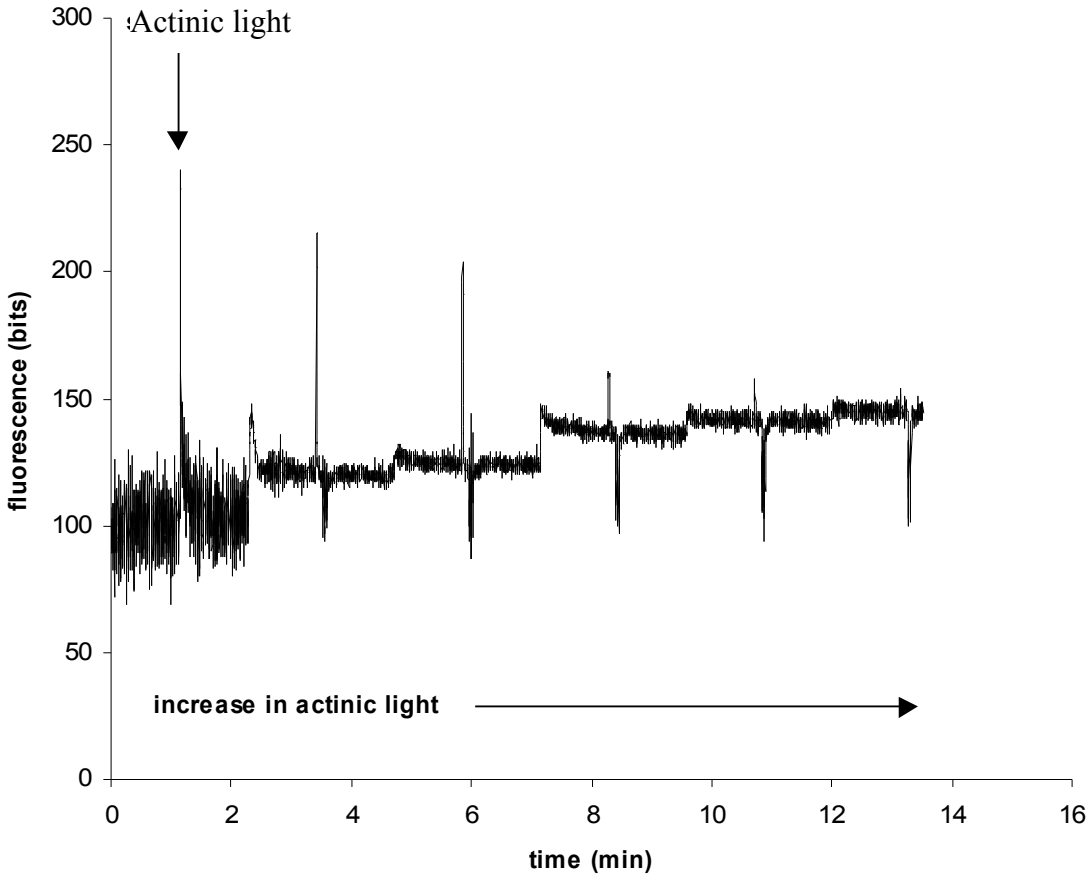

Figure 2.6 Induced chlorophyll fluorescence in a disc cut from the thallus of *Palmaria palmata*, measured using a Hansatech fluorescence monitoriing system.

Figure 2.6 shows the effect of actinic light on the variable fluorescence of P. palmata. Maximum fluorescence (Fm) is acquired by applying a saturating beam of actinic light to dark-adapted tissue, in which all Q_A is fully oxidised. Subsequently actinic light of increasing PFD are applied at regular intervals; the PFDs used in this experiment were 4.2, 9.5, 13, 18.5 and 25 umol m^{-2} s^{-1} respectively. After 30 seconds of exposure to each PFD a saturating beam of actinic light is applied to determine the maximum fluorescence yield from light-adapted tissue, Fm'. As increasing PFDs are applied, more QA is reduced and unable to accept electrons from chlorophyll. This results in a reduction in the

maximum fluorescence yield, which is shown by the decrease in values of Fm'.

2.4 Inhibitors of Bicarbonate Acquisition Mechanisms

Three inhibitors were used in the present study: the membrane-impermeable CA inhibitor acetazolamide (N-[5-Sulphamoyl-1,3,4-thiadiazol-2-yl]acetamide), and the AE1 inhibitors DIDS (4,4-Diisothiocyanatostilbene-2,2'-disulphonic acid) and SITS (4-Acetamido-4'-isothiocyanato-2,2'-stilbenedisulphonic acid).

Acetazolamide solution was prepared in 30mL polypropylene containers by initially dissolving the inhibitor in 3 drops of concentrated NaOH, then adding enough deionised water to submerse the probe of the pH meter. The pH was then adjusted to 8.2, and the resulting solution was diluted with deionised water to produce a 10mM working concentration.

100mM solutions of DIDS and SITS were made in 500uL polypropylene "eppendorf" tubes, by dissolving in dimethyl sulfoxide (DMSO) and deionised water respectively.

2.5 Analysis of nitrate and DIC concentrations in solution

Nitrate concentrations of water samples were determined using the well-known cadmium/copper reduction method, described by Strickland & Parsons (1972).

Briefly, 15 mL of the sample solution was diluted 10 times with deionised water, and passed through a column containing cadmium filings coated with metallic copper. The nitrite thus produced was quantified by firstly diazotizing with sulphanilamide, adding N-(1-napthyl)-ethylenediamine to form a coloured azo dye, and the extinction of this was measured using a spectrometer. To determine the efficiency of the column, a series of $NaNO_3$ solutions of known concentrations were passed through the column, to produce a calibration curve. Their spectrometrically-determined absorbencies were then compared to solutions of $NaNO_2$ of equal concentrations.

2.6 Total Alkalinity Determinations

Total alkalinity (TA) in aqueous solution is determined by titrating with a strong acid solution. The amount of acid used is proportional to the total amount of protons required to neutralise the negative charges of the solution. In seawater, this corresponds to the formation of carbonic acid from bicarbonate (Dickson, 1981). Therefore, it is possible to estimate the total DIC concentration.

In the present study, total alkalinities of natural seawater were measured using the method described by Gran (1952). Briefly, this is a step-wise procedure, whereby the volume of acid (HCl) required to decrease pH, are recorded between pH 4.4 and 3.7. These values are then used to calculate the Gran function F_2, given Equation 2.5.

$F_2 = [\text{antilog } (5\text{-pH})] \times (V_s + v)$ **Equation 2.5**

where V_s and v are the volume (mL) of the sample and of the titrant respectively. F_2 is plotted against v, so that, by extrapolation, the point of intersection with the horizontal axis (v_2) can be determined. The total alkalinity of the sample can then be obtained using Equation 2.6.

$TA\ (\text{mEq } l^{-1}) = v_2 \times (1000 / V_s) \times n$ **Equation 2.6**

where n is the concentration of the titrant, which was 0.01M HCl. Approximately 10g of sample was titrated at room temperature, using a motorized titrator (EDP Plus, RAININ instrument co, inc. USA). F_2 and TA values were calculated using a computer program.

2.7 Molecular Biology Methods

2.7.1 Preservation of nucleic acids in tissue

Immediately upon retrieval, thalli fragments of *Palmaria palmata*, cell pellets from centrifuged axenic cultures of *Emiliania huxleyi*, and a whole kidney extracted from *Rattus norvegicus*, were stored at –20°C, in a solution containing

25 mM $Na_3C_6H_5O_7 \cdot 2H_2O$ (sodium citrate), 10 mM EDTA, and 5.3 M $(NH_4)_2SO_4$. (ammonium sulphate). These substances are known to protect against the oxidation of nucleic acids, and inhibit the activity of DNases and RNases.

2.7.2 Genomic DNA extraction

Genomic DNA extractions were carried out using a potassium acetate protein precipitation method, modified from Cockburn & Seawright (1988). Briefly, samples of preserved tissue were homogenized in between 100 uL and 1 mL of extraction buffer (depending on the size of the sample), which comprised of 1% SDS, 50mM Tris biological buffer, pH 8.0, 25 mM EDTA. The homogenates were then transferred to an autoclaved polypropylene “eppendorf” vial, and placed in a waterbath heated to 68^{o}C, for approximately 20 minutes. A volume of potassium acetate (pH 7.2), equivalent to half the volume of the extraction buffer, is then added to the homogenate, mixed by inversion, and placed onto ice for 15 minutes, which separates proteins and lipids from nucleic acids by precipitation (i.e. the nucleic acids remain in the supernatant). The precipitates were removed by 10 min of high-speed micro-centrifugation, and the supernatant containing the nucleic acids was decanted into a vial. Three volumes of absolute ethanol were then used to precipitate nucleic acids from the supernatants, at –20^{o}C overnight. These were pelleted by 10 min of high-speed micro-centrifugation, and washed twice with 200 uL of 70% ethanol, and once with 100 uL of absolute ethanol. After the addition of the ethanol solutions at each wash step, the tube was micro-centrifuged at high speed for 5 minutes to maintain the nucleic acid pellet. After the final wash, the pellet was

dried in a vacuum desiccator for approximately 15 minutes, and re-suspended in autoclaved deionised water.

2.7.3 Polymerase Chain Reaction

The polymerase chain reaction (PCR) method was used to amplify the partial genomic DNA sequence of AE1 in *Rattus norvegicus*, and bicarbonate transporter genes in *P. palmata* and *E. huxleyi*. The required reagents were obtained from a Qiagen HotstarTaq® DNA polymerase kit. A single 50 µL PCR reaction mixture was created according to the Qiagen manual, and consisted of 50 µL 10x PCR buffer, 1 µL DNTP mix (10mM), 8 uL genomic DNA (10 ng / µL), 0.5 µL HotstarTaq® (5 U / µL), and 3 µL each of the forward and reverse primers (primer sequence design will be discussed shortly).

Genomic DNA concentrations were determined by measuring the absorbance at 260 nm (A_{260}) in a spectrophotometer. An absorbance of 1 unit at 260 nm corresponds to 40 ug of DNA per mL. Therefore:-

$$[\text{DNA}] \text{ in sample} = 40 \times A_{260} \times \text{dilution factor} \qquad \textbf{Equation 2.9}$$

The ratio of the absorbance readings at 260 nm and 280 nm provided an

estimate of the purity of DNA with respect to the contaminants that absorb in the UV, such as protein. A_{260}/A_{280} ratios of 1 and above were used in experiments.

The integrity of the DNA was assessed by agarose gel electrophoresis and ethidium bromide staining, using the protocol described in the Qiagen manual.

All PCR reactions were performed on a Techne Cyclogene thermal cycler, using the following program:-

1 cycle		95°C for 3 minutes
35 cycles	{	95°C for 20 seconds
		55°C for 30 seconds
		72°C for 1 minute
1 cycle		72°C for 15 minutes

2.7.4 Primer Design

Degenerate primers were designed by comparing the amino acid and nucleic acid sequences of AE1 genes from several different animals. This allowed for areas of the AE1 protein and gene sequences with greatest homology to be identified, with the prediction that this homology is likely be present in the algal sequence.

The animal AE1 sequences were firstly aligned using the fastPCR program. This program introduces colour coding to the aligned sequences, which allows them to be visualized according to their homology. By using this information, it was then possible to design degenerate primers.

2.7.5 pGEM® -T Easy Cloning of PCR Products

Agarose gel electrophoresis was used to separate, identify and purify the PCR pruducts. A 1 % agarose gel was routinely made by combining 1 g of electrophoresis-grade agarose powder in 100 mL of TAE buffer (ref), and heating in the microwave until the agarose dissolved. The solution was allowed to cool briefly, then ethidium bromide was added to a final concentration of 0.5 µg/mL. The agarose gel was then allowed to set at room temperature, for about 40 mins.

The DNA samples, containing 20 % DNA loading buffer (0.25 % bromophenol blue, 50 % glycerol, 50 % TE buffer), were loaded into the agarose gels, along with a molecular weight marker (Bioline). Electrophoresis was carried out at 70 volts for approximately 1 hour. Ethidium bromide is a fluorescent dye that intercalates between DNA base pairs, and re-emits UV light in the red-orange wavelength. Therefore, the separated bands of DNA were visualized by placing the gel onto a UV transilluminator. The gel was then photographed by a camera through a red filter.

The DNA band of interest was cut from the gel using a scalpel blade, and purified using a Qiagen QIAquick® gel extraction kit protocol, and purified with a QIAquick® PCR purification kit.

Purified DNA was cloned using the pGEM® -T Easy vector system from Promega, using the protocol described in the manual. The plasmids containing the DNA insert were used to transform *E. coli* cells (strain JM 109) which had previously been prepared according to the method described by Inoue *et al*. (1989). Super-competent cells were defrosted on ice before adding 5 µL of plasmid DNA. The mixture was then incubated on ice for 15 minutes, and then heat-shocked at 42^{o}C for 55 sec, before the addition of 200 µL Luria-Bertani (LB) broth (1 % tryptone, 0.5 % yeast extract, 0.5 % NaCl). The cells were then incubated, without shaking, at 37^{o}C for 30 mins to allow antibiotic resistance expression. This mixture was then spread onto an LB agar plate containing ampicillin and x-gal, and incubated at 37^{o}C overnight.

The following day, blue and white colonies were both normally produced. White colonies were produced by cells which had both ampicillin resistance, and contained the DNA insert. Under sterile conditions, these were removed from the agar plate with a sterile loop, and inserted into 10 mL of autoclaved LB solution. These were cultured on a shaker overnight at 37^{o}C.

Successful cultures acquired a cloudy appearance by the next morning, and these were centrifuged at 4^{o}C for 5 min to produce a pellet of cells, which were used in the isolation procedures.

2.7.6 Isolation of plasmid DNA and Restriction digest of DNA

A Qiagen QIAprep Miniprep kit was used for the purification of plasmid DNA, using the protocol described in the manual. The amplified DNA fragment was digested from the plasmid using the restriction enzyme, EcoR1. The EcoR1 digest reaction was allowed to proceed for 2 hours at 48^{o}C.

The digestion product was identified by agarose gel electrophoresis (as described previously). If the size the DNA band produced corresponded to the PCR product inserted into the plasmid vector, this indicated that the cloning was successful. Subsequently, about 10 µL of the digested DNA was sent for sequencing to the Qiagen DNA Sequencing Laboratories (Hilden, Germany).

Chapter 3

Mechanisms and kinetics of DIC Uptake in *Palmaria palmata*

3.1 Introduction

In terms of transporting inorganic carbon across cell membranes, algal cells face the same basic biochemical problem as erythrocytes: their cell membranes are somewhat impermeable to HCO_3^-. Bicarbonate transporters are well-characterised in animal systems, and at present 14 genes are known to encode proteins that mediate HCO_3^- transport activity (Cordat & Casey, 2009), and numerous isoforms of CAs have been identified (Sterling & Casey, 2002). Since Bradfield (1947) demonstrated ubiquitous presence of CA in higher plants, its role in carbon transport in higher plants and algae has also been widely examined (Giordano *et al*. 2005; Tiwari *et al*. 2005; Moroney *et al*. 2001). However, bicarbonate transporters are, in comparison to CAs, poorly examined in plants and algae, and no representative protein or gene sequence has been identified.

The experiments described in this chapter show that by taking into consideration what is known about bicarbonate transporters in animal systems, further knowledge of their function in algae can be obtained. Therefore, a summary of the two major mechanisms of carbon transport in animals is presented.

3.1.2 Carbonic Anhydrase

CA was first detected by Meldrum & Roughton (1933) in the erythrocytes of cow blood, and has since become recognised as an enzyme that is widespread in animals, plants, and many bacteria (Lindskog, 1997). Almost all CAs catalyse

the reversible hydration of CO_2 in an active site containing a zinc prosthetic group. However, a unique cadmium-containing CA has recently been isolated from the marine diatom *Thalassiosira weissflogii* (Lane *et al*. 2005).

The catalytic activity of CA involves the zinc-activation of water. After binding to a positively-charged zinc ion, the pK_a of the water molecule is reduced from 15.7 to 7, and dissociates to form a hydroxide ion. The CO_2 substrate then binds to the active site where it is optimally positioned to react with the hydroxide ion. Because of its greater electronegativity, the zinc-bound hydroxide attacks CO_2 much more readily than water, and rapidly converts it into HCO_3^-. The catalytic site is then regenerated by the release of the HCO_3^- ion and the binding of another water molecule (Berg *et al.* 2002)

CAs can be divided into five distinct groups, α, β, γ, δ and ε, which are functionally similar, but have no significant amino acid sequence homology, suggesting that they have evolved independently (Hewett-Emmett & Tashian, 1996).

α CA Mostly found in animals, this is the best studied group of CAs, whose active sites contain a zinc prosthetic group co-ordinated by three histidine residues and a hydroxyl group (Fisher *et al*. 2005). At present, 14 isoforms have been identified in mammals, which differ according to their distribution in tissues, catalytic activity, and sensitivity to inhibitors (Sterling & Casey, 2002; Lindskog, 1997). The most widely distributed isoform is CAII, which is found in the cytosol of the majority of mammalian tissues (Sly & Hu, 1995), and is the

most catalytically active CA, with a CO_2 hydration rate of 1 x 10^6 s^{-1} (Sterling & Casey, 2002). This group also contains two periplasmic CAs cloned from the green alga *Chlamydomonas reinhardtii (*Fukuzawa *et al. 1990),* which catalyse the extracellular conversion of HCO_3^- to CO_2 (Coleman *et al.* 1984), and therefore increase the concentration of CO_2 at the cell membrane surface.

β CA Represented by isoforms found in higher plants, this group also includes CA isolated from the red alga *Porphyridium purpureum* (Mitsuhashi *et al*. 2000). The active sites of βCAs contain a zinc group co-ordinated by one histidine and two cysteine residues, plus a hydroxyl group. Despite structural similarities, they share no significant amino acid sequence homology to the αCAs (Kimber & Pai, 2000, Bracey *et al.* 1994). Their primary function in plants is to increase the concentration of CO_2 in the proximity of the Rubisco active site, which contributes towards increasing the rate of carboxylation, and alleviating photorespiration by suppressing the oxygenase reaction (Giordano *et al*. 2005).

γ CA A prototype for this group has been reported for the methanogenic bacterium *Methanosarcina thermophila*, and shows a similar active site structure to the αCAs (Alber & Ferry, 1996). Smith *et al.* (1999) have demonstrated their widespread distribution in metabolically diverse species of archaea and bacteria, and have postulated that their presence in phylogenetically ancient chemolithoautotrophic bacteria suggests that CA had an important role in the proposed autotrophic origin of life (Wächtershäuser, 1989).

δ CA This group is made up of CAs which readily exchange cadmium and zinc at their active sites, and represent the only known biological use of cadmium. Originally isolated from *Thalassiosira weissflogii* (Lane *et al*. 2005), genes encoding cadmium-containing CAs (CDCA) have since been found in numerous other diatom species (Park *et al*. 2008). Despite having a substantial amount of amino acid sequence divergence with βCAs in higher plants, analysis of the crystal structure of CDCAs indicate that they possess striking similarities in the spatial organisation of their active site residues (Xu *et al*. 2008).

ε CA CAs which have an evolutionary lineage distinct from CAs previously sequenced in animals, plants and prokaryotes, have been identified in the carboxysomes of chemolithoautotrophs and cyanobacteria (So *et al*. 2004). Their function is analogous to CAs in plant chloroplasts, as they increase the CO_2 concentration at the Rubisco active site. Analysis of the crystal structure of a εCA from *Halothiobacillus neapolitanus* has revealed that, like CDCAs, its active site structure is similar to that of βCAs in higher plants, despite a lack of amino acid sequence homology (Sawaya *et al.* 2006).

The study of CAs has been helped considerably by the discovery that sulphonamides act as specific, high-affinity inhibitors of CA (Mann & Keilin, 1940). They are created by the reaction of sulphonyl chlorides with amines, and have the general formula RSO_2NH_2, where R is an organic group (Ch'En *et al.* 2008). Two sulphonamides often used in CA research are ethoxyzolamide, which is membrane permeable, and acetazolamide (Fig. 3.1) which is membrane-impermeable, and is used in the present study.

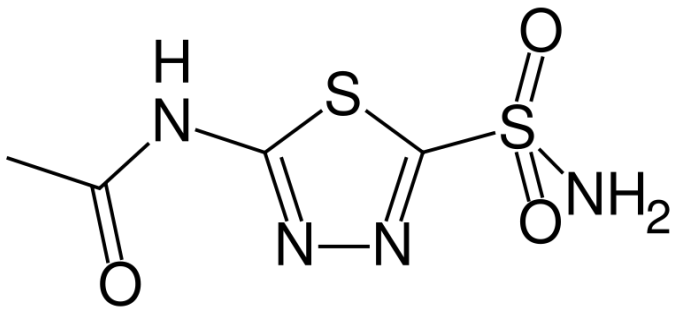

Figure 3.1 The chemical structure of acetazolamide (*N*-(5-sulphamoyl-1,3,4-thiadiazol-2-yl) acetamide) From Ch'En *et al.* (2008).

3.1.3 Anion exchangers

Anion exchangers mediate the 1:1 electroneutral exchange of HCO_3^- and Cl^- across cell membranes, and in animal systems they are central to the following processes:-

1) The efflux of respiratory CO_2
2) Regulation of cell pH
3) Excretion of HCO_3^-
4) Regulation of $[Cl^-]$
5) Regulation of cell volume (Cordat & Casey, 2009).

A multigene family of anion exchangers has been identified in animals, and because of its abundance in erythrocyte membranes, the most characterised member of this family is AE1, a 911 amino acid glycoprotein that was first cloned by Kopito & Lodish (1985). Each member of the HCO_3^-/Cl^- transporter

family possesses two structurally and functionally distinct domains: a 43 kDa amino-terminal cytoplasmic domain (Steck *et al.* 1976), which binds to components of the erythrocyte cytoskeleton, and functions mainly as an anchoring site for various other membrane-associated proteins (Harrison *et al.* 1994; Rybicki *et al*.1993; Rogalski *et al*. 1989), and a 55 kDa carboxyl-terminal domain which spans the cell membrane up to 14 times, and is responsible for HCO_3^- /Cl^- exchange activity (Tanner *et al.* 1988). Analysis of the crystal structure of the cytoplasmic domain has shown that the domain contains 11 b-strands and 10 helical segments (Zhang *et al.* 2000). A topological model for AE1 is shown in Figure 3.2.

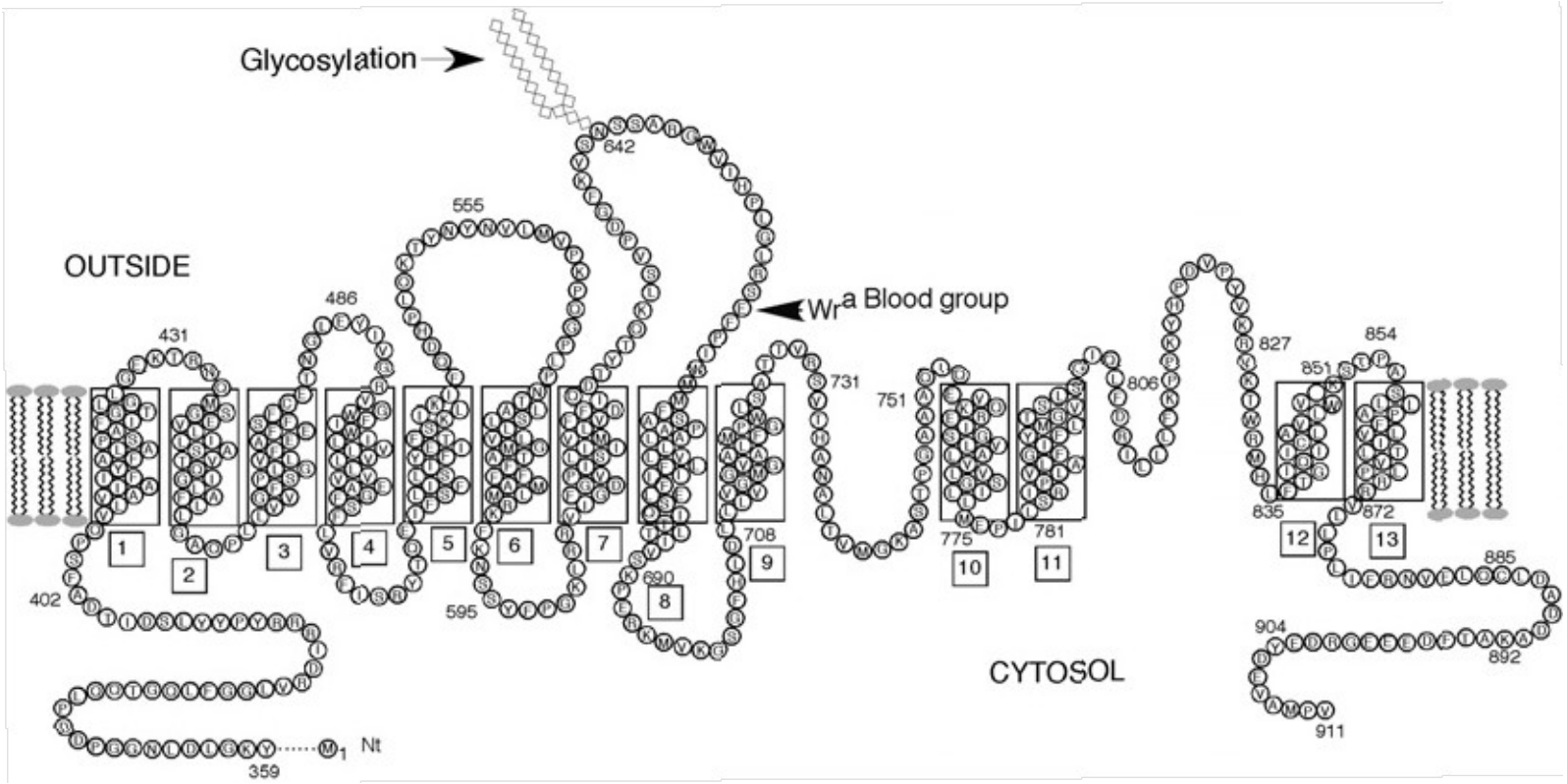

Figure 3.2 Topological model for Human AE1. Numbers indicate the residue number in erythrocyte AE1. The boxed numbers show the transmembrane segment number. This figure is reproduced from Cordat & Casey, (2009), where it was adapted from Zhu *et al*. (2003).

A truncated variant of the AE1 protein, kAE1, is expressed in the basolateral membrane of acid-secreting type-A intercalated cells of the renal collective duct (Kollert-Jons *et al.* 1993), and begins at Met79 of the erythrocyte AE1 sequence (Brosius *et al.* 1989). Screening of cDNA libraries with probes designed from the mouse sequence AE1 has also revealed two more members of the anion exchanger family, AE2 and AE3 (Alper *et al*. 1988; Kudrycki *et al*. 1990). Compared to AE1, their amino-terminal cytoplasmic domains are approximately 70kDa larger and have distinct amino acid sequences, and the third extracellular loop of the transmembrane domain provides the site for N-linked glycosylation (Zolotarev *et al.* 1996). Despite these differences, the transmembrane domain of all members are the AE family share 65% amino acid sequence homology, which suggests that they are functionally similar (Cordat & Casey, 2009; Alper, 1991). Like AE1, the expression of AE3 is restricted to specific tissues, which include the brain, heart, retina and pituitary gland (Kudrycki *et al.* 1990). The expression of AE2, however, is nearly ubiquitous (Alper *et al*. 1988).

None of these anion exchangers require metabolic energy to function, as ion transport is driven by differences in concentration gradients. This operates via a sequential “ping-pong mechanism”, by using a single ion exchange site which is accessible from different sides of the cell membrane. When an anion binds to AE1, it creates a conformational change which causes the binding site to move to the opposite side of the cell membrane, thus transporting the anion across the cell membrane. The bound anion then diffuses away, allowing another anion to bind and be transported in the opposite direction (Jennings,

1989; Frohlich & Gunn, 1986; Passow, 1986).

The specific inhibitor DIDS was first used to identify AE1 activity in erythrocytes by Cabantchik & Rothstein (1974), and since then the development of a stilbene disulphonate family of anion transport inhibitors has led to the extensive study of AE1 structure and function. The chemical structures of two such inhibitors used in the present study, DIDS and SITS, are shown in Figure 3.3.

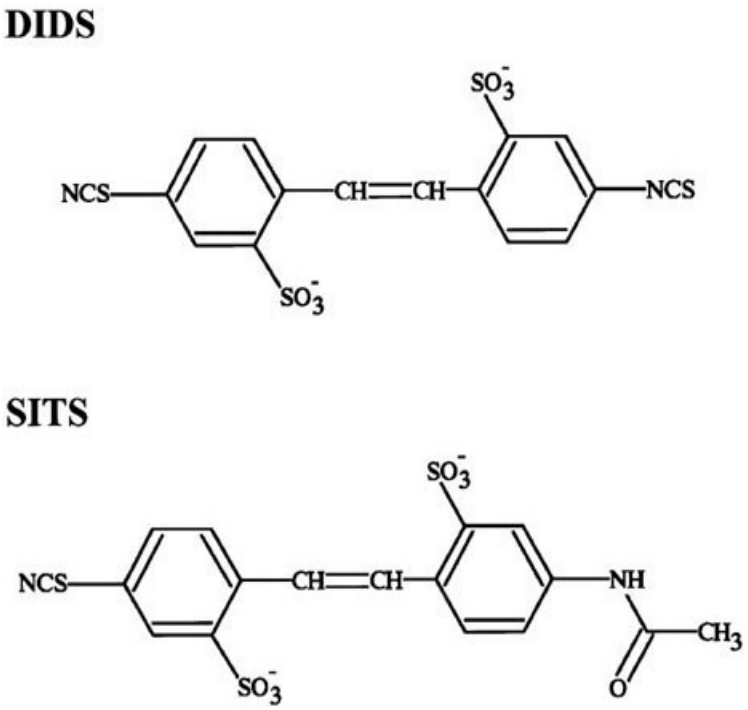

Figure 3.3 The chemical structures of two stilbene disulphonate anion exchange inhibitors, DIDS and SITS. From Fan *et al*. (2001).

It is established that the carboxyl terminal domain of AE1 possesses a binding site for CAII, a CA isoform expressed in erythrocytes, and that the two

mechanisms are physically linked to form a carbon-transport metabolon (Figure 3.4). The functional consequences of this were explored by Sterling *et al*. (2001), who showed that HCO_3^-/Cl^- exchange was reduced by 50-60% in the presence of the CA inhibitor acetazolamide, and when CAII was replaced with an functionally inactive CAII mutant. Moreover, an AE1 mutant that was unable to bind CAII was capable of only 10% of the ion transport activity achieved by the wild-type protein. This indicates that much of the transport activity of AE1 in erythrocytes is dependant on the simultaneous activity of CAII, and their arrangement in a metabolon structure substantially increases the rate of HCO_3^- transport across the cell membrane.

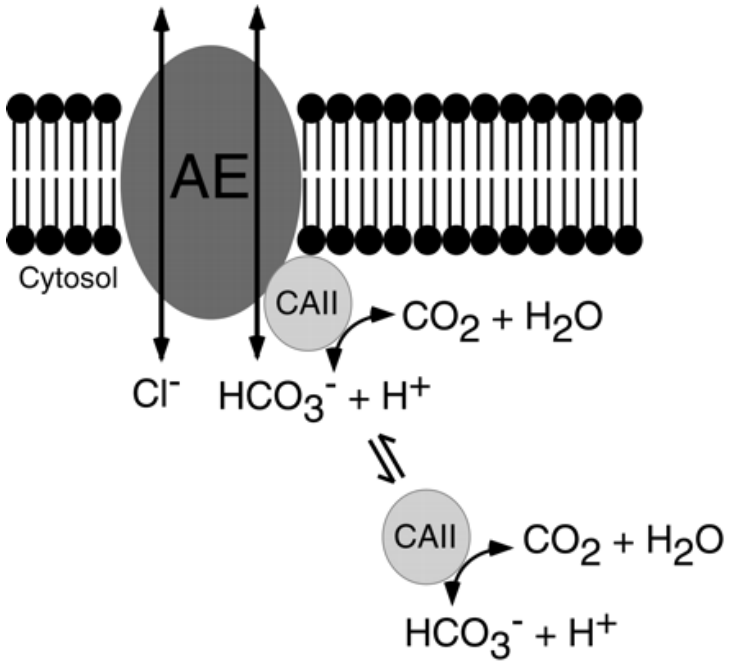

Figure 3.4 A schematic representation of the bicarbonate transporter metabolon thought to exist in human erythrocytes. From Sterling *et al*. (2001). AE = anion exchanger, CAII = carbonic anhydrase II.

3.1.4 Use of CA and AE in algae.

Although much is known about anion exchanger activity in animals, their role in in algae is presently under-investigated. In a recent review of carbon concentrating mechanisms in algae, direct bicarbonate transporters received little attention, whereas the role of CA was discussed at length (Giordano *et al.* 2005), There are a few reports, however, that some macro- and microalgae transport HCO_3^- into their cells using a mechanism similar to AE1 (Perez-Llorens *et al*. 2004; Miao & Wu, 2002; Andria *et al*. 2001; Granbom & Pederson, 1999; Larsson & Axelsson, 1999; Nimer *et al*. 1998; Merrett *et al.* 1996), and earlier work at the algal laboratory at QMUL has identified a bicarbonate transporter as the principal DIC acquisition mechanism in *Emiliania huxleyi*, the Earth's predominant calcifying microalga (Herfort *et al.* 2002). It is possible, therefore, that bicarbonate transporters are more common in algae than is currently thought, and that their importance has been underestimated.

The bicarbonate transporter in *E. huxleyi* was identified by showing that photosynthesis at the ambient DIC concentration was completely suppressed by the AE1 inhibitors SITS and DIDS (Herfort *et al.* 2002). These inhibitors were first used with algae by Smith & Bidwell (1989), to examine DIC uptake in the red macroalga *Chondrus crispus.* Although they found that this seaweed is not sensitive to SITS and DIDS, subsequent studies have shown that these inhibitors reduce the rate of photosynthesis in several species of marine macro- and microalgae (Table 3.1).

Table 3.1 Evidence of bicarbonate transporter activity in marine macroalgae and microalgae. In column 2, the method of detection and the inhibitor used is given. Rhodophytes and Chlorophytes are highlighted in red and green respectively.

Macroalgae	Method of AE detection	External CA activity	Reference	$K_{1/2}$ (mM DIC)
Ceranium diaphanum	O_2, DIDS, SITS	~	This study	
*Chaetomorpha linum**	O_2, DIDS	~	Larsson & Axelsson (1999)	
Chaetomorpha melagonium	O_2, DIDS	~	Larsson & Axelsson (1999)	
Cladophora sp.*	O_2, DIDS	~	Larsson & Axelsson (1999)	0.394*1
Corallina officianalis	O_2, SITS	~	This study	
Cryptopleura ramosa	O_2, DIDS, SITS	~	This study	
*Enteromorpha compressa**	O_2, DIDS	~	Larsson & Axelsson (1999)	0.263
*Enteromorpha flexuosa**	O_2, DIDS	~	Larsson & Axelsson (1999)	
Enteromorpha intestinalis	O_2, DIDS	~	Andria *et al* (2001)	0.2923
Euchema denticulatum	pH drift, DIDS	~	Granbom & Pederson (1999)	
Gracilaria gaditana	O_2, DIDS	~	Andria *et al.* (1999)	0.43*2
Gracilariopsis longissima	O_2, DIDS	~	Perez-Llorens *et al*. 2004	
Monostroma grevillei	O_2, DIDS	~	Larsson & Axelsson (1999)	
Palmaria palmata	O_2, DIDS, SITS		This study	0.63-0.71
Plumaria elegans	O_2, DIDS, SITS	~	This study	
*Spongomorpha arcta**	O_2, DIDS	~	Larsson & Axelsson (1999)	
*Ulva fasciata**	O_2, DIDS	~	Larsson & Axelsson (1999)	
Ulva lactuca	O_2, DIDS	~	Larsson & Axelsson (1999)	0.51*3
*Ulva rigida**	O_2, DIDS	~	Larsson & Axelsson (1999)	0.25

*1 Value for *Cladophora ruprestris*

*2 DIC dose response was measured in the presence of acetazolamide, to isolate AE activity.

*3 AE was induced at pH 9.4, and DIC dose response was measured at this pH.

Microalgae				
Chaetoceros compressus	DIC uptake, DIDS		Nimer *et al*. 1998	
Coccolithus pelagicus	pH drift, DIDS		Miao & Wu, 2002	
Ditylum brightwellii	O_2, DIDS, SITS	~	J. Roberts *pers comm*	
Emiliania huxleyi	O_2, DIDS, SITS		Herfort *et al.* 2002	2.6
Gephryrocapsa oceanica	pH drift, DIDS		Miao & Wu, 2002	
Glenodinium foliaceum	DIC uptake, DIDS		Nimer *et al*. 2000	
Nannochloropsis gaditana	mass spectrometry, DIDS		Nimer *et al*. 1997	
Nannochloropsis oculata	pH drift, DIDS		Merrett *et al.* 1996	
Prorocentrum micans	O_2, DIDS, SITS	~	J. Roberts *pers comm*	
Skeletonema costatum	O_2, DIDS, SITS	~	J. Roberts *pers comm*	
Thalassiosira pseudonana	DIC uptake, DIDS		Nimer *et al*. 1999	

Screening for the presence of bicarbonate transporters in a wide range of macroalgae has so far only been attempted by Larsson & Axelsson (1999). In this study, they examined the effect of the addition of 200μM DIDS and 100μM AZ on the photosynthetic O_2 production rate of 11 green, 5 red and 11 brown species. They found that DIDS-sensitivity was common amongst green algae, but often had to be induced by either increasing the ambient pH to 9.4 or above, by growth in strong light and nutrient-rich seawater, or by measuring photosynthesis in the presence of AZ. No response to DIDS was detected in any of the brown and red species, but AZ inhibited all algae tested, with the exception of *Palmaria palmata.*

Induction of bicarbonate transport activity by increasing the ambient pH of seawater has been described previously in green algae by Larsson *et al.* (1997) and Axelsson *et al*. (1995). They have suggested that this may confer a competitive advantage in green algae growing in rockpools that are isolated from open seawater for long periods of time, since the ambient pH is increased by photosynthesis, and the DIC supply is depleted. It possible, however, that the induction occurs not as a direct response to high pH, but in response to the loss of extracellular CA activity, since the capacity of green algae to acquire HCO_3^- using extracellular CA decreased sharply above pH 9.5.

Studies which have examined a large number of marine algae for extracellular CA activity have found that its use in DIC acquisition is widespread amongst both microalgae (Nimer *et al*. 1997), and macroalgae (Colman *et al*. 2002; Mercado *et al.* 1998; Giordano & Maberly, 1989). CA is also present in every

macroalga that has been shown to possess the bicarbonate transporter (Perez-Llorens *et al*. 2004; Andria *et al* 2001; Granbom & Pederson 1999; Larsson & Axelsson 1999; Beer, 1995). A macroalga which relies exclusively on a bicarbonate transporter mechanism has not yet been identified. It is possible, therefore, that CA and AE1 in macroalgae are associated in a carbon-transporting metabolon in order to increase the rate at which HCO_3^- is transported across their cell membranes, as they are in erythrocytes (Sterling *et al.* 2001). In 9 of the 11 microalgae that have been shown to possess bicarbonate transporters, however, no evidence of external CA activity was found (Miao & Wu, 2002; Nimer *et al*. 1999; Nimer *et al*. 1998; Nimer *et al*. 1997; Merrett *et al.* 1996), which indicates that the bicarbonate transporter may operate independently of any other mechanism. Whereas extraceullar CA has been identified in a large number of marine microalgae (reviewed by Colman *et al*. 2002), these studies may be misleading about the prevalence of the use bicarbonate transporters in microalgae, as once CA activity has been identified, evidence for bicarbonate transporters is not always sought.

DIC acquisition mechanisms are often characterised in terms of their substrate affinity and the maximum rate of their substrate transport. These are defined by the half saturation constant for DIC ($K_{½}$ DIC), and the maximum rate of photosynthesis (V_{max}), which can be obtained from a simple Michaelis-Menten kinetic transformation of the DIC dose response of photosynthesis at saturating light. However, the use of Michaelis-Menten kinetics is analogous to, not homologous with, DIC uptake, because they assume a one substrate, one enzyme reaction, whereas photosynthesis involves a far more complex set of

processes (Fogg & Thake, 1987). Therefore, it is difficult to compare, for example, the affinity of extracellular CA in one species of alga with another. When two mechanisms are present in the same organism, however, a more precise comparison can be made, since they are both functioning as part of the same complex set of processes. For example, in *E. huxleyi* a bicarbonate transporter is used alone at ambient DIC, whereas extracellular CA is active at low DIC, and the presence of these two mechanisms creates biphasic kinetics of photosynthesis with DIC concentration (Herfort *at al*. 2002). In this alga and in *Gracilaria gaditana,* which uses both mechanisms at ambient DIC, the bicarbonate transporter is characterised by high $K_{1/2}$ DIC (ie. low affinity for DIC) and high V_{max} kinetics, whereas extracellular CA is characterised by low $K_{1/2}$ DIC and low V_{max} kinetics (Herfort *et al.* 2002; Andria *et al.* 2001; Andria *et al*. 1999). Conversely, in *Enteromorpha intestinalis* and *Ulva lactuca*, which also use a bicarbonate transporter and extracellular CA, their bicarbonate transporters are high affinity and low V_{max} mechanisms, whereas external CA is defined by low affinity and high V_{max} kinetics (Andria *et al.* 2001; Axelsson *et al*. 1999). These findings indicate that general descriptions of the kinetics of bicarbonate transporters compared to those of CA cannot be made as this evidently varies depending on species. This may be possible, however, once bicarbonate transporters have been identified and examined in a larger number of species.

In this chapter, bicarbonate acquisition mechanisms were defined and characterised in *P. palmata* using both biochemical and molecular techniques (ie. the use of specific inhibitors and PCR), and by examining the kinetics of the

interaction between photosynthetic O_2 production and DIC concentration. For comparison, the kinetics of two extracellular CA-users, *Chondrus crispus* and *Laminaria digitata*, were also examined. Since biphasic kinetics have been found in other macroalgae that use bicarbonate transporters, evidence for this was also sought in *P. palmata*.

3.2 Aims

1. To identify the mechanisms of HCO_3^- uptake in *P. palmata* by using specific inhibitors of extracellular CA and AE1.

2. To use the polymerase chain reaction to determine the presence of an bicarbonate transporter gene in *P. palmata*.

3. To define and compare the kinetics of DIC use in photosynthesis in *P. palmata* and the two CA-users, *Chondrus crispus* and *Laminaria digitata.*

4. To determine if the kinetics of DIC use in photosynthesis in *P. palmata* are biphasic.

3.3 Materials and Methods

3.3.1 Photosynthesis versus irradiance (PI) curves

To determine what irradiance is saturating and subsaturating for photosynthesis in *P. palmata*, PI curves were obtained by measuring oxygen evolution at different photon flux densities (PFD) in buffered simple artificial seawater medium, maintained at 15°C by a thermostatted, refrigerated water bath (Techne, Cambridge, UK). Neutral density filters (Lee Filters, Hampshire, UK) were used to alter the light incident on the thallus surface in the O_2 electrode chamber. There were two experiments: during the first, PI curves were obtained for each sample (a 9 mm disc cut from young, healthy thallus) by measuring photosynthesis in increments from low to high PFDs, and during the second experiment, from high to low PFDs. At each PFD, photosynthesis was measured for about 5 min, followed by a 5 min dark period, followed by the next PFD increment, as described in Chapter 2. For each experiment six replicates were tested, using discs cut from separate thalli.

3.3.2 Primer Design for PCR

Degenerate primer sequences were based on highly conserved regions of the translated amino acid sequences of AE1 genes in various animals. This was achieved by obtaining cDNA nucleotide sequences for the AE1 gene in several animals, from the NCBI database (http://www.ncbi.nlm.nih.gov/), and aligning

the translated amino acid sequences using the GENEDOC program, version 2.6.02, which is available online at http://www.psc.edu/biomed/genedoc/. The species used in this alignment are displayed in table 3.2 with their NCBI-assigned "accession numbers".

Table 3.2 The AE1 sequences from different organisms that were used to identify conserved domains of the AE1 gene. The "accession number" assigned to each sequence on the NCBI data base is shown.

Species	**1. Accession Number**
1. Homo sapiens	M27819
Mus musculus	NM_011403
Gallus gallus	NM_205522
Danio rerio	NM_198338
Raja erinacea	AJ537571
Rattus norvegicus	JO4793
Bos taurus	NM_181036

forward primer, F1 and two reverse primers, R1 and R2, were used in the PCR reactions. The sequences of these are shown in Table 3.3.

Table 3.3 Primer sequences designed from the amino acid and nucleic acid alignments of AE1 genes in different organisms, and the corresponding non-degenerate nucleic acid sequences in *Rattus norvegicus*.

Primer Name	Primer Sequence
F1 (degenerate sequence)	GCNRTNATHTTYATHTAYTTYGC
F1 (non-degenerate rat sequence)	GCTGTCATCTTCATCTACTTTGC
R1 (degenerate sequence)	ATNAGCCARAANCCDATCCA
R1 (non-degenerate rat sequence)	ATAAGCGAGAAGCCGATCCA
R2 (degenerate sequence)	GGGCNGANGCRAACATCATCCA
R2 (non-degenerate rat sequence)	GGGCNGANGCRAACATCATCCA

Detailed descriptions of the PCR reactions, and subsequent amplification and cloning of the PCR products, are given in Chapter 2. Genomic DNA from *Rattus norvegicus* was used as a positive control, and as a negative control, PCR reactions were carried out with no added genomic DNA .

3.3.3 Curve-fitting

Biphasic (or "bivariate) data were analysed using Mathematica 5.0 (2003) (Wolfram Research Inc., Illinois, USA). The Henley equation (Henley, 1993) was used to determine the slope of α, and V_{max} for the first and second parts of the curve.

Inhibitor experiments were carried out as described in Chapter 2.

3.4 Results

Net photosynthesis (NPS) in *P. palmata* as a function of irradiance is shown in Figure 3.5. NPS measured in a high-low PFD direction was saturated by light at about 400 μmol m^{-2} s^{-1}, whereas NPS measured in a low-high PFD direction was saturated at about 150 μmol m^{-2} s^{-1}. The significance of the effect of PFD on NPS, and of the direction of change in PFD, was tested using 2-way ANOVA, the results of which are shown in Table 3.4. The effect of irradiance on NPS is highly significant (p=<0.05), whereas there is no significant difference in NPS measured from high-low PFDs compared to low-high PFDs (p=>0.05). Also no significant interaction between the two variables was shown (p>0.05).

Table 3.4 2-way ANOVA statistical test for the effect of the direction of changing irradiance from high to low PFDs and low to high PFDs.

Source of Variation	*SS*	*df*	*MS*	*F*	*P-value*	*F crit*
Light	983411.9	9	109268	14.21797	<0.05	1.974829
Direction	13242.87	1	13242.87	1.723165	0.192291	3.936143
Interaction	133637.9	9	14848.66	1.93211	0.055697	1.974829
Within	768520.5	100	7685.205			
Total	1898813	119				

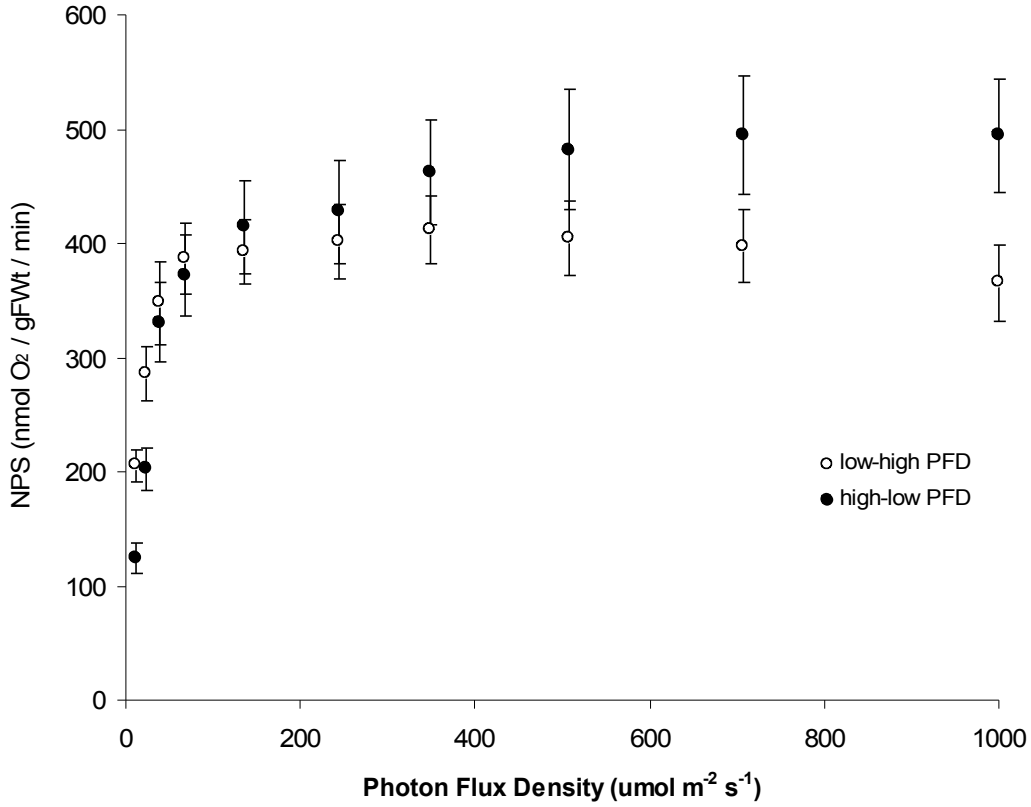

Figure 3.5 NPS in *P. palmata* as a function of irradiance. NPS was measured in individual samples whilst altering the irradiance in increments from either high-low PFDs, or low-high PFDs. Data points are means of +/- SE. *n*=6

To examine the effects of SITS on photosynthesis and to test for an interaction between SITS and DIC, NPS was measured in *P. palmata* at different DIC concentrations, with and without the addition of 1 mM SITS. These measurements are shown in Figure 3.6A, and shows that SITS inhibits photosynthesis between 0.25 mM and 3 mM DIC, whereas no inhibition is evident at 6 mM DIC. In Figure 3.6B these data are presented as double-reciprocal plots to highlight the differences in kinetic parameters, and indicate the inhibition was competitive since the apparent $K_{1/2}$ was increased by SITS from 1.4 to 2.75 mM DIC while the V_{max} remained similar with and without SITS, at 2500 and 2000 nmol O_2 / gFWt / min respectively.

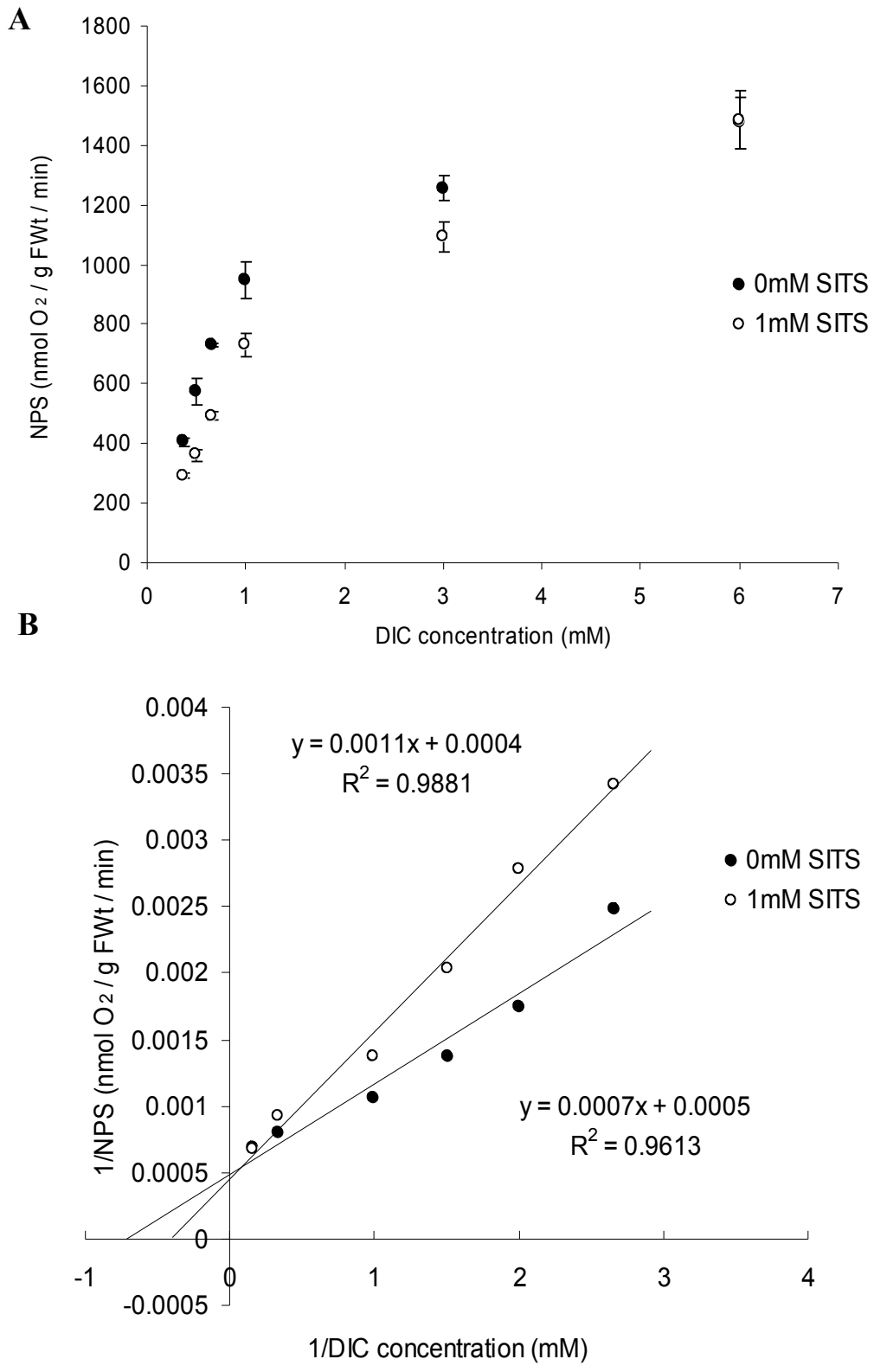

Figure 3.6 (A) NPS in *P. palmata* as a function of DIC concentration, with and without the addition of 1 mM SITS. (B) A double reciprocal plot of the data shown in (A). Data points are means of +/- SE (*n*=4).

The significance was tested with 2-way ANOVA, shown in Table 3.5, and demonstrated that DIC and SITS significantly affected NPS (p=<0.05). A significant interaction between DIC and SITS, which is characteristic of the competitive nature of SITS inhibition (p=<0.05), is also shown.

Table 3.5 2-way ANOVA for the effect of DIC and SITS inhibition of NPS in *P. palmata.*

Source of Variation	*SS*	*df*	*MS*	*F*	*P-value*	*F crit*
DIC	1462.81	7	208.97	188.1	<0.05	2.21
SITS	50.64	1	50.64	45.58	<0.05	4.04
Interaction	18.02	7	2.57	2.32	0.040	2.21
Within	53.33	48	1.11			
Total	1584.8	63				

Figure 3.7 shows dose response curves for DIDS (A) and SITS (B) of NPS in *P. palmata* photosynthesising at 2 mM DIC. The addition of 2 mM DIDS inhibited oxygen evolution rates by 90%, whereas the same concentration of SITS inhibited by 20%. Complete inhibition of NPS occurred when 8 mM SITS was added.

At an 8 mM concentration, SITS produced a yellow colour in solution, and because DIDS was dissolved in DMSO, this was also evident when 2 mM DIDS was used. To determine if this discolouration contributed to the reduction in NPS following the addition of inhibitors, the irradiance was increased by moving the projector lamps close to the electrode chambers, but no increase in NPS was measured.

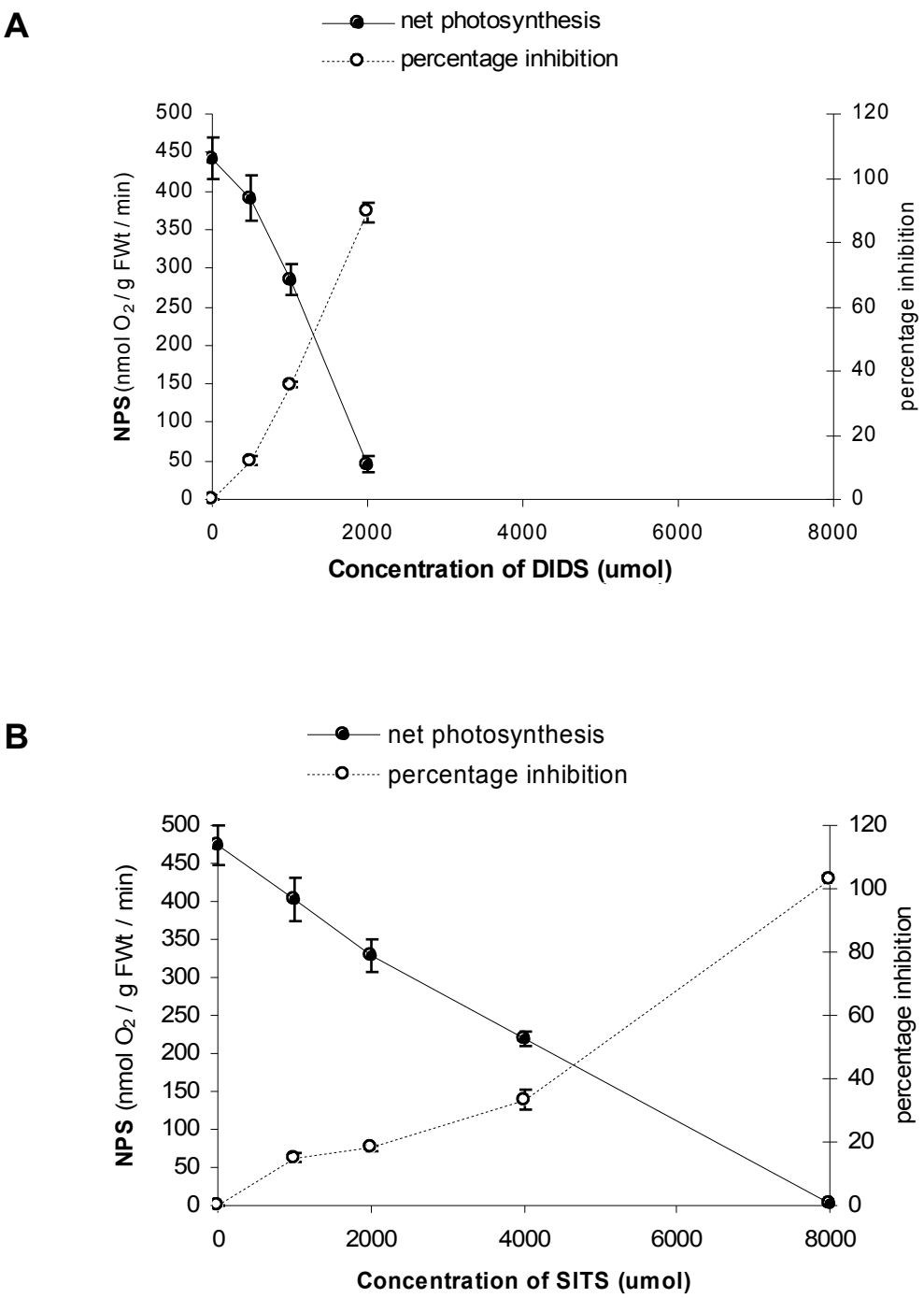

Figure 3.7 The dose response curves of the AE1 inhibitors DIDS (A), and SITS (B), on NPS in *P. palmata* photosynthesising at 2 mM DIC. Data points are means +/-SE (*n*=5).

Use of degenerate DNA primers with the polymerase chain reaction was successfully employed to identify gene sequences encoding functional regions of HCO_3^-/Cl^- transporter proteins. During PCR reactions, the F1 and R1 primers described in 3.3.2 amplified DNA of approximately 1500 base pairs in length from genomic DNA extracted from *P. palmata*, *E.huxleyi,* and *Rattus norvegicus* (the positive control), whereas the negative control, which contained the primers and all of the components of the PCR mixture, but no genomic DNA, did not contain an amplified DNA product.

Since the genetic code is degenerate, ie. different codons sequences can be translated as the same amino acids, amino acid rather than nucleotide sequence homology was analysed to identify the functional similarities between the three amplified sequences. The *R. norvegicus* sequence is identical to the rat AE1 sequence published on the NCBI database, indicating that a region of AE1 had been amplified in the positive control. This sequence corresponds to exonic regions of the highly conserved carboxyl-terminal domain of the protein, and therefore confers its function as a HCO_3^-/Cl^- transporter.

There is clear similarity between the amplified *R. norvegicus* sequence and the *E. huxleyi* and *P. palmata* sequences, which correspond to amino acid homologies of 94% and 80% respectively. The algal sequences were found to be unique, therefore it is likely that regions of bicarbonate transporter genes had been sequenced from these organisms.

The aligned amino acid sequences are shown in Figure 3.8.

A

```
                 420       430       440       450       460       470
Rat              TDALSPQVLAAVIFIYFAALSPAVTFGGLLGEKTRNLMGVSELLISTAVQGILFALLGAQ
                                           |||||| ||||||||||||||||||||||||
P.palmata        QTPASAXPXLALWAPGNDLLTLIPLXPLPTGEKTRNQMGVSELLISTAVQGILFALLGAQ
                      170       200       230       260       290       320

                    480       490       500       510       520       530
Rat              PLLVLGFSGPLLVFEEAFYSFCESNNLEYIVGRAWIGFWLILLVVLVVAFEGSFLVQYIS
                 ||||:|||||||||||||:|
P.palmata        PLLVVGFSGPLLVFEEAFFSVVLSLPHXPCHVPRTTCLMHGALPQGPLTDRLLLTTLQFC
                      350       380       410       440       470       500
```

B

```
                     420       430       440       450       460       470
Rat              ITDALSPQVLAAVIFIYFAALSPAVTFGGLLGEKTRNLMGVSELLISTAVQGILFALLGA
                                           |||||::|:|||||::|||:||::| ||||
E. huxleyi       GAAGXGEPSGRGRRGLPRAWPPAPELVPTPLGEKTQDLIGVSELIMSTALQGVVFCLLGA
                     390       360       330       300       270       240

                     480       490       500       510       520       530
Rat              QPLLVLGFSGPLLVFEEAFYSFCESNNLEYIVGRAWIGFWLILLVVLVVAFEGSFLVQYI
                 |||||:|||||||||||||:|
E. huxleyi       QPLLVIGFSGPLLVFEEAFFSVRALLAHLQPPLPCPRHLPTASPPRAQDLTAPPSSSVAA
                     210       180       150       120        90        60
```

Figure 3.8 Translated amino acid sequences for the amplified *R. norvegicus* AE1 gene fragment aligned against (A) the amplified *P. palmata* gene fragment, and (B) the amplified *E. huxleyi* fragment. Amino acids connected by vertical lines are identical, amino acids connected by dots are non-identical but functionally very similar. Dissimilar amino acids are not connected.

To examine and compare the kinetics of DIC in photosynthesis in *P. palmata* and two extracellular CA-users, *C. crispus* and *L. digitata,* it was first established with the use of inhibitors that these mechanisms were being used. Figure 3.9 shows the effect of 500 μM of the AE1 inhibitor DIDS, and 100 μM of the extracellular CA inhibitor AZ, on photosynthesis in these three macroalgae. Only in *P. palmata* was photosynthesis significantly inhibited by DIDS (t-tests: *P. palmata* + DIDS, p = <0.05, *C. crispus* + DIDS, p = 0.46; *L. digitata* + DIDS, p = 0.45), but no significant change in rate was measured in *P. palmata* after the addition of AZ (t-test p=0.81). Conversely, net photosynthesis was significantly inhibited by AZ in *C. crispus* (t-test p = <0.05) and *L. digitata* (t-test p = <0,05).

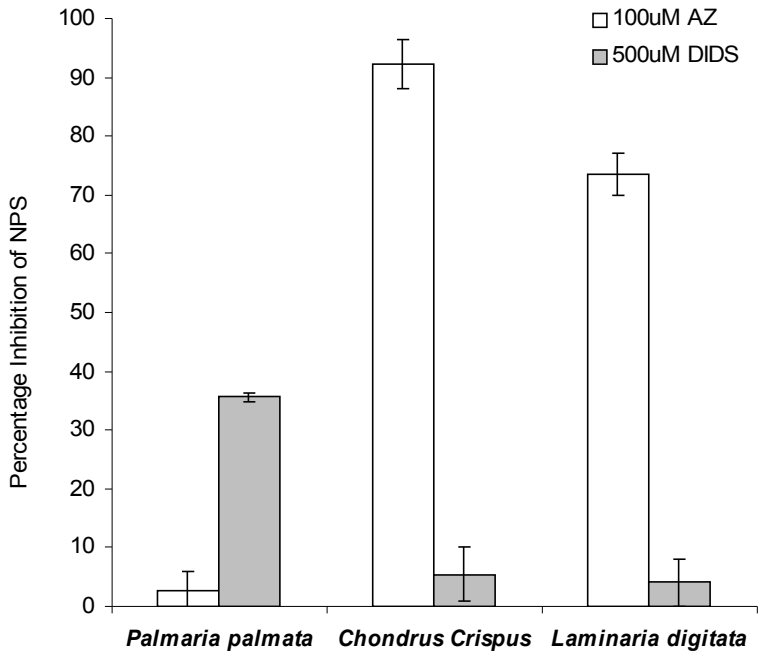

Figure 3.9 The effect of 100 uM AZ, and 500 μM DIDS, on rates of net photosynthesis in *Palmaria palmata*, *Chondrus crispus*, and *Laminaria digitata.* Data points are means +/- SE (n=4).

The photosynthetic responses of these macroalgae to DIC concentration is shown in Figure 3.10. In all species, photosynthesis was unsaturated at the ambient DIC concentration in seawater. Rates of photosynthesis at 2 mM DIC were greatest in *P. palmata,* followed by *L. digitata* and *C. crispus* respectively.

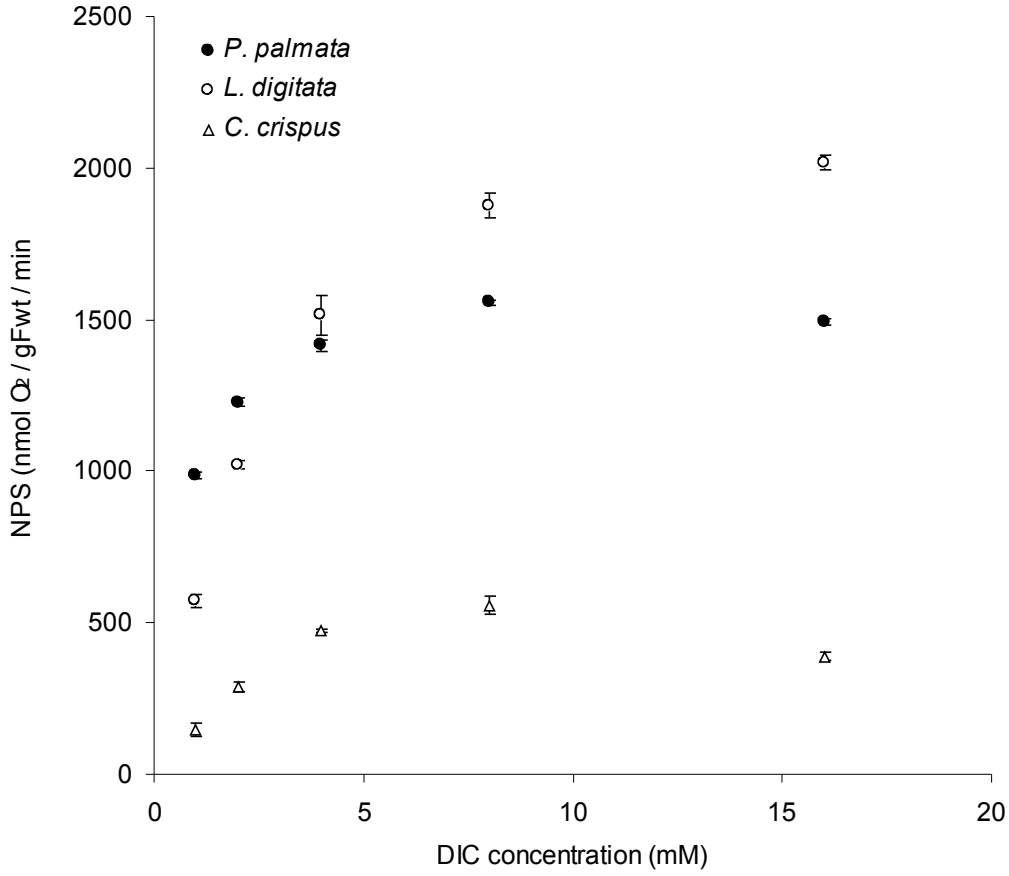

Figure 3.10 The effect of external DIC concentration on net photosynthesis (NPS) in *P. palmata*, *C. crispus*, and *L. digitata*. Data points are means +/- SE (*n*=6).

The $K_{1/2}$ and V_{max} of the kinetics of DIC use in photosynthesis in these species were determined using Michaelis-Menton kinetics (Michaelis & Menton, 1913) which were originally designed to analyse interactions between substrate concentration and enzyme activity. These were plotted using graphical methods for analysis of the Michaelis-Menton equation as proposed by Lineweaver & Burke (1934), Hofstee (1959), and Hanes (1932), and are shown in Table 3.6.

Table 3.6 Values of $K_{1/2}$ DIC, and V_{max} of net photosynthesis, for three macroalgae. Values were obtained using three linear plots of the data displayed in Fig 3.10

Species	Mechanism	Kinetic plot	r^2	$K_{1/2}$ DIC[*1]	V_{max}*[2]
Palmaria palmata	HCO_3^- transporter	Lineweaver-Burke	0.985	0.64	917
		Hanes-Woolf	0.998	0.42	875
		Eadie-Hofstee	0.96	0.63	914
Chondrus crispus	external CA	Lineweaver-Burke	0.987	7.72	320
		Hanes-Woolf	0.951	4.4	219
		Eadie-Hofstee	0.774	4.54	224
Laminaria digitata	external CA	Lineweaver-Burke	0.992	3.81	896
		Hanes-Woolf	0.005	2.67	13
		Eadie-Hofstee	0.942	3.15	815

[*1] $K_{1/2}$DIC = mM dissolved inorganic carbon.
[*2] V_{max} = maximum rate of NPS (nmol O_2 /g FWt /min).

According to the $K_{1/2}$ values, *P. palmata* possessed both the highest DIC affinity, and the lowest V_{max}, whereas *C. crispus* possessed the lowest DIC affinity and the highest V_{max}. In *C. crispus* and *L. digitata*, substantial variations in the values of both parameters were found when different methods were used to obtain them. In particular, the Hanes-Woolf plot gave a very low V_{max} value in *L. digitata*.

The photosynthetic response of *P. palmata* to small increments of DIC addition was measured between 0.125mM and 2mM DIC and is shown in Figure 3.11.

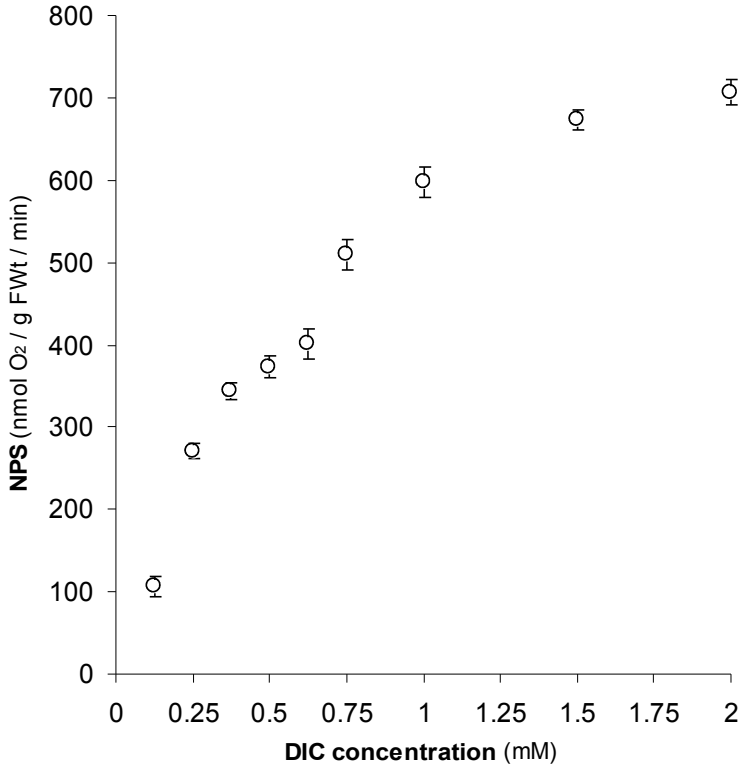

Figure 3.11 The effect of different DIC concentrations on NPS in *P. palmata*. Data points are means +/- SE (*n*=6).

The kinetics do not appear to follow a simple hyperbolic pattern, but appear to be biphasic, with a hiatus at 0.625 mM DIC. Analysis of this pattern according to the Henley equation (Henley, 1993) was carried out using the Mathematica 5.0 program and revealed that the initial slopes of α for the first and second kinetics were 1478.9 and 1262.6 respectively, wherease the V_{max} values of the first and second kinetics were 758.011 nmol O_2 / g FWt / min and 1020.58 nmol O_2 / g FWt / min respectively. Thus, in *P. palmata,* photosynthetic oxygen evolution shows high affinity, low V_{max} kinetics below 0.625 mM DIC, and low affinity, high V_{max} kinetics above 0.625 mM DIC.

3.5 Discussion

Experiments with the AE1 inhibitors SITS and DIDS indicate that at the ambient DIC concentration in seawater, photosynthesis in *P. palmata* is supported by a bicarbonate transporter mechanism. Since AZ did not significantly change the photosynthetic rate, it appears that this alga lacks extracellular CA. It is possible that other DIC uptake mechanisms are active that were not identified by this study, yet since net photosynthesis can be completely inhibited with SITS and DIDS, this suggests that the bicarbonate transporter is used alone. Although there are reports that some microalgae use a bicarbonate transporter as their sole DIC uptake mechanism (Herfort *et al*. 2002; Miao & Wu, 2002; Nimer *et al*. 1999; Nimer *et al*. 1998; Nimer *et al*. 1997; Merrett *et al.* 1996), this is the first report of this in a macroalga.

The concentrations of DIDS and SITS required to completely suppress photosynthesis in *P. palmata* were substantially higher than the concentrations used in previous studies to inhibit macro- and microalgae (Perez-Llorens *et al*. 2004; Herfort *et al*. 2002; Miao & Wu, 2002; Andria *et al.* 2001; Larsson & Axelsson 1999; Nimer *et al*. 1998; Nimer *et al*. 1997; Merrett *et al.* 1996). In green macroalgae, for example, bicarbonate transport is completely inhibited by only 200μM DIDS (Larsson & Axelsson. 1999; Larsson *et al*. 1997; Axelsson *et al*. 1995). The apparent insensitivity of *P. palmata* to SITS and DIDS may be caused by carrageenans in the thallus restricting the diffusion of these inhibitors to the cell surface, or the inhibitors may become adsorbed on the thallus surface. In experiments carried out at QMUL by Dong (1993), photosynthesis

in thalli of *P. palmata* that had been cut into 1 mm diameter discs before being placed in the oxygen electrode chamber, was completely inhibited by only 1mM SITS and 500μM DIDS. Since using small discs of thalli rather than one large disc would have increased the total surface area of the thallus that is exposed to the external medium, this may have introduced more cell surfaces to the inhibitors, thus increased the extent to which they bound to the bicarbonate transporters. Alternatively, there may be a molecular basis for this insensitivity, as it has been shown that creating minor changes in the amino acid sequence of AE1 in animal systems can substantially affect the affinity with which stilbene inhibitors bind (Salhany *et al*. 2003, 1996; Chernova *et al*. 1997, Bruce *et al*. 1993). Similarly, small differences that may naturally occur in the amino acid sequence of the *P. palmata* transporter could reduce the affinities with which SITS and DIDS bind, so that unusually higher concentrations are required. Therefore, Larsson & Axelsson (1999) were unable to detect bicarbonate transporter activity in *P. palmata* because the concentration of DIDS they used (200μM) was not sufficient to cause a significant reduction in photosynthesis. It is possible therefore, that bicarbonate transporters may prove detectable in a far wider range of marine plants if they are also screened with these inhibitor concentrations.

The concentration of SITS required to inhibit photosynthesis in *P. palmata* was four times greater than the required concentration of DIDS. This, however, is not unusual. DIDS is a more potent inhibitor of AE1 in animal systems, which is caused by chemical differences in the inhibitors that influence the stability with which they bind to AE1: both SITS and DIDS contain isothiocyano groups

that react covalently with lysine residues in the amino acid sequence of AE1, and in doing so prevent bicarbonate transport. But since DIDS contains two of these groups and SITS contains only one, DIDS forms a chemically more stable complex when it binds to AE1 (Cabantchik & Greger, 1992).

Because of its high concentration in seawater compared to the atmosphere, inorganic carbon is seldom regarded as an important limiting factor of algal photosynthesis and growth. Only rather recently have the photosynthetic responses of algae been explored at above ambient concentrations. When Mercado *et al*. (1998) and Holbrook *et al*. (1988) examined photosynthesis in numerous marine macroalgae at over-ambient DIC concentrations, they found that many are limited by DIC, in the sense that when more DIC was added , photosynthesis proceeds at a faster rate.

By measuring photosynthesis in *P. palmata* at a range of DIC concentrations, it was shown that the rate is unsaturated at the ambient concentration in seawater. This is in agreement with previous studies of DIC uptake in this species (Kubler & Raven, 1995; Johnston *et al*. 1992; Dong *et al*. 1991; Colman & Cook, 1985). The photosynthetic rate of *P. palmata* at the ambient DIC concentration is about 80% of its maximum DIC-saturated rate, indicating that its DIC uptake mechanism functions at close the its maximum rate in natural seawater, whereas extracellular CA in *C. crispus* and *L .digitata* functioned at about 50% of their maximum rates. This suggests that the bicarbonate transporter mechanism in *P. palmata* operates more efficiently compared to extracellular CA in the two other species, and thus *P. palmata* is less likely to be

limited by DIC in its natural environment.

According to the kinetics of photosynthesis as a function of DIC concentration in these species, *P. palmata* has the lowest $K_{1/2}$ for DIC compared to *C. crispus* and *L. digitata*, and V_{max} values that are slightly higher than *L. digitata* and over three time greater than those obtained for *C. crispus*. When different linear regression methods were used to analyse these data, however, there were substantial variations in the values obtained for $K_{1/2}$ DIC and, in *L. digitata*, for V_{max}. It is likely that these variations were caused by inaccuracies associated with using the different kinetic plots. With Lineweaver-Burk, since the *y*-axis represents the reciprocal of the rate of reaction, this means that small errors in measurements of low reaction rates can have a disproportionate effect on the linear slope. With Eadie-Hofstee and Hanes-Woolf plots, values for DIC concentration and NPS are dependant on the precision of NPS and DIC measurements respectively. Thus, experimental errors in these variables will be present in both axes. Although this questions the suitability of using such transformations to determine the kinetics of DIC use in photosynthesis, they are still useful in measuring changes in paramaters resulting from the action of an inhibitor. In this study, for example, the competitive nature of SITS inhibition was determined from a Lineweaver-Burk plot of NPS at different DIC concentrations, which showed that addition of the inhibitor increase $K_{1/2}$ but did not change V_{max}..

Since bicarbonate transporters have not yet been examined in many other macroalgae, it is difficult to determine if they are generally more efficient at

transporting DIC into cells compared to extracellular CA. Previous studies suggest that the kinetic parameters of DIC uptake in algae that use extracellular CA are somewhat variable, with $K_{½}$ ranging from 0.35 to 4.31 mM DIC, and V_{max} ranging between 29.2 and 688 µmol O_2 / g FWt / h (Zou *et al.* 2004; Israel & Hophey, 2002; Mercado *et al*. 2001; Axelsson *et a*l. 1999; Israel *et al*. 1999, Mercado & Neill 1999; Mercado *et al*. 1998; Smith & Bidwell 1987). The kinetic parameters in macroalgae that use bicarbonate transporters, however, are less variable, with $K_{1/2}$ between 0.25 and 0.71 mM DIC, and values for V_{max} between 85.7 and 160 µmol O_2 / g FWt / h (Andria *et al*. 2001, Mercado *et al*. 1998, Axelsson *et al.* 1995). This preliminary evidence suggests that algae that use bicarbonate transporters are more similar than CA-users in terms of their efficiency and capacity for DIC uptake. Perhaps, like AE1 in animal systems (Cordat & Casey, 2009; Sterling & Casey, 2002), the transport regions of bicarbonate transporter proteins in algae are phylogenetically highly conserved, whereas CAs are more variable.

It is established that external CAs differ considerably in terms of their catalytic activity and molecular structure (Lindskog, 1997). Mercado & Neill, (1999) have found evidence that different CA isoforms are present in the red macroalga *Porphyra leucostica*, and CAs isolated from microalgae show significant differences in molecular structure (Moroney *et al*. 2001). A CA gene cloned from the red microalga *Porphyridium purpureum*, for example, has shown substantial differences in amino acid sequence compared with CA genes cloned from other algae and higher plants (Mitsuhashi *et al*. 2000; Mitsuhashi & Miyachi, 1996). It is likely, therefore, that like the numerous isoforms of CA

isolated in animals, differences in the molecular structures of CAs expressed in algae determine substantial differences in their catalytic activity.

Bicarbonate transporter genes have been cloned from numerous animals, but no plant or algal sequences have yet been found. The only molecular evidence for bicarbonate transporters in algae has been provided by Sharkia *et al.* (1994), who used Western blotting to show that monoclonal and polyclonal antibodies raised against human AE1 are able to conjugate with a 95 kDa protein extracted from the cell membrane of *Ulva* sp. Because this protein is a similar size to AE1 in animals, the authors suggested that they had identified a an analogous algal bicarbonate transporter. Antibodies do not necessarily provide strong evidence for the presence of specific proteins, however, as they are often able to conjugate to regions of other proteins that possess regions which are homologous to the target protein, but functionally they may be very different (Dunbar, 1994).

In the present study, partial DNA sequences of three bicarbonate transporter genes were successfully cloned and amplified from genomic DNA extracted from the kidney of a rat *(R. norvegicus)*, and whole cells of *P. palmata* and *E. huxleyi*. The cloned rat sequence is identical to a previously published AE1 sequence cloned from this species (Kudrycki & Shull 1989), and sequence alignments of the *E. huxleyi* and *P. palmata* amino acid sequences demonstrated that they were highly homologous, by 93 % and 80 % respectively, within a 51 amino acid overlap corresponding to exonic regions of the rat AE1 gene. These are shown in Figure 3.12.

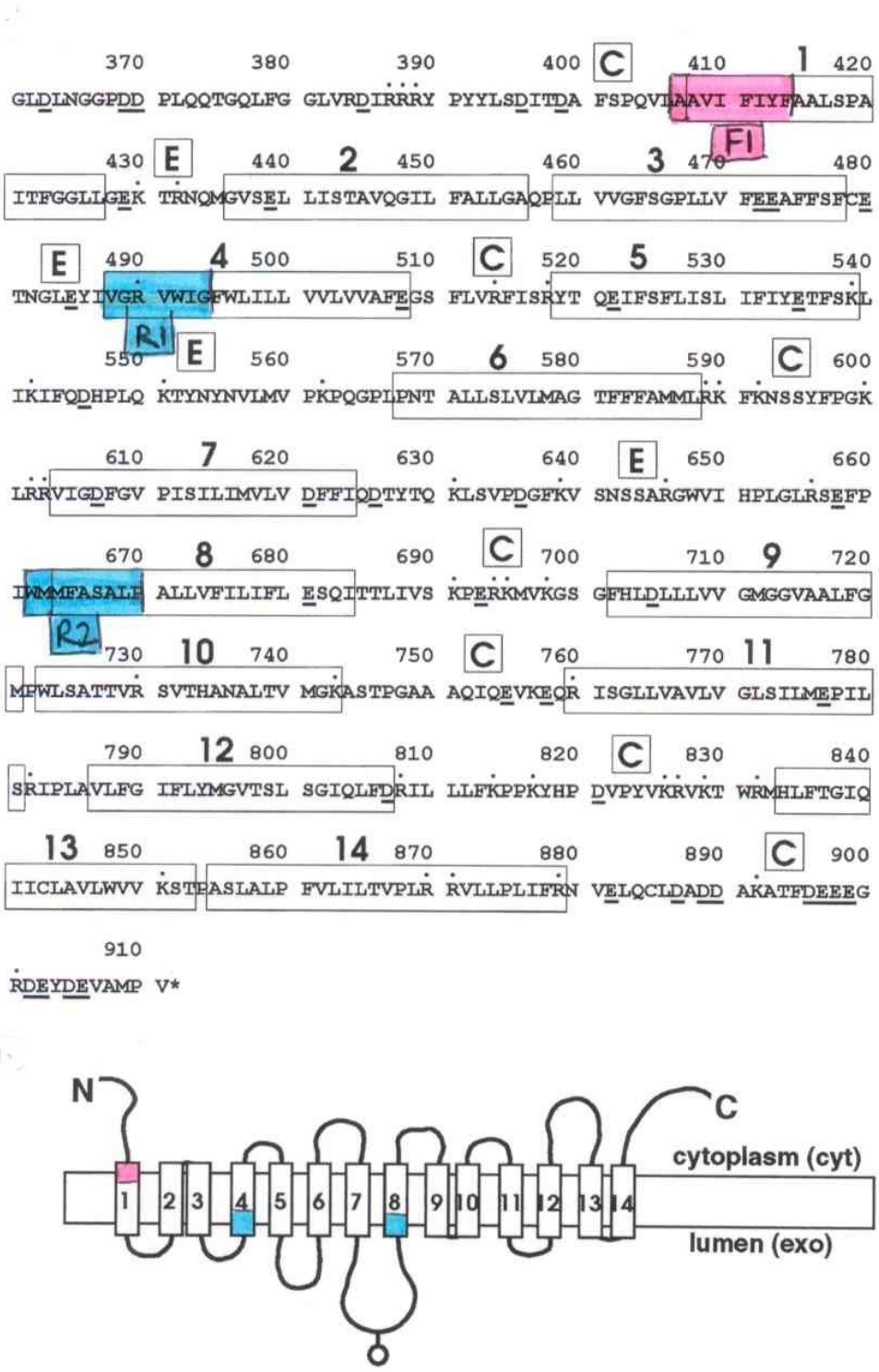

Figure 3.12 Part of the human AE1 amino acid sequence, showing the location of the degenerate primers F1, R1 and R2. The transmembrane domains are shown in boxes, and the cytoplasmic and extracellular domains are labelled “C” and “E” respectively.

The rat amino acid sequence contains pairs of lysine residues at positions 458, 472, 478 and 486, which are thought to be involved in HCO_3- binding in human AE1 (Jennings, 1995). These residues are also present in the algal sequences (with one exception in *E. huxleyi,* which has isoleucine instead of the lysine 459 found in the rat sequence), which indicates that they are functionally similar. It is evident, therefore, that the AE1 gene, or genes that encode proteins similar to AE1, were cloned from *E. huxleyi* and *P. palmata*.

Identification of these gene sequences does not reveal anything about where the bicarbonate transporter protein is used in the cell after it has been translated, however. Experiments with SITS and DIDS demonstrate that it is present in the cell membrane, but like CA, it could also be present in the chloroplast. Now the amino acid sequences are known, however, it will now be possible to design specific antibodies which can be labelled with fluorescent markers, and used to identify bicarbonate transporters in algal cells.

Previous work in the Algal Laboratory at QMUL has shown that photosynthesis and calcification measured in *E. huxleyi* at small increments of DIC addition showed biphasic kinetics, with a hiatus located at 1mM DIC. Similarly, Sekino *et al.* (1996) found evidence for biphasic kinetics of photosynthesis with DIC concentration in a South Pacific strain of *E.huxleyi.* Since Herfort et al. (2002) found that AZ inhibited photosynthesis in cells grown at 0.5mM DIC, they concluded that the biphasic kinetics were created by the presence of two mechanisms: extracellular CA, which is induced or activated at low DIC concentrations, and is characterised by high affinity / low V_{max} kinetics, and a

bicarbonate transporter, which is active at all DIC concentrations and is characterised by low affinity / high V_{max} kinetics.

In the present study. when photosynthesis in *P. palmata* was measured at small increments of DIC addition, a biphasic pattern was also produced, with a hiatus located at 0.625mM DIC. Since no extracellular CA activity is present at the ambient DIC concentration, as shown by the inhibitor experiments in the present study and in previous studies (Larsson & Axelsson, 1999, Giordano & Maberly, 1989), this suggests that, like *E. huxleyi*, a second DIC-uptake mechanism is activated at low DIC, and is characterised by low affinity / high V_{max} kinetics. As it is well-known that extracellular CA is induced in numerous algae at low DIC concentrations (Matsudo & Colman, 1996; Sasaki *et al*. 1997; Kaplan *et al*. 1998; Giordano *et al*. 2005), and has been shown to be almost ubiquitous in macroalgae (Colman *et al*. 2002; Mercado *et al.* 1998; Giordano & Maberly, 1989), therefore it is probable that this mechanism created the low DIC kinetics in *P. palmata,* and is examined in Chapter 4.

Chapter 4

Regulation of DIC acquisition mechanisms in *Palmaria palmata*

4.1 Introduction

Ribulose-1,5-bisphosphate (RuBisCO) is the principal enzyme of carbon fixation which forms more than 16% of the total protein content of chloroplasts, and is thought to be the most abundant protein in the biosphere. It consists of sixteen subunits, which include eight large "L" subunits of ~55 kDa, and eight small "S" subunits of ~13 kDa. The large subunits each contain a regulatory site and a catalytic site, and the small subunits serve to enhance the catalytic activity of the large subunits (Stryer *et al*. 1995).

Rubisco catalyses the CO_2 fixation stage of the Calvin cycle, where two molecules of 3-phosphoglycerate are formed from CO_2 and the five-carbon sugar, ribulose 1,5-*bis*phosphate. The catalytic activity of the enzyme is induced by the binding of a CO_2 molecule to an uncharged ε-amino group in the active site, to form a carbamate ion. This then binds to a positively-charged metal ion, either Mg^{2+} or Mn^{2+}, to form a positively-charged centre which acts as an electron acceptor during catalysis. The role of CO_2 at this stage is not as a substrate, but as an activator. The first step of catalysis is the formation of a six-carbon enediol intermediate from a molecule of ribulose 1,5-bisphosphate, which reacts with CO_2 to form a six-carbon intermediate, 2'-carboxy-3-keto-D-arabinitol. Subsequently this is hydrated to form an unstable gem diol intermediate. The C-2-C-3 bond of the intermediate is cleaved to yield a carbanion ion and one molecule of 3-phosphoglycerate. Finally, the protonation of the carbanion ion creates a second molecule of 3-phosphoglycerate. These reactions are described schematically in Figure 4.1.

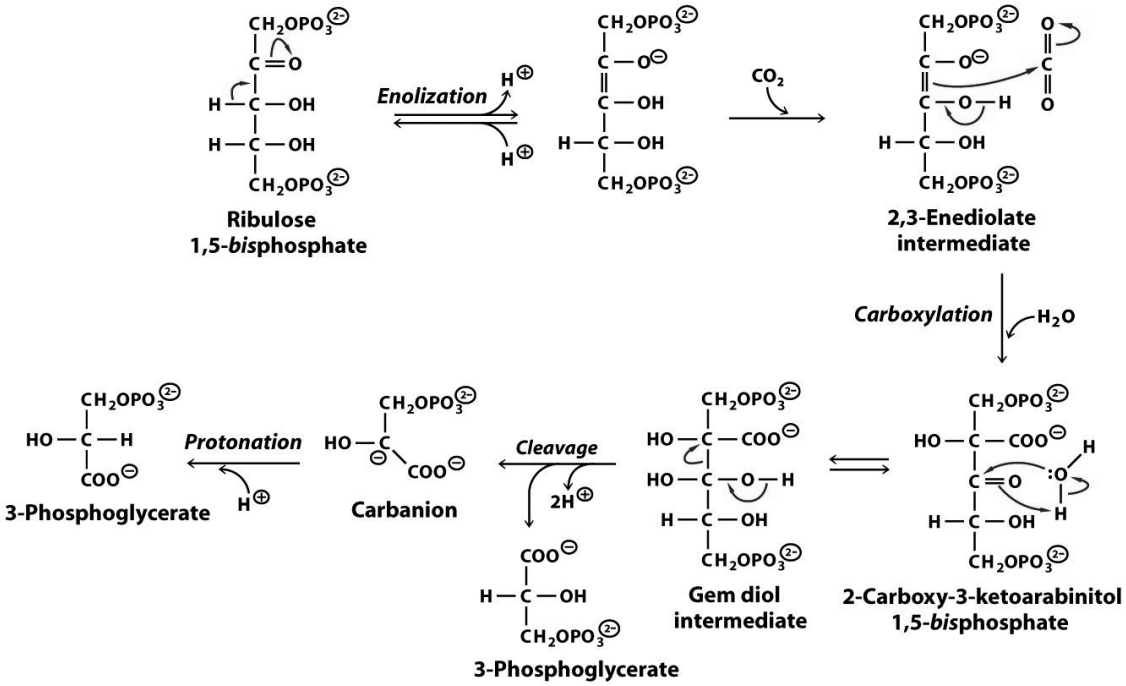

Figure 4.1 The carbon-fixation reaction catalysed by Rubisco.

The molecules of 3-phosphoglycerate produced by the carboxylase reaction are subsequently reduced in the Calvin cycle to form glyceraldehyde-3-phosphate, which is used in the synthesis of numerous essential compounds.

During the oxygenase reaction of Rubisco, the addition of O_2 instead of CO_2 to ribulose 1,5-bisphosphate produces only one molecule of 3-phosphoglycerate and a molecule of phosphoglycolate, which cannot be used directly in the Calvin cycle. Instead, a specific phosphatase converts it into glycolate, which is oxidised by the enzyme glycolate oxidase to form glyoxylate, the transamination of which yields glycine. Two molecules of glycine are used to form serine, a potential precursor of glucose.

When Rubisco operates as an oxygenase, no net carboxylation occurs. Therefore, it operates at a reduced rate and at a higher metabolic cost compared to the carboxylase reaction. Consequently, to maintain the energetic and nutritional budget of a cell, it is essential that the oxygenase reaction is suppressed (Giordano *et al.* 2005).

In all known Rubisco's, the carboxylase and oxygenase reactions are competitive, and the relative rates at which they occur depends principally on the CO_2 and O_2 concentrations in the proximity of the Rubisco active site, and on the molecular nature of Rubisco itself, which varies in different organisms. The capacity of Rubisco to discriminate between CO_2 and O_2 can be defined by a "Selectivity factor", shown in Equation 4.3

$$S_{rel} = \frac{K_{0.5}\,(O_2)\,.\,k_{cat}\,(CO_2)}{K_{0.5}\,(CO_2)\,.\,k_{cat}(O_2)} \qquad \textbf{Equation 4.3}$$

where $K_{0.5}$ (CO_2) and $K_{0.5}$ (O_2) are half-saturation constants for the carboxylase and oxygenase reactions respectively, and k_{cat} (CO_2) and $k_{cat}(O_2)$ are the corresponding substrate-saturated rates of catalysis (Ananyev *et al*. 2001). A low selectivity factor means that at given O_2 and CO_2 concentrations, the greater the oxygenase function of Rubisco. Therefore, more phosphoglycolate is formed.

The advent of oxygenic photosynthesis has led to a long-term reduction in atmospheric CO_2 coupled with an increase in O_2. Consequently CO_2 fixation in

modern plants and algae can be restricted if they rely exclusively on the diffusive entry of CO_2 (Beardall & Raven, 2004).

Many aquatic plants and some higher plants have developed carbon concentrating mechanisms (CCMs) which create high CO_2 concentrations at the active site of Rubisco. They suppress the oxygenase reaction whilst promoting the carboxylase reaction, and thus greatly increase the rate and efficiency of DIC assimilation. They also minimise nutrient and energetic losses that are associated with phosphoglycolate production. Mechanisms which contribute towards CO_2 accumulation are widespread in algae, and have been reviewed by Giordano *et al.* (2005). These are summarised below.

The C_4 pathway, which is well-characterised in higher plants, involves CO_2 fixation which is spacially seperated from Rubisco. Initially, pyruvate is converted to phosphoenolpyruvate (PEP) by the enzyme pyruvate-phosphate dikinase, in a reaction which consumes ATP. The PEP is then combined with CO_2 to form oxaloacetate, a reaction catalysed by the enzyme PEP carboxylase, which has a higher affinity than Rubisco and therefore is more active at low CO_2 concentrations, and avoids the wasteful oxygenase reaction. Oxaloacetate is converted to malate for transport, which in higher plants is into bundle sheath cells, where it undergoes decarboxylation to yield CO_2 and pyruvate. The CO_2 enters the Calvin Cycle and the pyruvate is used again by pyruvate-phosphate dikinase. Malate can be stored in cells and therefore inorganic carbon can be accumulated. C_4 photosynthesis is thought to be rare in marine algae (Raven, 1997), but there is convincing evidence that it occurs in the benthic marine maroalga *Udotea flabellum* (Reiskind & Bowes, 1991), and

in the marine diatom *Thalassiosira weisflogii* grown under DIC-limited conditions (Reinfelder *et al.* 2004; Morel *et al*. 2002). Crassulacean acid metabolism (CAM) photosynthesis is similar to C_4 photosynthesis, except CO_2 fixation occurs during the night, and is not spacially separated from Rubisco. CAM photosynthesis is found in cacti and other plants that inhabit arid environments, and allows stomata to be closed during the day, thus curtailing water loss from transpiration, and when they open at night, CO_2 is fixed by PEP carboxylase and stored as malate. During the day, CO_2 is released from the malate and used by Rubisco. Like C_4 photosynthesis, CAM photosynthesis is seldom found in marine algae, but there is evidence that it occurs in some brown macroalgae (Raven, 1997; Johnston, 1991).

Active uptake of DIC involves ATP-dependant mechanisms of CO_2 or HCO_3^- uptake, which is widespread in cyanobacteria and occurs across one or more of the membranes that separate Rubisco from the external medium. CA in the carboxysome converts HCO_3^- to CO_2, which accumulates and thus increases the CO_2 concentration at the Rubisco active site. These mechanisms are well-characterised in cyanobacteria, and have been reviewed by Badger *et al*. (2002).

CMMs in eukaryotic micro- and macroalgae involve not only mechanisms that facilitate the uptake inorganic carbon across the cell membrane, but also those that transport inorganic carbon across the chloroplast membrane. As well as catalysing the conversion of HCO_3^- to CO_2 in the periplasmic space, the roles of CA in the CMM also extends to the cytosol and chloroplast envelope, and have

been reviewed by Badger & Price, (2002). A schematic model for inorganic carbon transport and CO_2 accumulation processes is shown in Figure 4.2.

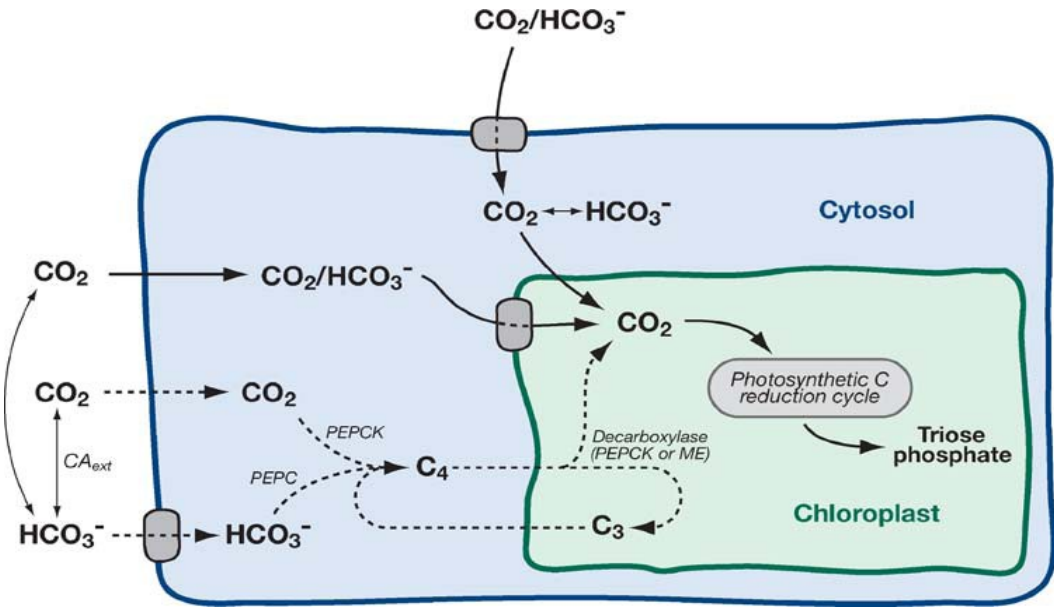

Figure 4.2 Inorganic carbon transport and CO_2 accumulation processes in eukaryotic algal cells. Active transport is shown by the shaded bases. From Girodano *et al*. (2005).

Because they increase the rate of DIC flux from the external medium into the cytoplasm, DIC acquisition mechanisms are a crucial component of CCMs, but their synthesis (and if they are ATP-dependent mechanisms, their activity) represents a considerable investment in valuable cellular resources of energy and nutrients. It is no surprise then, that experimental evidence indicates that nutrient availability and energy supply in the environment significantly affect the activity and expression of these mechanisms (Beardall *et al.* 2002). However, if the CCM is efficient, the incurred energetic and nutritional costs may be offset by the advantages associated with minimising phosphoglycolate production. Part of this efficiency results from regulating the expression CCMs, since if the external inorganic carbon concentration is high, for example, it would be

wasteful to express proteins that facilitate carbon uptake at the same rate as when the external inorganic carbon concentration is low.

The influence of DIC concentration on the regulation of CCM activity and mechanisms of DIC uptake has been investigated in several algae. It is established that extracellular CA expression is regulated by the external DIC concentration for example, and there is strong evidence to suggest that CO_2 is the regulatory carbon species. In most algae that use CA, its activity is suppressed at elevated atmospheric CO_2 and DIC concentrations, (Matsudu & Colman 1996; Palmqvist *et al*, 1988; Shiraiwa & Miyachi, 1985), and increases at low pCO_2 and DIC (Andria *et al*. 2001, Sültemeyer 1998).

Extracellular CA activity is not always associated with low concentrations of DIC. In *Chlamydomonas reinhardtii* for example, there are two forms of extracellular CA, *Cah1* and *Cah2*, which are regulated differently with DIC concentration; *Cah1* is only expressed at low CO_2 concentrations, whereas *Cah2* is expressed poorly at low CO_2, but is more active at elevated CO_2 (Fukuzawa *et al*. 2001; Fujiwara *et al.* 1990).

Little is known about the regulation of algal bicarbonate transporters in response to DIC supply. Because they are only detectable in some green macroalgae when the external pH is high, Axelsson *et al* (1999) have suggested that they may be induced in response to low CO_2 concentrations. Only Andria *et al* (2001) have measured bicarbonate transporter activity in algae cultured at different DIC concentrations, and they found that it was suppressed at low DIC in *Enteromorpha intestinalis*, whereas in *Gracilaria* sp. it became more active.

Therefore, it appears that like extracellular CA, bicarbonate transporters are regulated differently with DIC concentration, depending on species.

Experiments with *Emiliania huxleyi* by Herfort *et al* (2002) showed that although a bicarbonate transporter is the principal DIC acquisition mechanism at ambient DIC, external CA is induced at low DIC. They also demonstrated that the kinetics of photosynthesis as a function of DIC concentration were biphasic, and were produced by the presence of these two mechanisms. Since biphasic kinetics were also measured in *P. palmata* in the present study, it was hypothesised that both the bicarbonate transporter and external CA operate in these species, with CA being induced or activated at low DIC. Therefore, in this chapter, evidence for external CA activity below the ambient DIC concentration was sought.

Carbon uptake in *P. palmata* was also examined in plants cultured for 6 days in artificial seawater containing different concentrations of DIC. Low DIC concentrations were created by making solutions of artificial seawater to which no DIC was added, and to prevent it absorbing CO_2 from the atmosphere it was aerated with air that had been passed through a 1M solution of NaOH. As well as low-DIC seawater, plants were cultured in seawater containing 2mM and 8mM DIC. The hypothesis that the expression of bicarbonate transporters is induced in CA-users by increasing DIC concentration was investigated in *Chondrus crispus* by culturing plants for 6d in artificial seawater containing 2mM and 8mM DIC, and subsequently testing the effect of the bicarbonate transporter inhibitor DIDS on net photosynthesis.

4.2 Aims

To test the following hypothesis:-

At low concentrations of DIC, *Palmaria palmata* uses extracellular CA to acquire DIC.

And to answer the questions:-

1. How is the activity of the bicarbonate exchanger mechanism in *Palmaria palmata* affected by high and low DIC concentrations?

2. Is a bicarbonate transporter mechanism induced in the CA-user *Chondrus crispus* by high concentrations of DIC?

4.3 Materials and Methods

4.3.1 Culture of *P. palmata* and *C. crispus* at different DIC concentrations

Young, healthy fronds of *Palmaria palmata* and *Chondrus crispus* were cultured in cylindrical glass tanks containing artificial seawater medium prepared as described in Chapter 2, after Harrison *et al*. (1980). Three different DIC concentrations were used: 0 mM (or "low DIC"), 2 mM and 8mM. The 2 mM and 8 mM DIC concentrations were created by adding $NaHCO_3$ to the seawater to the required concentrations, whereas the 0 mM DIC seawater contained no added $NaHCO_3$, and to prevent the absorption of atmospheric CO_2, the culture medium was continuously aerated with CO_2-free air, created by passing air through a 1M NaOH solution. The 2 mM and 8 mM tanks, however, were aerated with untreated air. Fronds from the two different species were cultured separately in 5L of the ASW, and were maintained at 15°C, with a downwelling photon flux density of 100 µmol m^{-2} s^{-1} provided by white fluorescent lights, and the photoperiod was set at a 12:12 hour light:dark cycle. The pH of the seawater was measured daily and did not increase above 8.3. To avoid a change in pH over time because of photosynthesis or respiration, the growth medium was changed daily. Discs of thalli, 9 mm in diameter, were cut from fronds of *P. palmata* on the 6th day of culture, and used in oxygen electrode experiments. Segments of *C. crispus* were cut from the tips of thalli, blotted onto tissue paper, and their fresh weight measured before being used in experiments. Segments with fresh weights between 8-10mg were selected for

experiments, and supported in the oxygen electrode chambers with an acetate panel, as described for *P. palmata* in Chapter 2.

4.3.2 Short-term incubation of *P. palmata* at different DIC and $NaNO_3$ concentrations

Discs of *P. palmata*, 9 mm in diameter, were cut from thalli and incubated for 2 hours in sealed 40 mL cylindrical glass vials containing 30 mL unbuffered ASW with different concentrations of DIC, $NaNO_3$, and NH_4Cl, according to the experiment in question. The glass vials were placed horizontally on a rotating shaker at 100 rpm, under a continuous downwelling PFD of 120μM μmol m^{-2} s^{-1}. The movement of the air bubbles in the tubes ensured that the solutions were aerated. After incubation, the thallus discs were placed in oxygen electrodes containing 1 ml of fresh buffered ASW, which contained the same concentrations of DIC and $NaNO_3$ as used in the incubation medium.

4.4 Results

To determine if extracellular CA was induced by low DIC in *P. palmata*, a preliminary experiment was carried out in which the effect of the specific inhibitor AZ on photosynthesis was measured in discs of *P. palmata* incubated for 2 h in ASW containing no added DIC. No CA activity was detected, and it was hypothesised that since the alga had been maintained in N-free ASW it may have become N-limited which decreased the expression of this mechanism. Subsequently, it was found CA activity could be detected in discs of *P. palmata* that had been incubated for 2h in ASW containing no added DIC + 50μM of $NaNO_3$ (t-test p = 0.012), and ASW containing no added DIC + NH_4Cl (t-test p = 0.031). The results of this experiment are shown in Figure 4.3.

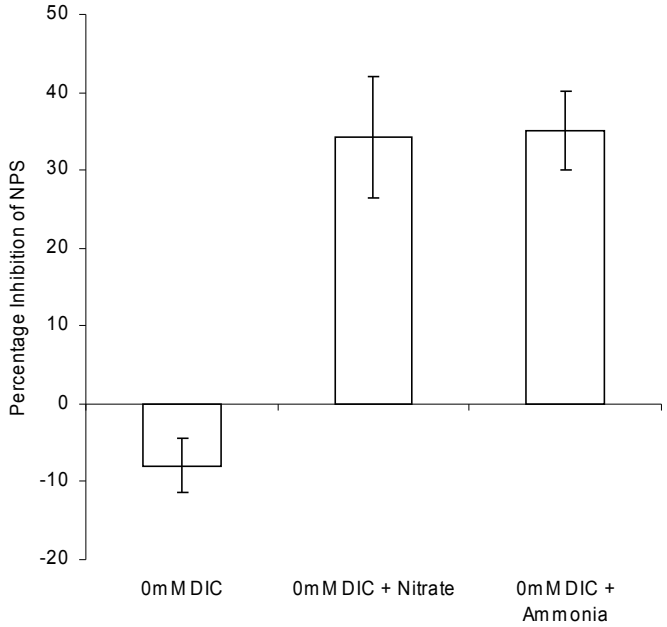

Figure 4.3 Percentage inhibition of NPS in *P. palmata* incubated for 2h in seawater containing no added DIC, with and without the addition of 50 μM $NaNO_3$ or 50 μM NH_4Cl. Date are +/-SE (n=3).

Since atmospheric CO_2 would have been absorbed by the DIC-free seawater during this experiment, and therefore the DIC concentration at which CA activity was induced was unknown, AZ inhibition was examined in discs that were incubated for 2h seawater containing known concentrations of DIC, which were 0.25 mM, 0.5 mM and 2 mM. Each solution also contained 50µM $NaNO_3$. The results of this experiment are shown in Figure 4.4. At 0.25 mM DIC, the percentage inhibition of photosynthesis was equal to that shown in "DIC-free" seawater in the preliminary experiments, suggesting CA was active. At 0.5 mM DIC however, there was a substantial decrease in inhibition, and almost no inhibition at 2 mM DIC.

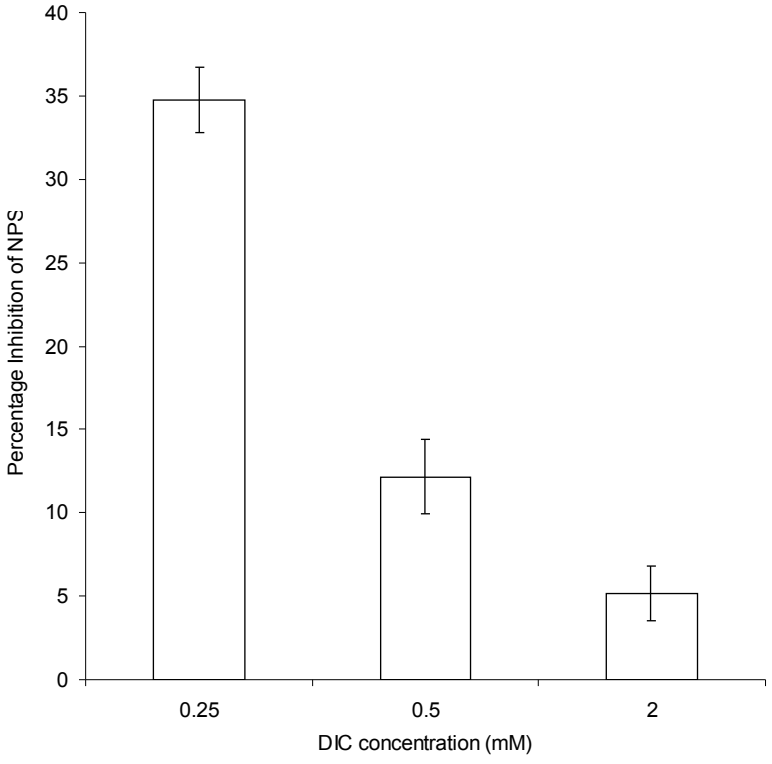

Figure 4.4 Percentage inhibition of net photosynthesis (NPS) by 50uM AZ addition, in *Palmaria palmata* incubated for 2 h in ASW containing 50µM $NaNO_3$ and DIC concentrations of 0.25mM, 0.5mM and 2mM. Data are means +/-SE (*n*=3)

The effect of DIC supply on bicarbonate transporter activity in *P. palmata* was examined in plants cultured for 6 days in ASW containing 0mM, 2mM and 8mM added DIC. Photosynthesis and DIDS inhibition were measured in buffered ASW containing 2mM DIC, and the results of these experiments are shown in Figure 4.5. The greatest percentage inhibition of 40% was measured in the 8mM culture, followed by the 2 mM culture, which was similarly inhibited by 34%. Inhibition was lowest in the 0 mM DIC culture, at only 13%

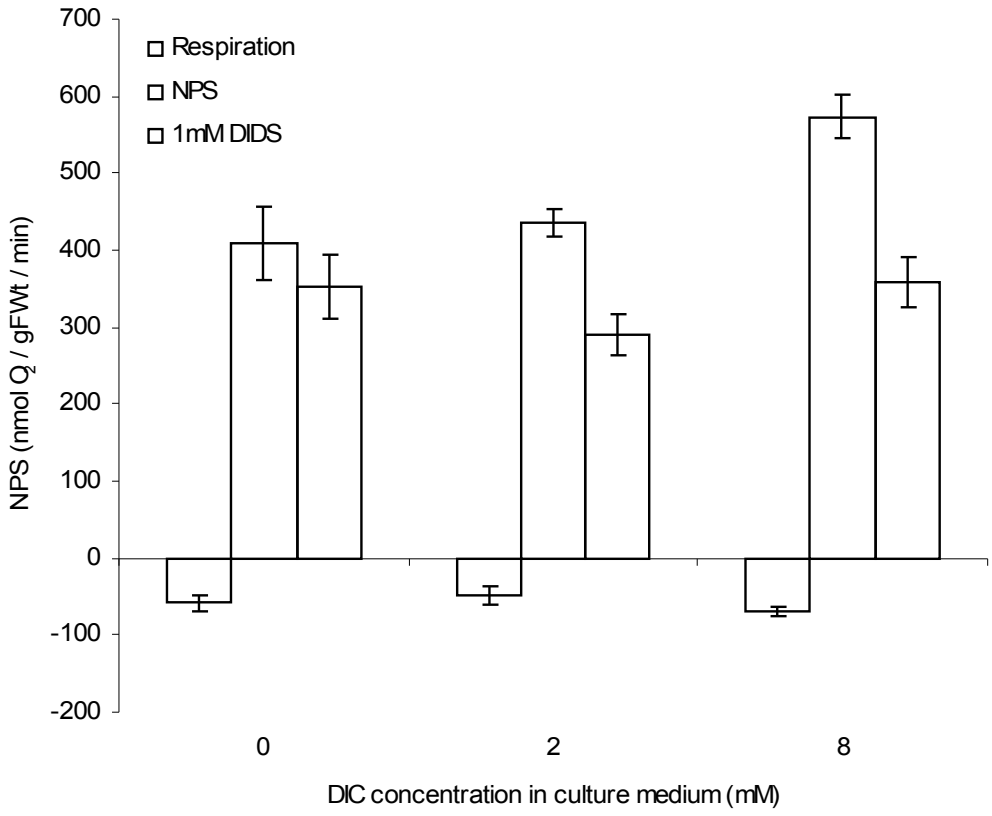

Figure 4.5 Respiration and net photosynthesis of *Palmaria palmata* cultured for 6 days in ASW with 8mM, 2mM, and 0mM added DIC, before and after the addition of 1mM DIDS. Measurements were made in buffered ASW containing 2mM DIC. Data are means +/-SE (n=6).

The effect of DIC concentration on respiration rates was tested for significance using 1-way ANOVA, but no significant differences were found (Table 4.1)

Table 4.1 1-way ANOVA to analyse the effect of DIC concentration in the culture medium on rates of respiration.

Source of Variation	*SS*	*df*	*MS*	*F*	*P-value*	*F crit*
Respiration	0.572893	2	0.286447	1.326142	0.301756	3.885294
Within Groups	2.592	12	0.216			
Total	3.164893	14				

Rates of photosynthesis were similar in the 0 mM and 2 mM treatments, but were higher in plants cultured at 8mM DIC. The addition of 1mM DIDS inhibited photosynthesis in the 2 mM and 8 mM culture treatments, though little inhibition was evident in the 0 mM DIC culture. The significance of the differences in NPS with and without DIDS were analysed with 2-way ANOVA, the results of which are shown in Table 4.2

Table 4.2 2-way ANOVA to analyse the effect of DIC concentration in culture medium on the NPS with out without DIDS addition in *P. palmata*.

Source of Variation	*SS*	*df*	*MS*	*F*	*P-value*	*F crit*
DIC	17.22372	2	8.611858	6.018886	0.006342	3.31583
SITS	42.22834	1	42.22834	29.51367	6.87E-06	4.170877
Interaction	10.78424	2	5.392119	3.768588	0.034665	3.31583
Within	42.92418	30	1.430806			
Total	113.1605	35				

Photosynthesis was also measured in buffered ASW containing no added DIC (Figure 4.6). Plants cultured for 6d at 2mM and 0mM DIC achieved rates of photosynthesis of approximately 100 nmol O_2 / g FWt / min, suggesting that some DIC had been absorbed into the ASW, or that photosynthesis was supplied by internal stores of DIC. Oddly, the photosynthetic rate of the 8mM DIC cultured-plant, at around 550 nmol O_2 / g FWt / min, was much greater, and was sustained for over 40 mins.

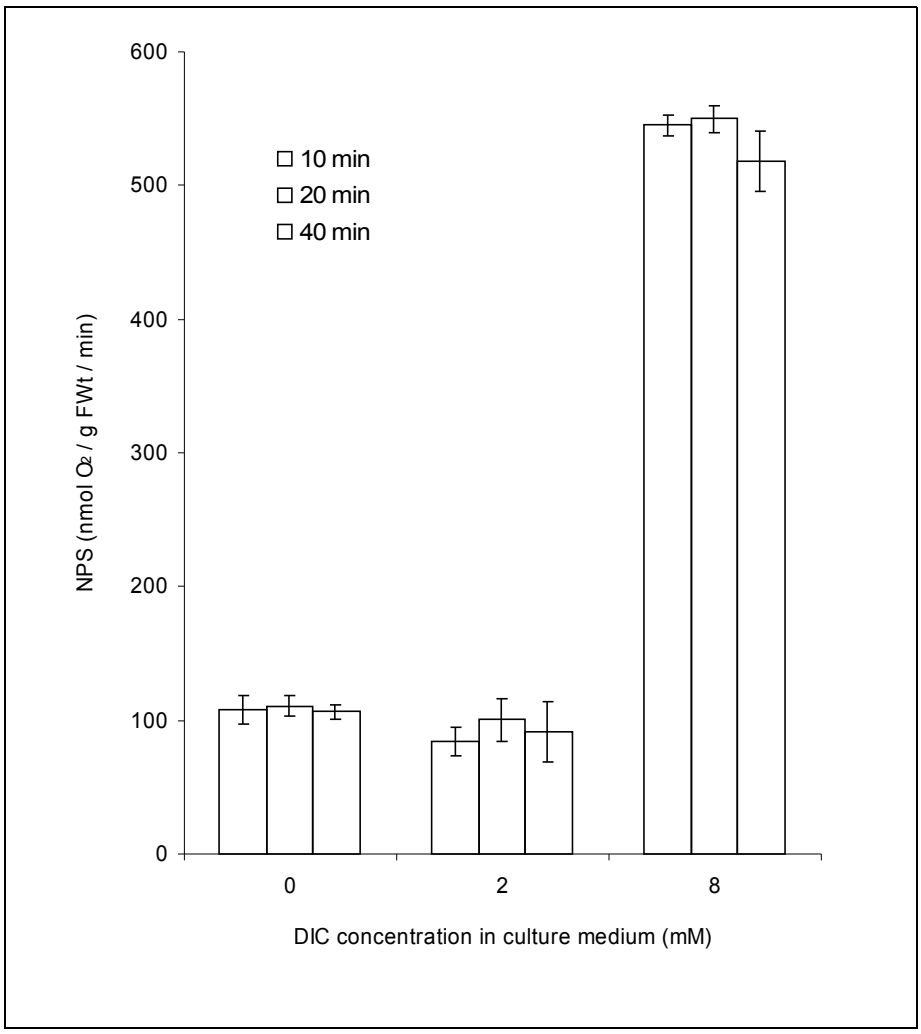

Figure 4.6 Photosynthesis of *Palmaria palmata* that had been cultured for 6d in ASW with 0mM, 2mM and 8mM DIC, measured in buffered ASW with 0mM DIC addition. Photosynthetic rates measured after 10, 20 and 40 min spent in the oxygen electrode chamber are given. Data are means +/- SE (n=4).

Thalli that had been cultured for 6 d in 8 mM DIC had become rigid, whereas fronds in the 0 mM and 2 mM DIC cultures were not noticeably different. It was hypothesised that because of the high alkalinity of the 8mM DIC culture medium, $CaCO_3$ had precipitated on the thallus surface or somewhere within the thallus, and its dissolution was supplying DIC for use in photosynthesis. Therefore, even in a low DIC solution, high rates of photosynthesis were achieved. To test this, thallus discs were submersed for approximately 15 seconds in 1M HCl, to dissolve any $CaCO_3$ crystals that may have formed. They immediately became more flexible, and photosynthesised at a much slower rate. By comparison, fronds cultured at 2mM DIC that were subjected to the same acid treatment photosynthesised at a similar rate compared to fronds that had not been exposed to HCl (Figure 4.7).

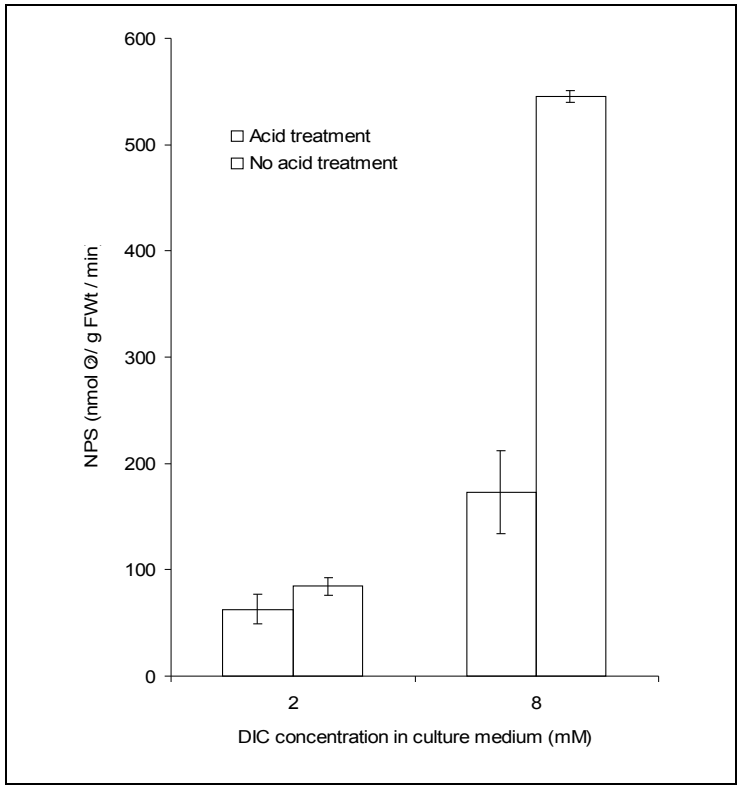

Figure 4.7 Photosynthesis of *P. palmata* that had been cultured for 6d at 2mM and 8mM DIC, measured in buffered ASW containing 0mM DIC, after being submersed briefly in 1M HCl solution. Data are means +/- SE (n=4).

The effect of 500µM DIDS addition on photosynthesis was tested in *Chondrus crispus* that had been cultured for 6 days in ASW containing 2 mM and 8 mM DIC. Before the inhibitor was added, photosynthesis was measured in buffered ASW containing 2mM DIC, and was similar in both cultures (t-test, p = 0.83). After the addition of DIDS, however, the rates of photosynthesis became significantly different (t-test, p = <0.05); no DIDS inhibition was measured in the 2mM DIC cultures (t-test, p = 0.68), whereas photosynthesis was significantly reduced in the 8mM DIC-cultured plants (t-test, p = <0.05) (Figure 4.8). The percentage inhibition of photosynthesis by DIDS is shown in Figure 4.9.

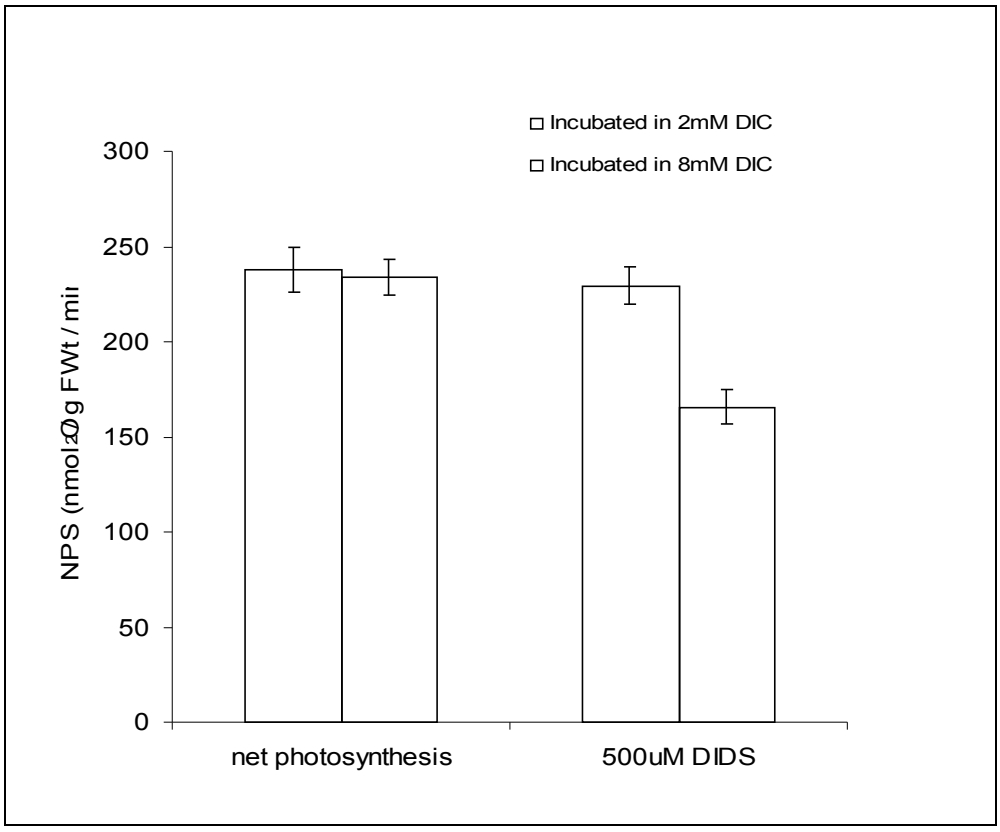

Figure 4.8 Photosynthesis of *C. crispus,* cultured for 6d at 2mM and 8mM DIC, before and after the addition of 500µM DIDS. Measurements were made in buffered ASW containing 2mM DIC. Data are means +/-SE (n=11-16).

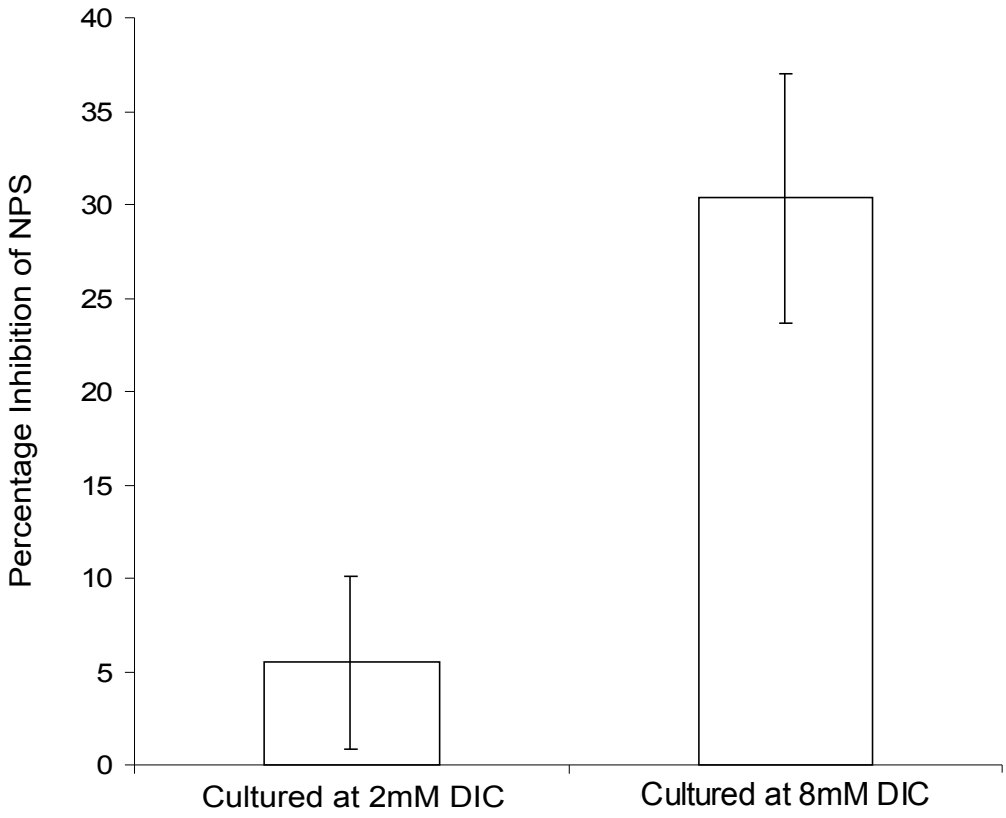

Figure 4.9 Inhibition of net photosynthesis in *Chondrus crispus* cultured for 6d at 2mM and 8mM DIC, after 500 μM DIDS addition. Measurements were made in buffered ASW containing 2mM DIC. Data are means +/-SE (n=11-16).

The effect of 100 uM AZ addition on photosynthesis was tested in buffered seawater containing 2 mM DIC. After AZ was added and the rate of photosynthesis had been measured, 500μM DIDS was added. (Figure 4.10).

The rates of photosynthesis before AZ addition were not significantly different (t-test, p = 0.36). After AZ was added, photosynthesis decreased in both cultures, but inhibition was significantly greater in the 2 mM DIC culture (t-test,

p = <0.05). After the addition of DIDS, photosynthesis was completely inhibited in the 8 mM culture, but there was no significant difference in photosynthesis in the 2 mM DIC culture before and after the addition of DIDS (t-test, p = 0.66).

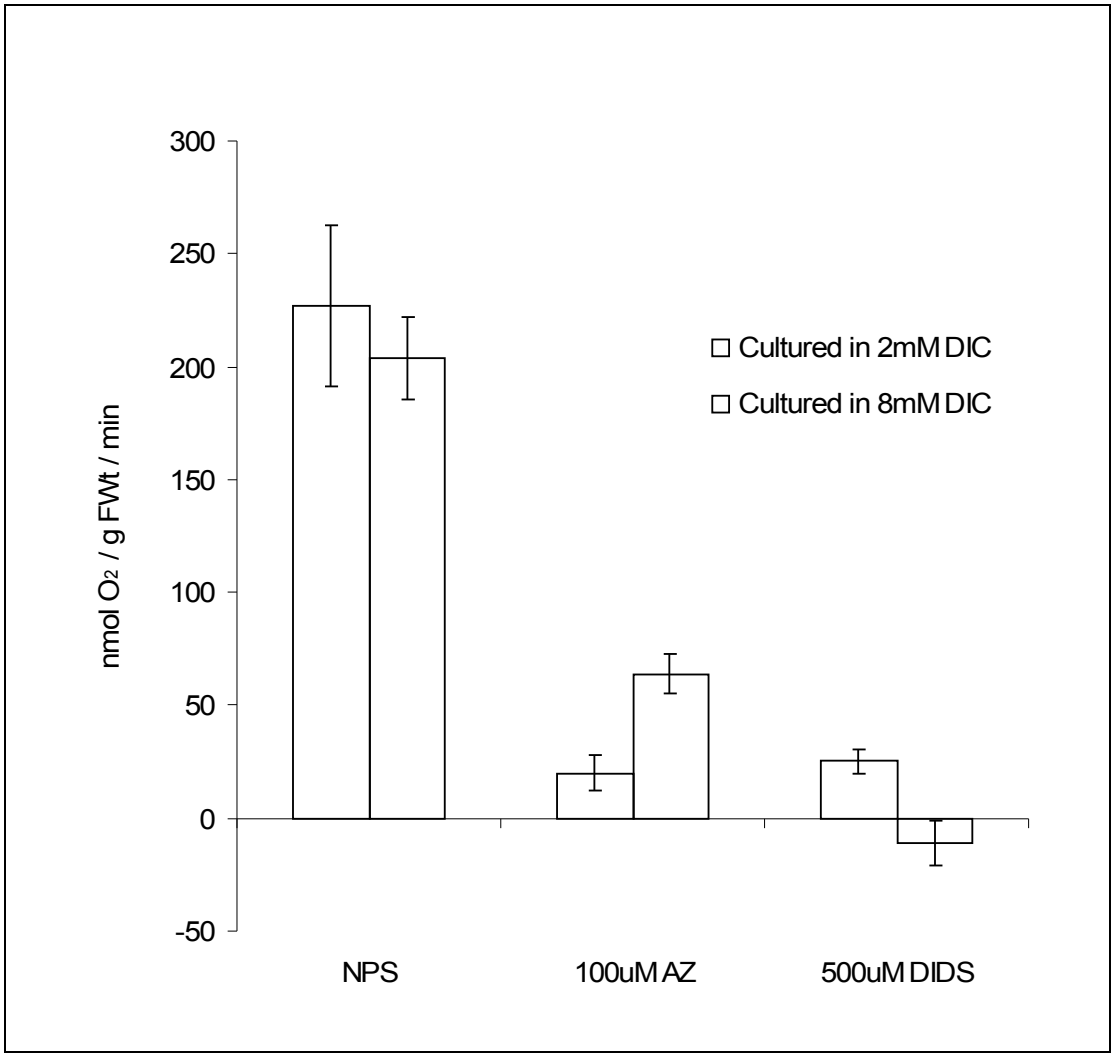

Figure 4.10 Net photosynthesis of *Chondrus crispus* cultured for 6 days in seawater containing 2 mM and 8 mM DIC, which was measured in buffered ASW containing, 2 mM DIC, Photosynthesis was measured before and after the addition of 100uM AZ, and after AZ was added and photosynthesis had been measured, 500µM DIDS was added. Data are means +/- SE (n=6).

4.5 Discussion

The results of these experiments indicate that inorganic carbon acquisition in *P. palmata* is mediated by two separate mechanisms. Although it was shown in Chapter 3 that a bicarbonate transporter is the major mechanism of DIC uptake in *P. palmata*, and is active above and below the ambient DIC concentration, the experiments described in this chapter indicate that external CA is induced or activated at low DIC. These findings support the idea that biphasic kinetics of photosynthesis with DIC concentration in *P. palmata* were produced by the interaction of two mechanisms. Below 0.625 mM DIC, photosynthesis is supported by both CA and a bicarbonate transporter, whereas above this concentration, CA is no longer active, and the bicarbonate transporter is the sole mechanism of HCO_3^- uptake. This suggests that *P. palmata and E. huxleyi* have similar DIC acquisition strategies in relation to DIC supply, since *E. huxleyi* also uses a bicarbonate transporter as its major mechanism of DIC uptake, and extracellular CA activity is present below 1 mM DIC. Similarly, the kinetics of photosynthesis as a function of DIC concentration in this alga are also biphasic (Herfort *et al*. 2002).

It appears that a source of N is required to induce CA activ*ity in P. palmata*. Although the effect of N-supply on CA activity was not determined in *E. huxleyi*, since it had been grown in a nutrient-rich artificial seawater medium, it is unlikely to have been N-limited. A direct interaction between N supply and extracellular CA is not established in algae, yet the modulation of CCM activity in relation to N supply has been examined. N-limitation in *Chlamydomonas reinhardtii*, for example, leads to a suppression of the CCM, and downregulation

of mitochondrial CA (Giordano *et al*. 2003), whereas it has been shown that CCM activity in this alga increases with N concentration (Beardall & Giordano, 2002). Conversely, some algae show an up-regulation of CCMs when N is limiting (Be*ardall* et al. 1991). It has been suggested that this may improve the efficiency with which algae assimilate N, by increasing the rate of CO_2 fixation per unit of nitrogen (Gi*ordan*o *et al*. 2005; *Raven* et al. 1985).

Whereas extracellular CA is the principal mechanism of DIC uptake in many marine macroalgae (Mercado *et al*. 1998; Giordano & Maberly, 1989), in P. palmata it appears to function as a supplementary mechanism to the bicarbonate transporter, for increasing DIC uptake in carbon-limited cells. Extracellular CA in *E. huxleyi* was described by Herfort *et al*. (2002) as a supplementary DIC scavenger, analogous to C_4 metabolism in plants.

Unlike external CA, bicarbonate transporter activity appears to be suppressed or down-regulated by long-term exposure to low DIC. In thalli that were cultured for 6 days in low DIC seawater and then examined at 2 mM DIC, the addition of SITS inhibited net photosynthesis by only 10%, compared to 35% in the other DIC treatments. However, it photosynthesised at a similar rate to the other DIC treatments, indicating that the apparent decrease in bicarbonate transporter activity did not affect the rate at which it acquired DIC. In future experiments, it would be interesting to investigate if this long-term exposure to low DIC had induced extracellular CA activity in *P. palmata*, to an extent that this mechanism had become a major mechanism of DIC uptake, rather than merely a supplementary mechanism that supports the bicarbonate transporter after short-term exposure to low DIC.

In similar experiments, Andria *et al*. (2001), found that DIDS inhibition of photosynthesis in *Gracilaria* sp. decreases in plants cultured at 1.2 mM DIC compared to 2.2 mM DIC, indicating that the activity of its bicarbonate transporter mechanism is also reduced at low DIC concentrations. This challenges the suggestion made by Larsson & Axelsson (1999), that low CO_2 concentrations induce bicarbonate transporter activity in green macroalgae. It is possible, however, that the role of the bicarbonate transporter in this species, which uses CA as its principal mechanism at the ambient DIC concentration in seawater, is analogous to extracellular CA in *P. palmata*, and *E. huxleyi*., ie. as a supplementary DIC scavenger. It is also possible that bicarbonate transporter activity is regulated in green macroalgae by factors other than DIC, such as ambient pH (Larsson & Axelsson, 1999, Axelsson *et al.* 1999, Larsson et al. 1997).

Although the DIDS experiments in this chapter show that bicarbonate transport activity in *P. palmata* was similar in thalli cultured at 2mM and 8mM DIC, rates of photosynthesis were slightly higher in the 8 mM culture, and after they had been placed in seawater containing no added DIC, photosynthesis proceeded at a high rate for over 40 minutes, whereas much lower rates of photosynthesis were measured in the 0mM and 2mM cultured plants. This suggested that photosynthesis in thalli cultured at 8mM DIC was supported by an internal DIC store.

Because fronds that had been cultured for 6 days in 8 mM DIC had become rigid, it was thought that the high DIC concentration in the external medium had

caused $CaCO_3$ to precipitate somewhere within the thallus tissue. Since no $CaCO_3$ deposition was visible on the thallus surface, it is possible that this occurred in the periplasmic space. When fronds were submersed in ASW containing lower DIC concentrations, dissolution of the $CaCO_3$ may have provided a source of HCO_3^- for photosynthesis, which would allow the alga to maintain high rates of photosynthesis in ASW containing no added DIC. This idea was supported by experiments in which fronds were briefly submersed in a 1M HCl solution in an attempt to dissolve any $CaCO_3$ deposits. After being exposed to HCl rates of photosynthesis in thalli cultured at 8mM DIC were substantially reduced. Photosynthesis in fronds cultured at 2mM DIC were not affected by the acid treatment, however, suggesting that the brief exposure to acid was not harmful.

The deposition of $CaCO_3$ has been localised to numerous sites in algal tissue, including the cell wall surface, within cell walls, and in both inter- and intracellular regions (Lobban & Harrison, 1997). Although calcification in some algae may have a physiological purpose, such as discouraging grazers or providing physical support, Simkiss & Wilbur (1989) have suggested that calcification in algal tissue often results from localised increases in pH due to photosynthesis, and rather than being beneficial, may limit light penetration and nutrient uptake and cause tissue damage. It is possible that in *P. palmata*, because photosynthesis is increased by DIC addition to seawater, regions of high pH were created in thalli cultured 8 mM DIC, which caused $CaCO_3$ to precipitate. Once thalli were placed in low DIC seawater, the $CaCO_3$ dissolved and thus provided a source of DIC for photosynthesis.

With the use of inhibitors of CA and AE1, Smith and Bidwell (1989) have shown that photosynthesis in *Chondrus crispus* is supported mainly by external CA in the absence of bicarbonate transporter mechanism, and their findings are in agreement with the inhibitor experiments in chapter 3. The experiments in this chapter suggest that bicarbonate transport activity is induced in *C. crispus* plants that have been cultured for 6 days in seawater containing 8mM DIC, whereas external CA is suppressed. This is the first report that a bicarbonate transporter can be induced in an alga which does not normally possess the mechanism, by increasing the external DIC concentration.

The function of the bicarbonate transporter in *C. crispus* is not clear. It does not appear to increase DIC uptake, as rates of photosynthesis were similar in thalli cultured at 2 mM and 8 mM DIC. Moreover, experiments in chapter 1 indicate that photosynthesis in *C. crispus* is saturated at 8mM DIC, therefore inducing a bicarbonate transporter for the purpose of acquiring DIC would be futile at this DIC concentration.

Since AE1 is used in animal tissues to maintain cellular pH (Sterling & Casey 2002), it is possible the bicarbonate transporter in *C. crispus* was induced at high DIC to prevent an increase in cytoplasmic pH caused by high rates of photosynthesis. This would suggest, however, that the bicarbonate transporter mechanism in *P. palmaria* also regulates cellular pH, which challenges the hypothesis that $CaCO_3$ is deposited in thalli grown at high DIC. However, since a bicarbonate transporter is the principal mechanism of DIC uptake in this species, it may have evolved to only transport HCO_3^- into cells, whereas the

bicarbonate transporter in *C. crispus* may also be used to transport HCO_3^- out of the cytoplasm, as it does in erythrocytes.

Alternatively, even though bicarbonate transporters have been reported in rather few algae, it is possible that they were more common when the DIC concentrations in the ocean were much higher. Therefore, although they are seldom expressed in algae at the ambient DIC concentration, they are induced at high DIC. If DIC acquisition is examined more at above ambient DIC concentrations, it may emerge that this mechanism is present in a larger number of marine plants than is currently thought.

Chapter 5

The effect of light and DIC concentration on photosynthesis in *Palmaria palmata*

5.1.1 Introduction

There is a long-held view in biology that inorganic carbon limitation does not occur at subsaturating light. This belief began with the influential work of F. F. Blackman: “Optima and limiting factors” (1905), in which he discussed his experiments on the effect of light and temperature on photosynthesis in the aquatic willow moss, *Fontinalis antipyretica* (Blackman & Mathaei, 1905), which showed that:-

1. At saturating light, the rate of photosynthesis increases with increasing temperature. At subsaturating light, increasing temperature has little effect on photosynthesis.
2. At constant temperature, photosynthesis increases with increasing irradiance until it reaches a saturating plateau.

Based on these findings, Blackman adapted Liebig’s “Law of the minimum” (Rabinowitch 1951), and postulated:-

“When a process is conditioned as to its rapidity by a number of separate factors, the rate of the process is limited by the pace of the ‘slowest’ factor.”

Thus, photosynthesis can only be limited by one factor at a time. Blackman illustrated this by producing a family of PI curves similar to those shown in Figure 5.1A. Bose (1924) disagreed with this theory of a single limiting factor, and to illustrate his argument, he produced the set of curves shown in Figure 5.1B.

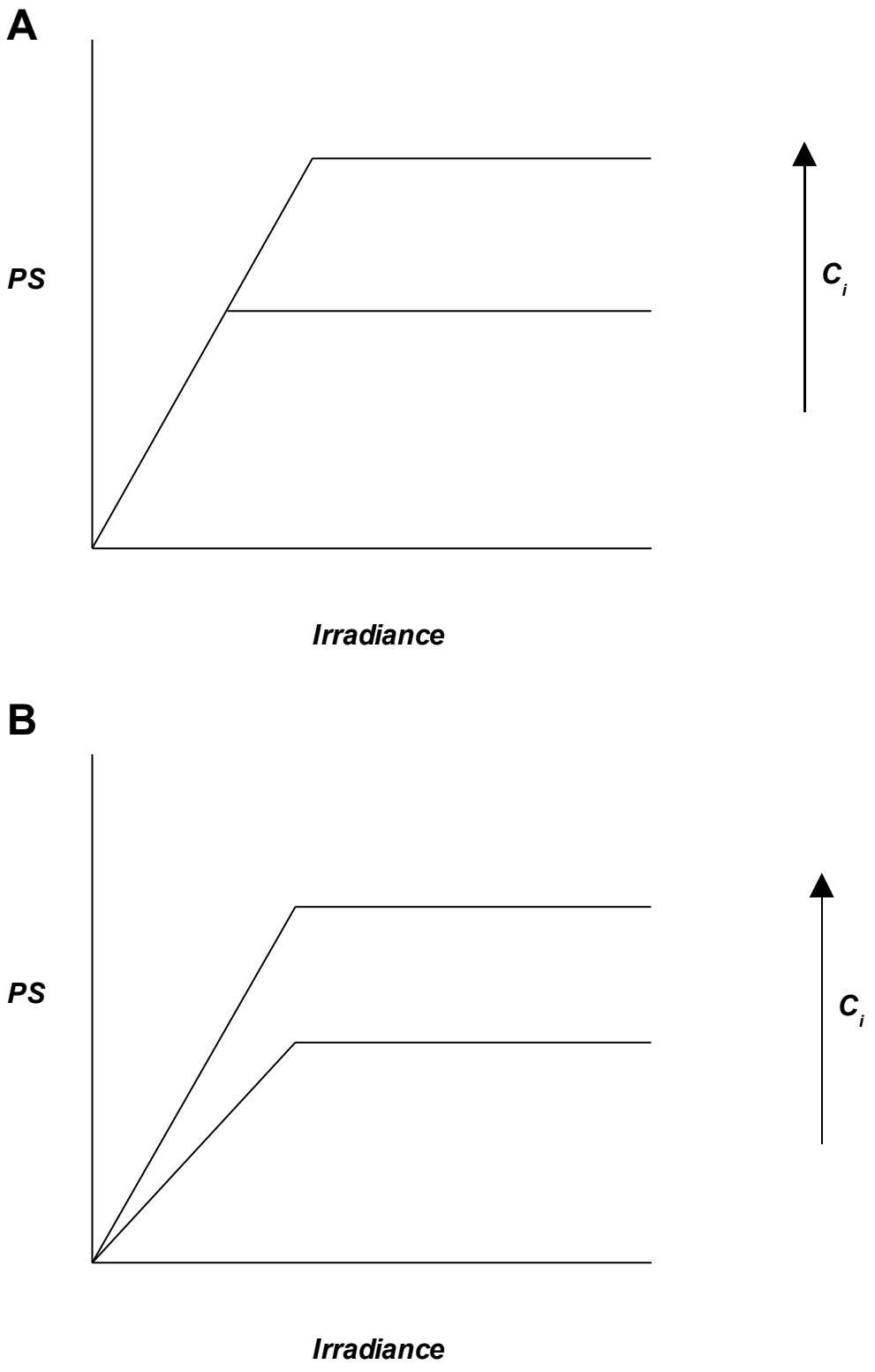

Figure 5.1 Schematic representation of PI curves that represent models proposed by (**A)** Blackman (1905), and (**B)** Bose (1924). *PS* = photosynthetic rate, C_i = inorganic carbon concentration.

Another important aspect of Blackman's work is it demonstrates that photosynthesis involves two processes: one of which is which is independent of carbon and temperature, and dependent on light, and another which is dependent on temperature and carbon concentration and independent of light. Subsequently, Warburg (1919) described these respective processes as the light and dark reactions of photosynthesis.

5.1.2 A brief overview of photosynthesis

During photosynthesis, solar energy is used to assimilate inorganic carbon, and in the case of oxygenic photosynthesis, which is carried out by plants, algae and cyanobacteria, it also yields O_2 and H_2O. The general equation for photosynthesis is shown in equation 5.1.

$$CO_2 + 2\ H_2O + \text{photons} \rightarrow (CH_2O)_n + H_2O + O_2 \qquad \textbf{Equation 5.1}$$

The first stage of photosynthesis involves a series of light-dependent reactions which take place in the thylakoid membrane of the chloroplast. Light energy is absorbed by chlorophyll and accessory pigments, and is transferred to a central chlorophyll located at the core of the protein complex, Photosystem II. When sufficient energy is transferred, this chlorophyll donates an electron to an electron acceptor molecule, Pheophytin, and subsequently a series of redox reactions form an electron transport chain between the four major protein complexes: Photosystem II (PSII), Cytochrome b6, PSI and NADP reductase. This creates a chemiosmotic potential across the thylakoid membrane which is

used by ATP synthase to create ATP, and the final redox reaction of the electron transport chain leads to the formation of NADPH. Collectively, these reactions are often described schematically in a "z-scheme" diagram, which was first proposed by Hill & Bendall (1960), and is shown in Figure 5.2.

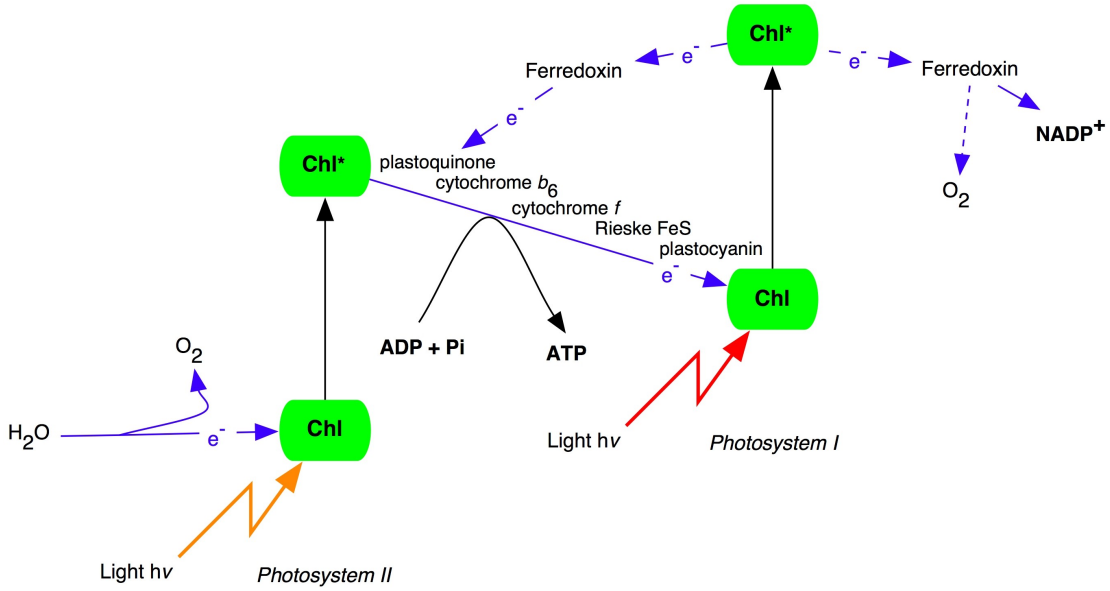

Figure 5.2 The z-scheme of photosynthesis in plants, reproduced from Allen (2004).

The light independent or "dark reactions" of photosynthesis take place in the stroma of the chloroplast, and use the NADPH and ATP produced by the light reactions to assimilate CO_2. The first major step of carbon fixation is carried out by Rubisco, and in a series of reactions which collectively are described as the Calvin cycle (Bassham *et al.* 1950), and use the NADPH and ATP formed by the light reactions, 3-carbon sugars are produced which subsequently combine to form sugar and starch. The overall equation for the light-independent reactions in photosynthesis is shown in equation 5.2.

$$3\ CO_2 + 9\ ATP + 6\ NADPH + 6\ H^+ \rightarrow C_3H_6O_3\text{-phosphate} + 9\ ADP + 8\ P_i + 6\ NADP^+ + 3\ H_2O$$

Equation 5.2

The biochemical explanation behind Blackman's model is that at saturating light, the rate of photosynthetic electron transport is limited by the rate of CO_2 fixation by Rubisco. Therefore, in the presence of excess ATP and NADPH (the products of the light reaction), an increase in CO_2 concentration will result in an increase of Rubisco activity, and thus an increase in the photosynthetic electron transport rate (ETR). By contrast, at subsaturating light, Rubisco activity is limited by the availability of ATP and NADPH, and not by CO_2. Therefore, an increase in ambient inorganic carbon concentration will not increase photosynthetic ETR. Bose's model, however, implies that at subsaturating light although Rubisco is limited by the availability of NADPH and ATP, it can also be limited by the availability of CO_2. Therefore, increasing the carbon concentration increases the ETR.

There is some evidence to suggest that HCO_3^- ions can increase the photosynthetic ETR directly, by providing an alternative source of electrons for the reduction of PSII. Although it is established that the electrons transported in the photosynthetic transport chain are obtained from water molecules, Warburg and Krippahl (1958) found evidence that HCO_3^- may also be used. They demonstrated that the addition of HCO_3^- increases O_2 production in isolated chloroplasts of *Chlorella* in the presence of an electron acceptor such

as ferricyanide. This is often referred to as “the bicarbonate effect” (Stemler, 2005).

Although the experiments of Warburg and Krippahl did not reveal anything about the mechanism of HCO_3^- stimulation of the light reaction, there is evidence to suggest that HCO_3^- ions bind to the electron acceptor and donor sides of PSII (reviewed by Dismukes *et al*. 2001). A study by Klimov *et al*. (2001) also shows that HCO_3^- ions represent an integral part of the water-splitting complex, and are required for the efficient functioning of the Mn cluster. The authors have speculated that HCO_3^- can increase photosynthetic ETR either by acting as a substrate for Rubisco, or by stimulating the light reaction directly.

Since HCO_3^- is the predominant form of DIC in seawater, it is possible that, increasing the DIC concentration may stimulate the light-dependant reaction of photosynthesis at subsaturating light in marine algae.

In this chapter, the effect of DIC concentration on photosynthesis was examined at both saturating and subsaturating light in *P. palmata*, *L. digitata*, and *Alaria esculenta*. Photosynthetic ETR was measured at different irradiances and DIC concentrations using a fluorescence monitoring system (FMS). This technique was chosen because it is a rapid, non-intrusive method for obtaining measurements of gross photosynthesis (Schreiber *et al.* 1994), and since the emission of chlorophyll fluorescence is high at subsaturating PFD, preliminary experiments revealed that precise measurements of photosynthesis could be

made at low PFDs. To identify which irradiances were subsaturating, PI curves were obtained for each species. The parameters of a PI curve are as follows:-

1. $\mathbf{P_{max}}$ = the maximum rate of photosynthesis
2. **α** = the initial ascending slope
3. $\mathbf{I_K}$ = the photon flux density at which P_{max} occurs
4. **LCP** (light compensation point) = PFD at which respiratory O_2 consumption is equal to photosynthetic O_2 production, therefore no net photosynthesis occurs.
5. **R** = respiration,

These are identified on the schematic representation of a PI curve shown in Figure 5.3.

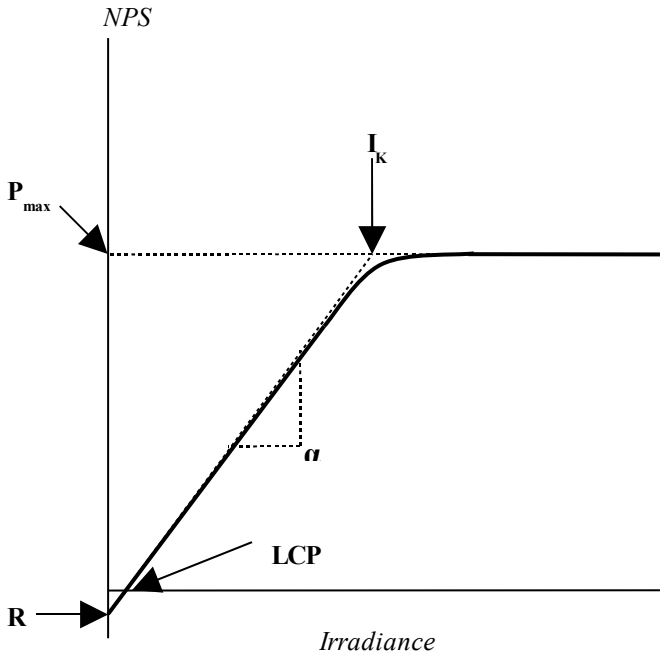

Figure 5.3 The parameters of a PI curve.

Since the ascending slope of α represents photosynthesis at subsaturating light, if DIC addition increased photosynthesis at PFDs that correspond to this region of the PI curve, it would indicate that, contrary to Blackman's theory of limiting factors, photosynthesis can be simultaneously limited by both light and inorganic carbon. Therefore, the effect of DIC addition on photosynthetic ETR was examined at PFDs below the I_k of each PI curve.

5.2 Aims

To test the following hypothesis:-

Photosynthetic electron transport rate in macroalgae is stimulated by DIC addition at both saturating and subsaturing light.

5.3 Materials and Methods

P. palmata, *Laminaria digitata*, and *Alaria esculenta* were harvested in April 2003 at low tide from a shore next to Dale Fort Field Centre in Milford Haven, Pembrokeshire. Plants were harvested daily at about 8am, and transported to the lab in a bucket of natural seawater. Upon arrival at the lab 5 min later, they were immediately placed in a tank of natural seawater which had been obtained from the collection site the same morning. The tank was placed outdoors in a shaded area next to the lab, and was vigorously aerated with airlines.

Induced chlorophyll fluorescence was measured in buffered natural seawater containing no added DIC, and 6 mM added DIC, using the Hansatech FMS. Seawater was collected daily from the harvesting site, and vacuum-filtered through a 2µm polycarbonate membrane to remove suspended solids, then buffered to pH 8.2 with 20 mM Bicine. Before experiments, a 9 mm disc was cut from the thallus, and incubated for 30 mins in a 100 mL plastic electrode chamber containing 80 mL filtered natural seawater at the DIC concentration that was being used in the subsequent experiment. The seawater was stirred with a magnetic stirrer, and illuminated by a projector lamp at PFD 100 µmol m^{-2} s^{-1}. After incubation, the thallus disc was placed in a DW2/2 Hansatech liquid-phase chamber (Hansatech Instruments, Norfolk, UK), containing 1 mL of fresh seawater medium. This chamber is similar to the oxygen electrode chamber described in Chapter 2, and consists a borosilicate tube which can be sealed from the air with a stopper, surrounded by a water jacket coated in black acetate to completely obscure light, other than that provided by the FMS probe. As for the oxygen electrode experiments, the thallus disc was supported in the

chamber with an acetate panel. The seawater was constantly stirred with a stirrer bar, and maintained at 20°C with a water bath. The FMS probe was inserted into a port at the side of the chamber, and positioned horizontally to the thallus disc.

Once placed in the experimental chamber, the thallus disc was incubated in the dark for 10 min, to allow it to reach a "dark-adapted" state, during which the primary electron acceptor of PSII, Q_A, is fully oxidised (Schreiber et al. 1994). As described in Chapter 2, chlorophyll fluorescence was measured after exposure of the thallus disc to increasing irradiances. Briefly, after 1 min exposure to actinic light, a short intense beam of saturating light was used to measure the maximum fluorescence yield of light-adapted tissue. This was followed by a 2 min period of darkness before the next irradiance was applied.

Chlorophyll fluorescence was also measured in *P. palmata* collected from St. Margaret's Bay, in simplified Harrison's artificial seawater medium, as described previously, buffered to pH 8.2 with 20mM Bicine.. DIC concentrations of 1, 2, 4 and 8 mM were used in these experiments, and before fluorescence was measured, 9 mm discs of thalli were incubated for 30 min in 30 mL polypropylene tubes containing 20 mL of the seawater medium, which were placed on a mechanical shaker, under a downwelling PFD of 100 µmol m^{-2} s^{-1}. After incubation, the tubes were placed in a dark chamber for 10 min to allow thalli to reach a "dark-adapted" state, and chlorophyll fluorescence was then measured using the FMS in an experimental setup described in detail in Chapter 2. Like the Dale Fort experiments, the thalli received 1 min exposure

to actinic light followed by a measurement of the maximum fluorescence yield, followed by a 2 min dark period.

5.4 Results

5.4.1 The effect of light and DIC concentration on photosynthesis

The effect of 6 mM DIC addition on photosynthetic electron transport rate at different irradiances are shown for *P. palmata*, *A. esculenta* and *L. digitata* in Figures 5.4- 5.6. To obtain PI curves from these data, relative ETRs were calculated by multiplying ΦPSR by the PFD at which they were measured, and were then plotted against irradiance (PFD) to give a rectangular hyperbola. This made it possible to identify light-limited regions of the PI curve, ie. the initial ascending slope (α), and light-saturating regions. Part "A" of each figure shows the measurements from PFD 0-1020 μmol m^{-2} s^{-1}, and in *L. digitata*, from 0-2000 umol m^{-2} s^{-1}, since ΦPSR measurements indicated that photosynthesis was not saturated by light (although subsequent calculation of the relative ETR suggested it had been saturated). To show more clearly the effect of DIC addition at low light, part "B" shows the measurements from 0-75 μmol m^{-2} s^{-1}.

The significance of the effects of DIC concentration and irradiance on photosynthetic ETR was tested for each species using 2-way ANOVA (with replication). This included measurements of ETR at both DIC concentrations, and at all PFDs tested. The results of the 2-way ANOVA tested three nul hypotheses: that irradiance does not affect ETR, that DIC concentration does not affect ETR, and that no interaction occurs between irradiance and DIC. The results of this are shown in Tables 5.1-5.3.

A

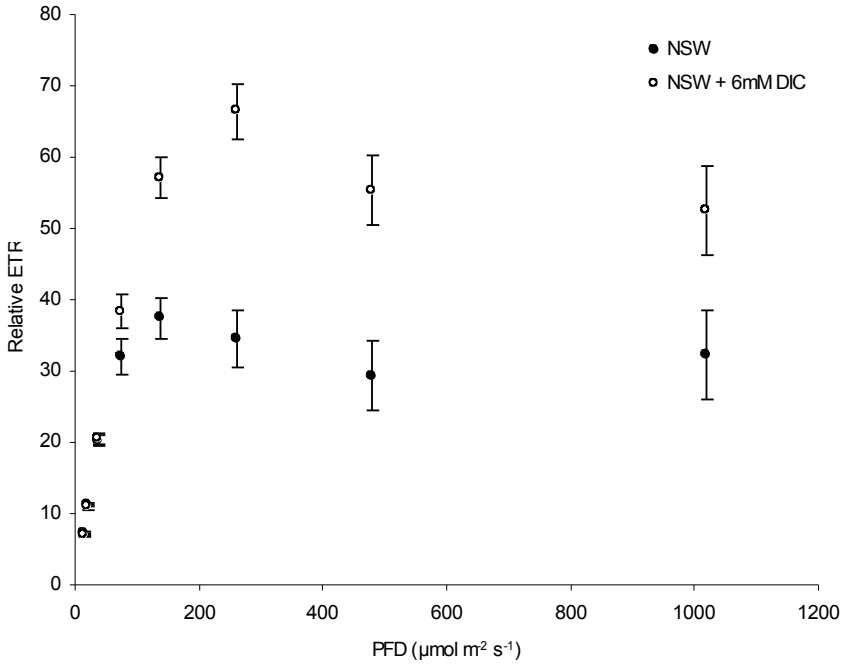

B

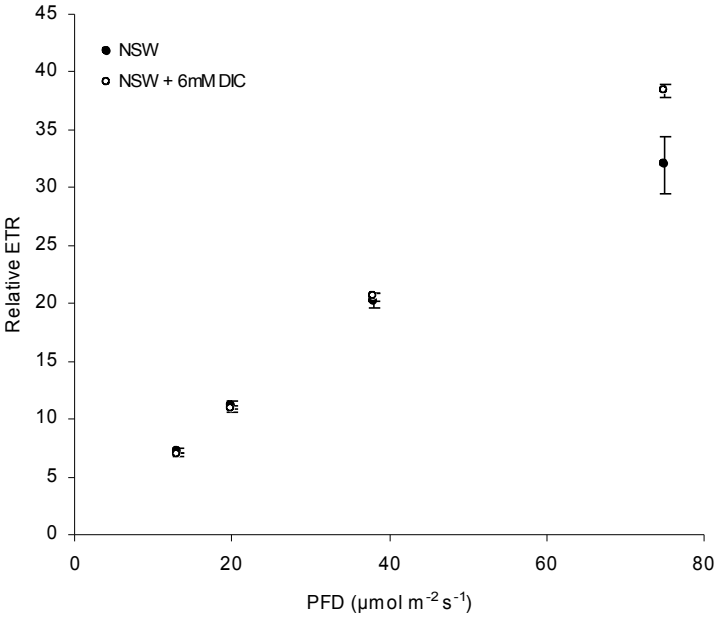

Figure 5.4 The effect of different irradiances (PFD) on relative ETR in *Palmaria palmata*, measured in buffered natural seawater containing no added DIC and 6mM added DIC. **A** shows measurements made at PFD 0-1020 µmol m^{-2} s^{-1}, **B** shows measurements between 0-75 µmol m^{-2} s^{-1}. Data are means +/- SE (*n*=6).

A

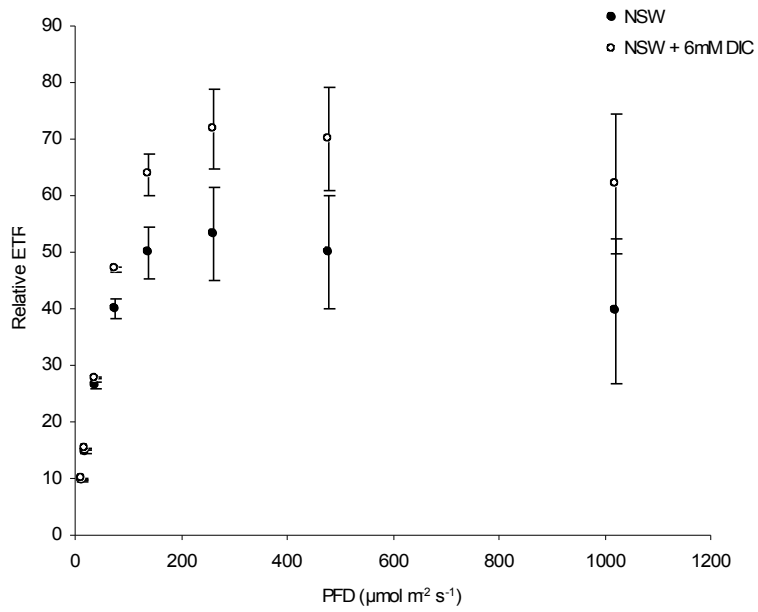

B

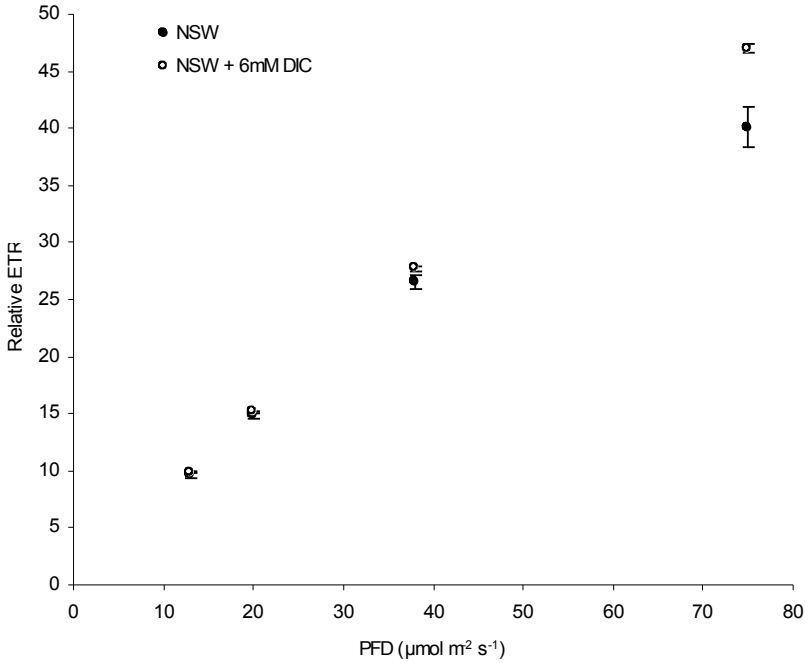

Figure 5.5 The effect of irradiance (PFD) on relative ETR in *Alaria esculenta*, measured in buffered natural seawater containing no added DIC and 6mM added DIC. **A** shows measurements made at PFD 0-1020 µmol m^{-2} s^{-1}, **B** shows measurements between 0-75 µmol m^{-2} s^{-1}. Data are means +/- SE (*n*=6).

A

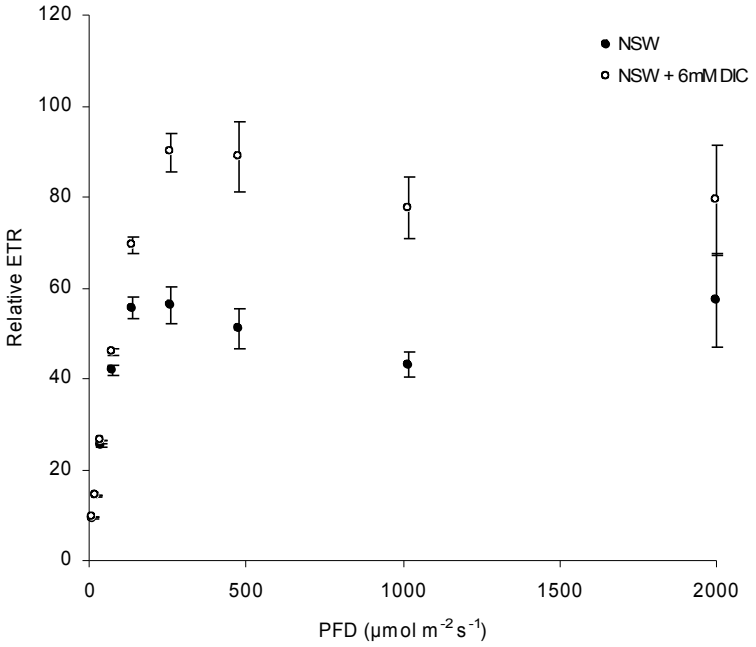

B

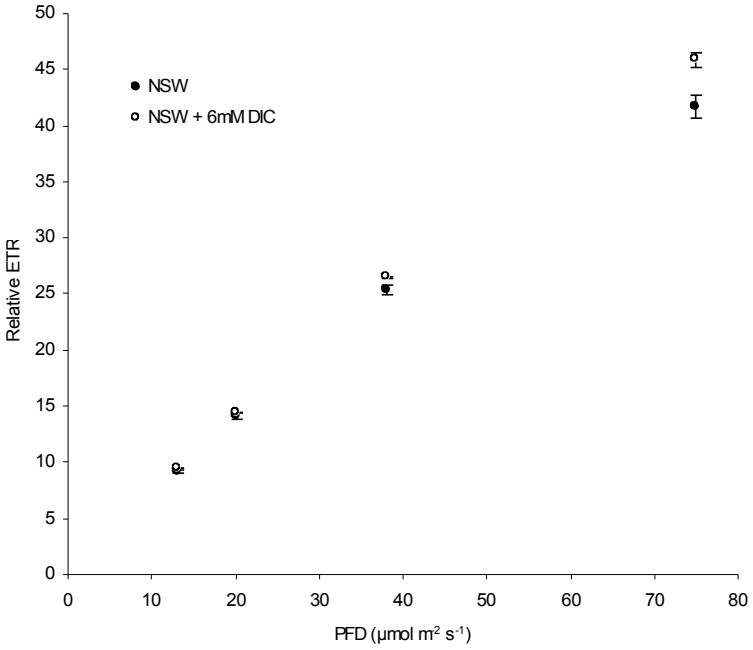

Figure 5.6 The effect of irradiance (PFD) on relative ETR in *Laminaria digitata*, measured in buffered natural seawater containing no added DIC and 6mM added DIC. **A** shows measurements made at PFD 0-2000 µmol m^{-2} s^{-1}, **B** shows measurements between 0-75 µmol m^{-2} s^{-1}. Data are means +/- SE (*n*=6).

Table 5.1 2-way ANOVA for the effect of PFD and DIC concentration on photosynthetic ETR between PFD 13-1020 umol m^{-2} s^{-1} in *Palmaria palmata*.

Source of Variation	*SS*	*df*	*MS*	*F*	*P-value*	*F crit*
Light	23918.23	7	3416.89	40.05	<0.05	2.13
DIC	4050.1	1	4050.1	47.47	<0.05	3.96
Interaction	3543.84	7	506.26	5.93	<0.05	2.13
Within	6825.63	80	85.32			
Total	38337.8	95				

Table 5.2 2-way ANOVA for the effect of PFD and DIC concentration on photosynthetic ETR between PFD 13-1020 umol m^{-2} s^{-1} in *Alaria esculenta.*

Source of Variation	*SS*	*df*	*MS*	*F*	*P-value*	*F crit*
Light	36299.9	7	5185.7	58.74	<0.05	2.13
DIC	2597.32	1	2597.32	29.42	<0.05	3.96
Interaction	1837.29	7	262.47	2.97	<0.05	2.13
Within	7062.21	80	88.28			
Total	47796.71	95				

Table 5.3 2-way ANOVA for the effect of PFD and DIC concentration on photosynthetic ETR between PFD 13-1020 umol m^{-2} s^{-1} in *Laminaria digitata..*

Source of Variation	*SS*	*df*	*MS*	*F*	*P-value*	*F crit*
Sample	54205.74	7	7743.68	116.05	<0.05	2.13
Columns	5919.76	1	5919.76	88.71	<0.05	3.96
Interaction	5981.21	7	854.46	12.8	<0.05	2.13
Within	5338.28	80	66.73			
Total	71444.99	95				

According to the PI curves obtained by plotting relative ETR against irradiance, the I_K for each species was located at, or close to, 75 µmol m^{-2} s^{-1}. Therefore, it was decided that PFD measured between 13-38 µmol m^{-2} s^{-1} were within the

ascending slope of α on the PI curves, and thus represented photosynthesis at subsaturating light. Therefore, 2-way ANOVA was used to determine if DIC significantly stimulated photosynthesis at these PFDs. The results of this are shown in tables 5.4-5.6.

Table 5.4 2-way ANOVA for the effect of PFD and DIC concentration on photosynthetic ETR between PFD 13-38 umol m^{-2} s^{-1}in *Palmaria palmata*.

Source of Variation	*SS*	*df*	*MS*	*F*	*P-value*	*F crit*
Light	1119.26	2	559.63	690.47	<0.05	3.32
DIC	0.07	1	0.07	0.08	0.77	4.17
Interaction	0.67	2	0.33	0.41	0.67	3.32
Within	24.32	30	0.81			
Total	1144.31	35				

Table 5.5 2-way ANOVA for the effect of PFD and DIC concentration on photosynthetic ETR between PFD 13-38 umol m^{-2} s^{-1}in *Alaria esculenta*.

Source of Variation	*SS*	*df*	*MS*	*F*	*P-value*	*F crit*
Light	1904.94	2	952.47	968.29	<0.05	3.32
DIC	3.19	1	3.19	3.25	0.08	4.17
Interaction	1.92	2	0.96	0.98	0.39	3.32
Within	29.51	30	0.98			
Total	1939.56	35				

Table 5.6 2-way ANOVA for the effect of PFD and DIC concentration on ΦPSR between PFD 13-38 umol m^{-2} s^{-1}in *Laminaria digitata*.

Source of Variation	*SS*	*df*	*MS*	*F*	*P-value*	*F crit*
Light	1741.08	2	870.54	2646.89	<0.05	3.32
DIC	2.97	1	2.97	9.04	<0.05	4.17
Interaction	1.41	2	0.7	2.14	0.14	3.32
Within	9.87	30	0.33			
Total	1755.33	35				

The PI curves followed a typical hyperbolic pattern – an increasing initial slope followed by a saturating plateau, which increased with DIC addition, showing that DIC addition to buffered natural seawater increases photosynthetic ETR at saturating light. At subsaturating light, however (between 13-38 μmol m^{-2} s^{-1}), DIC addition caused no apparent increase in ETR, although at 75 μmol m^{-2} s^{-1} a small increase was visible. The ANOVA analysis demonstrated that the stimulation of ETR by DIC and irradiance were both significant between 13 and 1020 μmol m^{-2} s^{-1}, and that there was a significant intereraction between these two factors.. ANOVA analysis of ETR values between 13-38 μmol m^{-2} s^{-1} however, revealed that although irradiance significantly increased ETR in all species, in *P. palmata* and *A. esculenta,* DIC addition did not., and there was no significant interaction between these factors. In *L. digitata*, significant differences in ETR were caused by both irradiance and DIC addition, yet no significant interaction occurred between these factors. In *L.digitata*, the Fv/Fm value in the high DIC samples (0.73) was significantly higher than the Fv/Fm value of 0.7 measured in seawater with no added DIC (t-test, p = 0.017), whereas no differences in Fv/Fm were found in *P. palmata* (t-test p = 0.35) and *A. esculenta* (t-test, p = 0.42).

The effect of light and DIC on photosynthesis was also examined in *P. palmata* in artificial seawater medium at DIC concentrations between 1mM and 8mM, at PFDs between 0 and 1020 μmol m^{-2} s^{-1}. In this experiment, a larger number of subsaturating PFDs were tested. Measurements of ETR plotted against irradiance are shown in Figure 5.7. Part “A” shows the measurements from PFD 0-1020 μmol m^{-2} s^{-1}, and part “B” shows the measurements from 0-55 μmol m^{-2} s^{-1}. The significance of the effects of DIC concentration and irradiance on

ETR was tested using 2-way ANOVA. Table 5.7 shows the results of ANOVA which included all DIC concentrations and PFDs tested, whereas Table 5.8 shows the results of ANOVA which included all DIC concentrations, but only subsaturatiing PFDs (between 4-34 µmol m^{-2} s^{-1}).

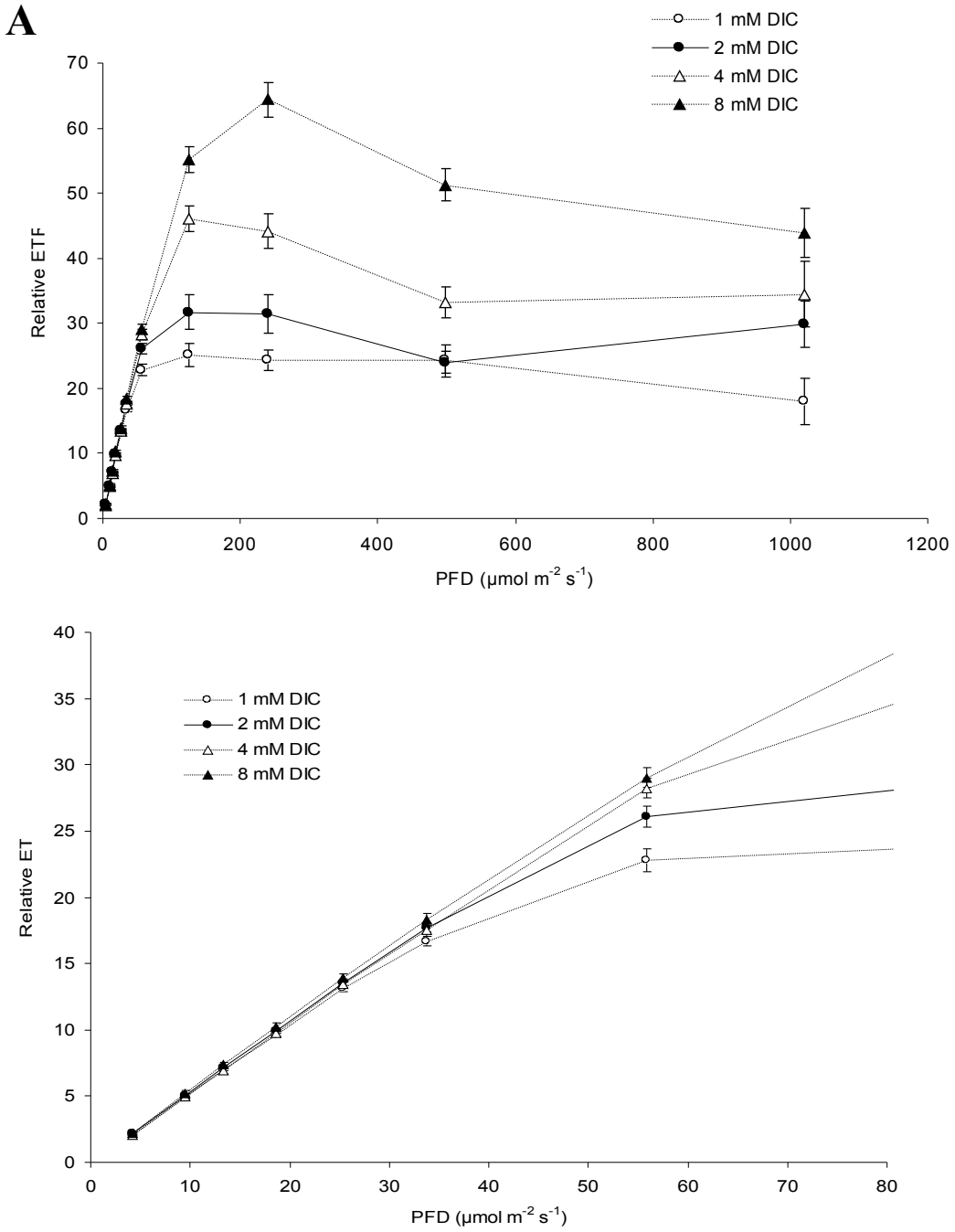

Figure 5.7 The effect of irradiance (PFD) on relative ETR in *Palmaria palmata*, measured in aritificial seawater containing1-6 mM DIC. **A** shows measurements made at PFD 0-1020 µmol m^{-2} s^{-1}, **B** shows measurements between 0-75 µmol m^{-2} s^{-1}. Data are means +/- SE (*n*=5).

Table 5.7 2-way ANOVA for the effect of PFD and DIC concentration on photosynthetic ETR between PFD 4-1020 umol m^{-2} s^{-1} in *Palmaria palmata*.

Source of Variation	*SS*	*df*	*MS*	*F*	*P-value*	*F crit*
Sample	41499.57	10	4149.96	177.92	<0.05	1.88
Columns	5087.37	3	1695.79	72.7	<0.05	2.66
Interaction	7854.78	30	261.83	11.23	<0.05	1.52
Within	4105.24	176	23.33			
Total	58546.96	219				

Table 5.8 2-way ANOVA for the effect of PFD and DIC concentration on photosynthetic ETR between PFD 4-34 umol m^{-2} s^{-1} in *Palmaria palmata*.

Source of Variation	*SS*	*df*	*MS*	*F*	*P-value*	*F crit*
Sample	1540.32	4	385.08	2485.11	<0.05	2.49
Columns	2.74	3	0.91	5.88	<0.05	2.72
Interaction	0.81	12	0.07	0.44	0.94	1.88
Within	12.4	80	0.15			
Total	1556.26	99				

The data in Figure 5.7 (A) show that each DIC addition between 1mm and 8mM DIC caused a stimulation of ETR at saturating PFDs. Analysis of these data with 2-way ANOVA demonstrated that the effects of irradiance and DIC addition on ETR were both significant between 4-34 umol m^{-2} s^{-1} (Table 5.7). DIC addition at low irradiances shown in Fig. 5.7 (B) appeared to cause a small increase in ETR, and analysis with 2-way ANOVA inducated that at these PFDs, the effects of both light and DIC were significant, although no interaction between the two factors occurred.

Using Microsoft Excel software, a trendline was fitted to the relative ETR values of the data shown in Figure 5.7, to determine the slope of α for each DIC

concentration, and is shown in Figure 5.8. Excel calculates the least squares fit for a line bases on equation 5.4.

$y - mx + b$ **Equation 5.4**

Where *m* is the slope, and *b* is the intercept. The R^2 values for 1 mM and 8 mM DIC were >0.99 indicating that the increase of relative ETR with irradiance was linear. DIC addition caused a small increase in the slope of α of 0.5 to 0.55.

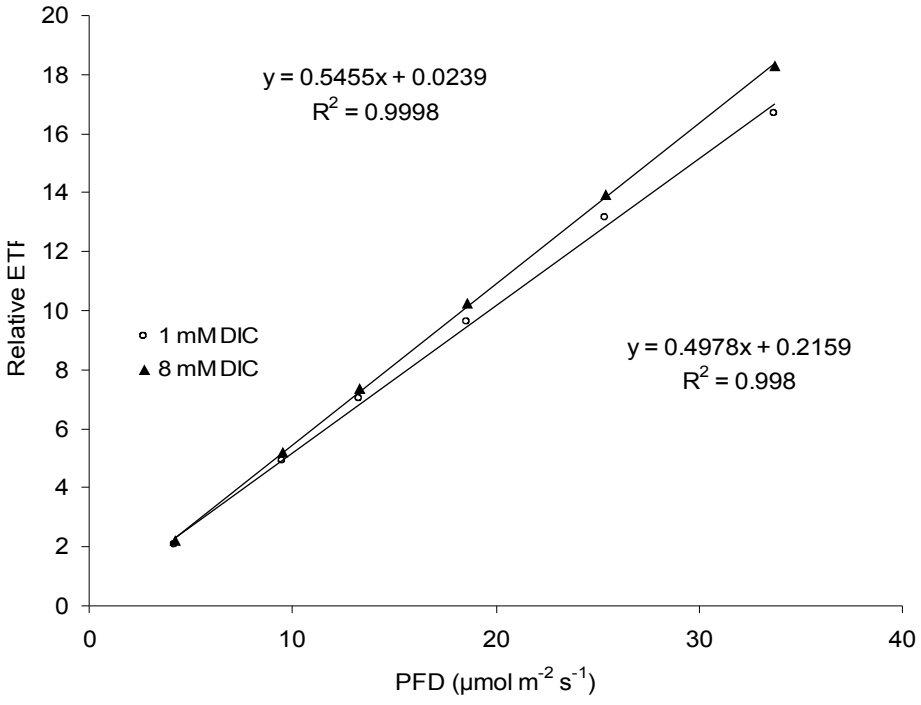

Figure 5.8 The effect of irradiance (PFD) on Relative ETR in *Palmaria palmata*, measured in artificial seawater containing 1 and 8mM DIC at PFD 4-34 µmol m^{-2} s^{-1}. Data are means +/- SE (*n*=5).

5.5 Discussion

There is evidence that HCO_3^- is directly involved in PSII photochemistry as an integral part of the water-splitting complex (Zouni *et al*. 2001), and is associated with the acceptor and donor side of Q_A (Dismukes *et al*. 2001). Therefore, it is possible that the stimulation of photosynthesis in macroalgae by DIC addition arises not only from a substrate effect on Rubisco, but also from a bicarbonate effect on PSII. It is not possible to distinguish between the former and latter effects at saturating light, since P_{max} is determined by the rate of CO_2 fixation by the Calvin cycle. The initial slope of a PI curve however, depends on the photochemical reaction, as Rubsico activity is limited by the rate of NADPH and ATP production (Falkowski & Raven 1997). Therefore, if light-limited photosynthesis increases with DIC addition, this would suggest that HCO_3^- may be stimulating the light reaction directly.

Against this background, it was hypothesised that increasing the DIC concentration in seawater would increase the rate of photosynthetic electron transport in macroalgae at subsaturating PFDs. By determining the effect of DIC addition on photosynthetic ETR at both saturating and subsaturing irradiances, the experiments described in this chapter were designed to investigate a possible bicarbonate effect in macroalgae.

It is shown in Chapter 3 that the ambient DIC concentration in seawater limits photosynthetic oxygen evolution in *P. palmata*, *C. crispus*, and *L. digitata*. Using a fluorescence monitoring system, DIC limitation was also demonstrated by the experiments in this chapter in *P.palmata*, *A. esculenta* and *L.digitata*,

which showed an increase in photosynthetic ETR at saturating light in response to DIC addition to natural seawater. By measuring induced chlorophyll fluorescence at a wide range of irradiances, it was possible to create PI curves to determine which PFDs limited the rate of photosynthetic electron transport, ie., the initial ascending slope α, and subsequently the effect of DIC concentration on light-limited photosynthesis could be investigated.

In the first experiments, which examined the effect of 6 mM DIC addition to buffered natural seawater on photosynthesis of *P. palmata*, *A. esculenta* and *L. digitata*, photosynthetic ETRs were substantially higher in all species at saturating light, yet at subsaturating PFDs between 13-38 μmol m^{-2} s^{-1}, there was no obvious stimulation of ETR. This is typical of the Blackman model, which shows no change in α with DIC addition, and an increase in V_{max} at saturating light. Use of 2-way ANOVA revealed that both light and DIC significantly increased ETR between 13-1020 μmol m^{-2} s^{-1}, and there existed an interaction between light and DIC. Since large differences were evident from the PI curves this significance was not unexpected, but the effect of DIC addition at low PFDs was less obvious. 2-way ANOVA confirmed that no significant effect of DIC was present at subsaturating PFDs in *P. palmata* and *A. esculenta*. In *L. digtata*, however, a significant effect of DIC was shown, and closer examination of the data points between 13-38 μmol m^{-2} s^{-1} showed a stimulation of ETR, although the increase was very small. Therefore, Bose's model appears to be true for this species.

Experiments with *P. palmata* in which ETR was measured at a wider range of irradiances and at DIC concentrations between 1mM and 8mM DIC, the findings

were similar to those of *L. digitata*: ETR increased with DIC addition at both saturating and subsaturating PFDs, though only slightly at subsaturating PFDs, and according to 2-way ANOVA the effect of DIC was significant at both saturating and subsaturating light.

A trendline fitted to the ETR values measured between 4-34 μmol m^{-2} s^{-1} in ASW containing 1mm and 8mM DIC showed a very high R^2 value, indicating that the relationship between ETR and irradiance at these PFDs is linear, and they therefore represent α. The slope of these trendlines was calculated to be 0.5 and 0.55 in the 1mM and 8mM DIC treatments respectively, indicating that DIC addition produced a 10% increase in α.

Previously, only Mercado *et al.* (2001) have examined the interaction of light and DIC at above-ambient DIC concentrations in marine macroalgae, and they concluded that, in three *Gelidiales* species, DIC is not limiting at subsaturating light. The discrepancies between their findings and the findings of the present study may have arisen from species differences: indeed, the present study has shown that photosynthesis was stimulated at low irradiance in only one of the three species tested, and significant stimulation was detected in *P. palmata* only when photosynthesis was examined at a below-ambient DIC concentration. Since different techniques were used to measure photosynthesis in each study (photosynthesis was measured by Mercado *et al*. (2001) using oxygen electrodes), a direct comparison of the data is not possible. It is clear from the data presented in this chapter that chlorophyll fluorescence measurements were precise at subsaturating light, since standard error was small in groups of ETR measurements taken at low PFDs. Therefore, this may have allowed for

the small differences in ETR to be detected in *P. palmata* and *L. digitata*. In conclusion, DIC stimulation of light-limited photosynthesis may not have been reported in previous studies of marine macroalgae because the resopnse is species-dependent, and can only be detected when photosynthesis is measured at above-ambient DIC concentrations, or (as is the case with *P. palmata*), when rates of photosynthesis is compared between below-ambient DIC and above-ambient DIC concentrations. To establish this it would be necessary to examine a larger number of species at a wide range of DIC concentrations and irradiances, and if photosynthetic oxygen evolution and induced chlorophyll fluorescence were measured simultaneously, this would provide stronger evidence.

Since DIC stimulation of light-limited photosynthesis was very small in *L. digitata*, put in an ecological context, this suggests that for macroalgae growing in seawater, an increase in the ambient DIC concentration is unlikely to produce a substantial increase in photosynthesis at subsaturating irradiances. Blackman's adaptation of Leibig's "law of the minimum" is, therefore, more accurate than Bose's model for the light-limited environments occupied by benthic marine macroalgae. Therefore, the predicted rise in seawater DIC concentration is unlikely to stimulate photosynthesis in light-limited environments, but will increase photosynthesis at saturating light. However, in laboratory conditions where photosynthesis is examined below and above the ambient DIC concentration, Bose's model may be more accurate for some species.

Chapter 6

Seasonal variations of DIC uptake in *Palmaria palmata*

6.1.1 Introduction

A decrease in irradiance caused by the scattering and absorption of light as it passes through water is known as attenuation, and has profound effects on productivity in aquatic environments. In pure water, the penetration of light is at least 2000-fold less than in air, and in seawater, attenuation of light by various processes and particles determines the quality and quantity of light that is available for photosynthesis.

An attenuation coefficient can be calculated after measuring irradiance at two different depths, by using Equation 6.1.

$$\text{Attenuation coefficient, } K(m^{-1}) = \frac{\log I_1 - \log I_2}{d_2 - d_1} \qquad \textbf{Equation 6.1}$$

where I_1, I_2 = irradiance at depths 1 and 2

d_1, d_2 = depths of two measurements in metres (Dring, 1982).

Other than by seawater itself, scattering of light in the ocean is caused by particles > 2μM, which contribute to attenuation by increasing the length of the optical path of quanta Light that leaves the water due to scattering is defined as water-leaving radiance (L_W), and can be remotely sensed with satellites. Some marine algae produce structures that scatter light, and thus increase the length and optical path of photons which have not been absorbed by reaction centres and the molecules in seawater. These include silica frustules synthesised by diatoms, and $CaCO_3$ plates such as the coccoliths that are

synthesised by *E. huxleyi* , which scatter light to such an extent that it can be seen in satellite images. Falkowski & Raven (1997) have suggested that such light-scattering structures increase the amount of light available for photosynthesis, although it is possible that they are used to cause heterogeneity in the light field, since this stimulates photosynthesis and growth in some algae (Greene & Gerard 1990; Drew 1983).

The spectral composition of natural light is altered by its penetration through water. Seawater maximally absorbs light energy in the infrared and far-red regions (wavelengths >700 nm), and since the bulk of this is absorbed by the first 1 m of water in the sea, it accounts for the strong heating effect of surface waters by solar radiation. Also, because the photosynthetic pigments in algae absorb wavelengths of light between 400 nm to 700 nm, this means most of the light below the first meter of seawater is in the photosynthetically active range.
In optically uniform waters, irradiance decreases exponentially with depth, and in surface waters this determines rates of photosynthesis in phytoplankton (Figure 6.1).

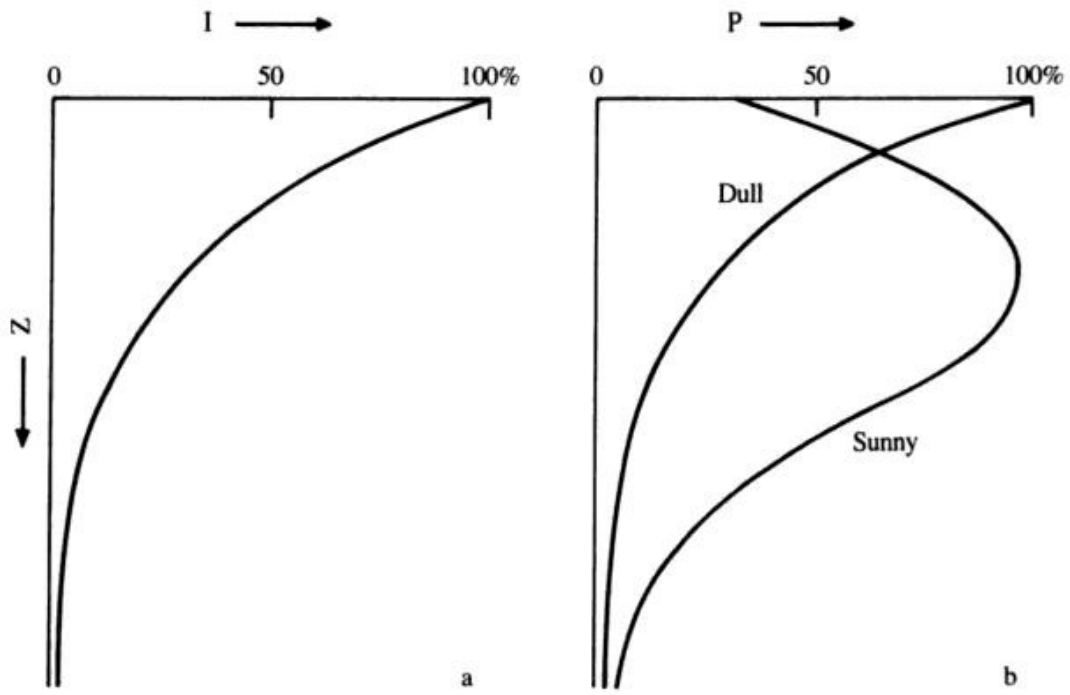

Figure 6.1 (a) penetration of light into water; irradiance (I) as a percentage of that at the surface as a function of depth (Z); (b) rate of photosynthesis (P) as a percentage of the maximum as a function of depth under dull and bright conditions. Reproduced from Fogg & Thake (1987).

Figure 6.1 shows that under dull light conditions, the rate of photosynthesis in phytoplankton decreases exponentially with depth. In bright light, however, photosynthesis initially increases with depth, then decreases. This results from photoinhibition of photosynthesis in phytoplankton inhabiting surface waters.

Components of seawater that absorb light include phytoplankton cells and colonies, phaeocopigments (the degradation products of phytoplankton pigments), and chromophoric dissolved organic matter (Kirk, 1994). Waters containing large quantities of phytoplankton and phaeocopigments tend to be green in colour because the chlorophyll pigments absorb short wavelengths of light, although this can vary depending on the pigments that are present.

Chromophoric dissolved organic matter, also known as “yellow substance” and “gelbstoff”, is the name given to dissolved organic matter which is most concentrated in productive waters, and is transported to the sea in runoff water. This absorbs light mostly in the blue spectrum.

Jerlov (1976) has classified seawaters according to their spectral transmittance, and distinguished three ocean-water types and nine coastal water types. Coastal type nine, for example, represents eutrophic coastal waters that contain large quantities of algae and organic solutes, which absorb approximately 50 % per meter of the shorter wavelengths of light, up to 550 nm. Therefore, most of transmitted light is in the green region (575 nm) and is photosynthetically inactive, except in some red algae and cyanobacteria where it is absorbed by phycobiloproteins (Falkowski & Raven, 1997) .

As well as attenuation, the interaction of light with seawater is also affected by its heterogenicity over time, and the effect of the water surface on light penetration. Unpredictable changes in light heterogenicity result from cloudiness, turbidity caused by storms, runoff and seasonal plankton blooms, whereas more predictable changes occur seasonally and diurnally. The interaction of light with the sea surface also influences light penetration into seawater, because some light is always reflected. The extent of reflection varies depending on the solar angle, which is determined by the roughness of the water (Lobban & Harrison, 1997).

6.1.2 Seasonal patterns of productivity in algae.

Although light is an important limiting factor of productivity in the marine environment, spatial and temporal fluctuations of environmental factors can significantly influence algal growth (Lobban & Harrison, 1997; Fogg & Thake, 1987; Dring, 1982). The success of phytoplankton populations, for example, can be determined by interactions between mixing in the water column and light and nutrient availability, and grazing by zooplankton. The size of phytoplankton populations in temperate waters typically follows a distinct seasonal pattern, which is characterised by a spring peak, followed by a rapid decrease during summer, a second, smaller peak in autumn, and another rapid decrease in winter which persists until the next spring.

During winter, the water column is well-mixed, and in the absence of phytoplankton growth, nutrient concentrations are high. Because of the water mixing, that total amount of radiation received by cells will be very small, since they spend little time in photic zone. The average radiation available to a phytoplankton population per day ($\bar{I}$) can be calculated by Equation 6.2, after Riley (1957).

$$\bar{I} = \frac{I_o(1-e^{-kz})}{Kz} \qquad \textbf{Equation 6.2}$$

Where I_o is the incident radiation, z is the depth of the water column, and k is the vertical extinction coefficient. When $\bar{I}$ is too small to support net photosynthesis, no growth of phytoplankton will occur. During spring, as I_o increases, and thermal stratification reduces the depth of mixing in the water column, phytoplankton are able to photosynthesise and grow, and a spring peak

or “spring bloom” in phytoplankton growth and population size occurs.

The decline in the phytoplankton population during summer can be attributed to three factors: light limitation caused by self-shading in dense population, a depletion of nutrients in surface waters, and grazing by zooplankton. By late summer, once the phytoplankton population has remained low for long enough to cause a concomitant decrease in grazing zooplankton, and an increase in the concentration of nutrients, a second peak in autumn often occurs. This is short-lived, however, as thermal stratification decreases, and the depth of the mixed layer increases (Fogg & Thake, 1987).

Macroalgae also experience large changes in physical and chemical factors such as light, temperature, and nutrient availability (Davison & Pearson, 1996), and Dring (1982) has suggested that the intertidal habitat is among the most variable to be found on Earth. When macroalgae are transferred from an aquatic to a terrestrial environment, for example, they endure sudden changes in temperature, and reductions in water supply and the availability of essential solutes. During submersion, they are also subjected to light and nutrient limitation, high salinity, and physically damaging wave action. Seasonal environmental changes are less abrupt by comparison, yet considerable variations in light, temperature and inorganic nutrient concentrations can occur (Perez-Llorens *et al*. 2004; Martinez & Rico 2002; Esminger *et al*. 2000).

When King & Schramm (1976) monitored photosynthesis in 27 benthic seaweeds from the Western Baltic Sea during spring, summer, autumn and winter months, and discovered that there were seasonal patterns of

photosynthesis which varied in different species. Photosynthesis in macroalgae does not always appear to follow a distinct seasonal pattern, however. Maximum rates of photosynthesis in *Fucus serratus* for example, remained relatively constant throughout the year, and photosynthesis in *Himanthalia elongata* collected from a nearby shore varied considerably during the year, but lacked a distinct seasonal pattern (Brenchly *et al.* 1997).

In the present study, seasonal changes in photosynthesis and bicarbonate transporter activity were monitored in *P. palmata* growing at St. Margaret's Bay near Dover, where it predominates in pools and streams that are filled with water that can be observed emanating from springs during low tide. Because the tides on this shore are semi-diurnal, at its highest position on the shore of about 1.5 metres above chart datum, *P. palmata* is submersed in the springwater for up to five hours each day. Although the springwater is clear, at high tide the seawater covering the macroalgae is chalky and turbid, and at low tide thalli can often be observed covered in particulate chalk. *P. palmata* growing in the *Laminaria digitata* zone at St. Margaret's Bay is also exposed to the springwater at low tide, but only briefly.

Seasonal changes in photosynthesis at the ambient DIC concentration were determined by making monthly measurements of photosynthetic oxygen evolution in ASW containing 2mM DIC, between February 2003 and April 2004. DIC limitation was examined by comparing photosynthesis at 2mM DIC with photosynthesis in DIC-saturated ASW, containing 8mM DIC. Bicarbonate transporter activity was determined by measuring the effect of SITS addition on

photosynthesis. It was hypothesised that plants growing in the *Laminaria* zone would show different seasonal patterns of photosynthesis, since they are more deeply submerged at high tide (thus, more light-limited), and are less exposed to springwater at low tide compared to high shore plants. Therefore, for comparison, photosynthesis was also examined in low-shore plants.

6.2 Aims

To answer the following questions:-

What are the seasonal variations in photosynthesis and DIC uptake in *P. palmata* ?

Are there seasonal changes in bicarbonate transporter activity in *P. palmata*?

Do high and low shore plants show different seasonal variations in photosynthesis and DIC uptake?

6.3 Materials and Methods

Seasonal measurements of photosynthesis and bicarbonate transporter activity in *P. palmata* growing at St. Margaret's Bay were carried out each month between February 2003 and May 2004. High shore plants were collected approximately 1.5 m above chart datum, whereas low shore plants were collected approximately 0.5 m above chart datum. Plants were transported to the lab and maintained as described in Chapter 2. Experiments were completed within 16 hours of collection. Photosynthetic oxygen evolution was measured using Hansatech oxygen electrodes, in simplified Harrison's seawater medium buffered to pH 8.2 with 20 mM Bicine. Photosynthesis was measured at 2 mM and 8 mM DIC, and at 2 mM DIC after the addition of 1 mM SITS.

At the time of collection, the temperature of the spring water in which the *P. palmata* used in experiments was growing, was measured using a mercury thermometer. Samples of spring water of approximately 50 mL were collected in plastic polypropylene tubes, and immediately upon arrival at the laboratory their salinity was determined and they were then stored at -20°C. The nitrate contents of defrosted samples were determined using the cadmium/copper reduction method, as described in Chapter 2.

6.4 Results

Light-saturated rates of net photosynthesis in *P. palmata* were measured monthly from February to December during 2003. Fig. 6.2 shows the rates of photosynthesis measured in artificial seawater containing 2mM DIC and 8mM DIC, and 2 mM DIC after the addition of 1mM SITS.

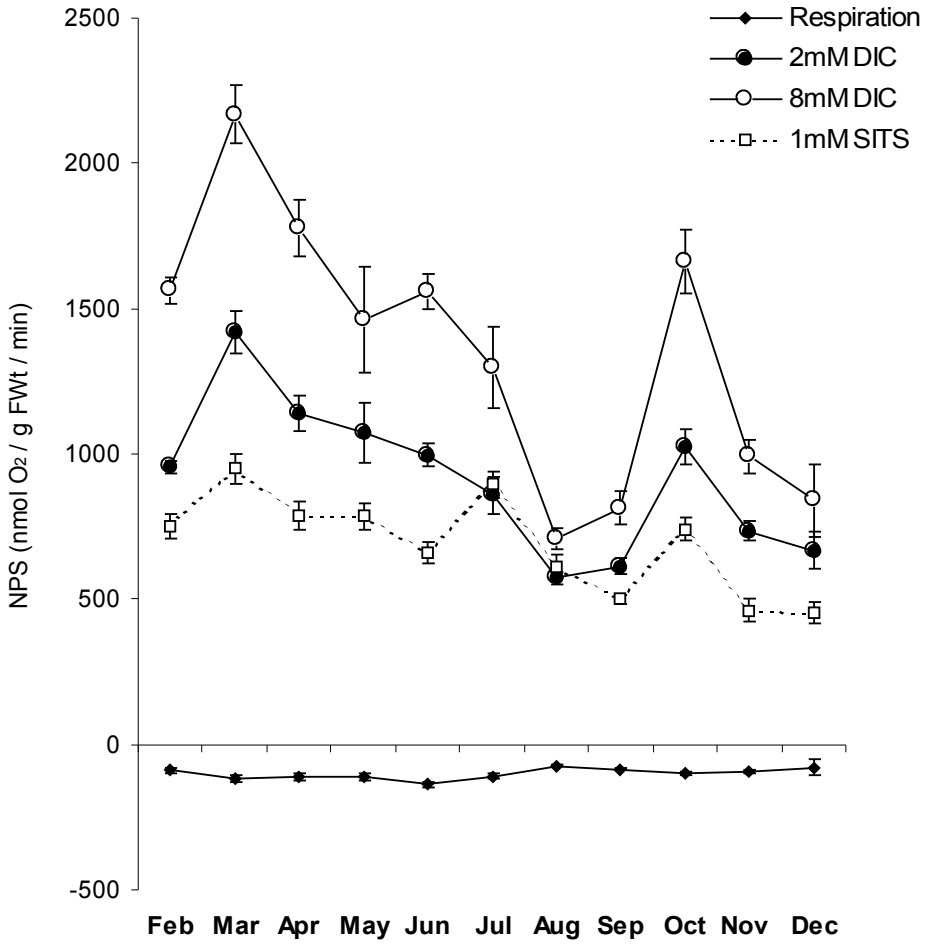

Figure 6.2 Dark respiration rates and net photosynthesis (NPS) of *P. palmata* collected from St. Margaret's Bay at monthly intervals during 2003, measured at 15°C in artificial seawater medium containing 2mM DIC, 8mM DIC, and 2mM DIC + 1mM SITS. Data points are means SE +/- *n*=6-8.

Distinct peaks in photosynthesis occurred during March and October. Rates of photosynthesis increased from February and peaked in March, then gradually decreased from March until August, and increased again towards a second peak in October. Rates of photosynthesis increased between 2mM and 8mM DIC in samples collected throughout the year, and was most pronounced in Spring and early Summer. Inhibition of net photosynthesis by the addition of 1mM SITS was also greatest during Spring and early Summer, but declined towards August, when no significant SITS inhibition was measured (t-test p = 0.27). The effect of DIC addition and SITS inhibition were tested for significance with 2-way ANOVA, shown in tables 6.1 and 6.2 respectively.

Table 6.1 2-way ANOVA for the effect of DIC stimulation on photosynthesis from February to December in *P. palmata* growing at St. Margaret's Bay.

Source of Variation	*SS*	*df*	*MS*	*F*	*P-value*	*F crit*
Month	15988148	10	1598815	28.00851	<0.05	1.917827
DIC	6526215	1	6526215	114.3282	<0.05	3.927393
Interaction	1480723	10	148072.3	2.593974	0.0073	1.917827
Within	6279150	110	57083.18			
Total	30274235	131				

Table 6.2 2-way ANOVA for the effect of SITS on photosynthesis from February to December in *P. palmata* growing at St. Margaret's Bay.

Source of Variation	*SS*	*df*	*MS*	*F*	*P-value*	*F crit*
Month	4977680	10	497768	25.24512	<0.05	1.917827
SITS	1772654	1	1772654	89.90307	<0.05	3.927393
Interaction	960604.8	10	96060.48	4.871865	<0.05	1.917827
Within	2168913	110	19717.39			
Total	9879852	131				

Net photosynthesis at 2mM and 8 mM DIC in low shore plants are plotted against the rates in high shore plants in Fig 6.3A and 6.3B respectively. Low shore rates were generally lower than high shore rates at both DIC concentrations. However, in July and August high and low shore rates were similar at both DIC concentrations..

Differences in high shore and low shore rates of photosynthesis at 2mM and 8mM DIC were tested for significance using 2-way ANOVA. This is shown in tables 6.3 and 6.4.

A

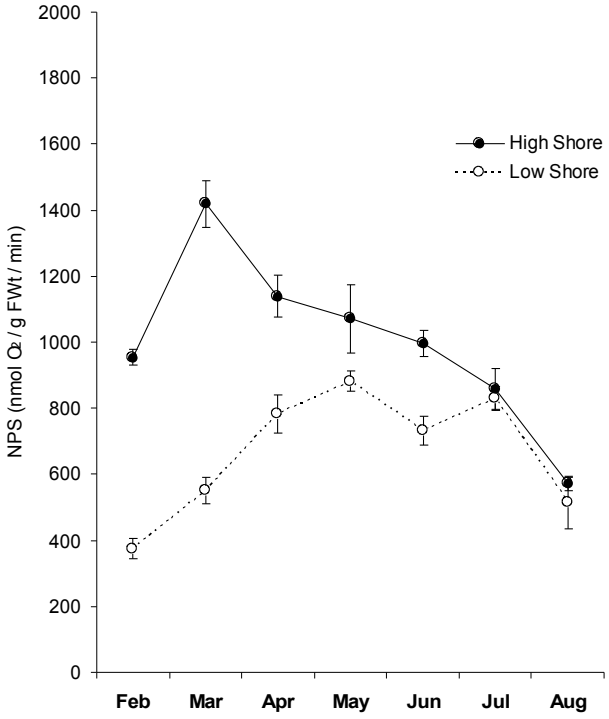

B

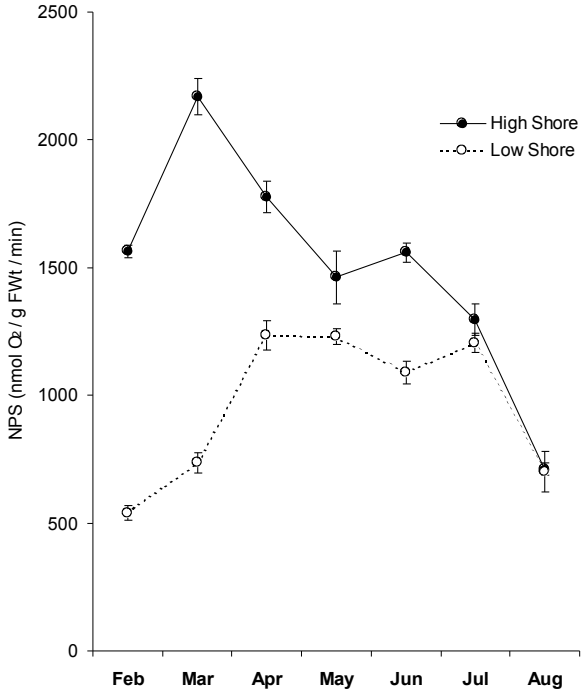

Figure 6.3 Net photosynthesis of *Palmaria palmata* in artificial seawater containing **A** 2mM DIC and **B** 8mM DIC, in high shore and low shore plants. Means are +/- SE *n*=(6-8)

Table 6.3 2-way ANOVA for the effect of month of measurement and height on shore on photoynthesis in *P. palmata* at 2mM DIC.

Source of Variation	*SS*	*df*	*MS*	*F*	*P-value*	*F crit*
Month	2101353	6	350225.5	18.15149	<0.05	2.231192
Height on shore	2422880	1	2422880	125.5731	<0.05	3.977779
Interaction	1733751	6	288958.5	14.97615	<0.05	2.231192
Within	1350621	70	19294.58			
Total	7608605	83				

Table 6.4 2-way ANOVA for the effect of month of measurement and height on shore on photoynthesis in *P. palmata* at 8mM DIC.

Source of Variation	*SS*	*df*	*MS*	*F*	*P-value*	*F crit*
Sample	5408048	6	901341.3	15.14142	<0.05	2.231192
Columns	6329292	1	6329292	106.3243	<0.05	3.977779
Interaction	5118405	6	853067.4	14.33048	<0.05	2.231192
Within	4166974	70	59528.2			
Total	21022718	83				

Net photosynthesis in *P. palmata* was also measured from January to April during 2004, to investigate if a similar March peak in photosynthesis occurred again. Photosynthesis measured at 2mM DIC and 8mM DIC are shown in Fig 6.4 A and Fig 6.4 B respectively, and demonstrates that the rates during 2003 and 2004 are very similar. This was tested statistically using 2-way ANOVA, shown in tables 6.5 and 6.6, and no significant difference was found.

A

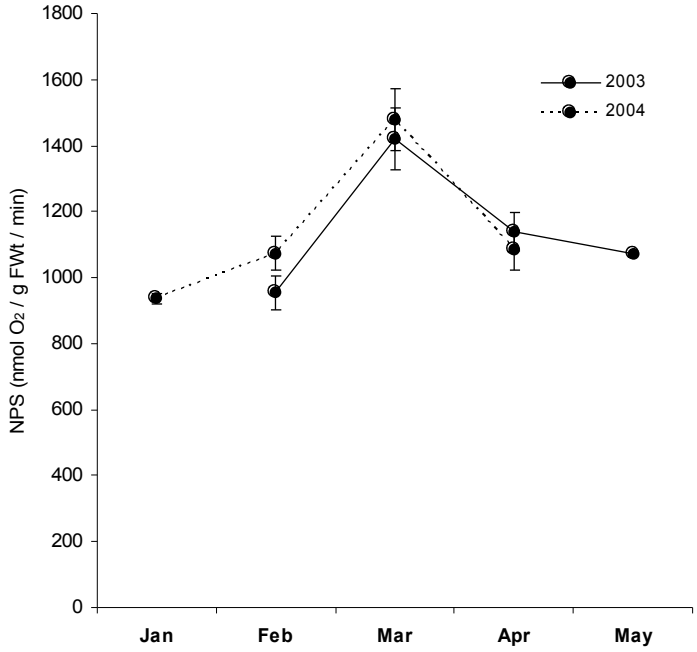

B

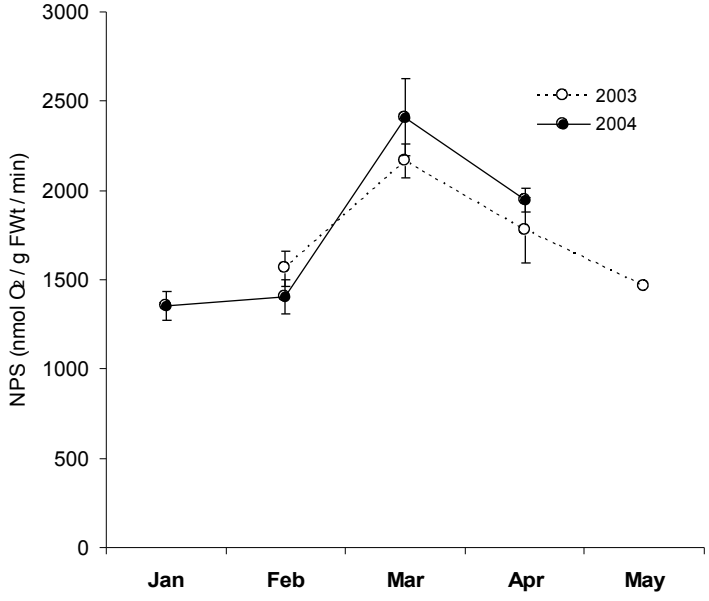

Figure 6.4 Net photosynthesis of *Palmaria palmata* in artificial seawater containing (A) 2mM DIC , and (B) 8 mM DIC, measured in plants collected from St. Margaret's Bay during 2003 and 2004. Means are +/- SE (*n*=6-8)

Table 6.5 2-way ANOVA for rates of photosynthesis in *P. palmata* at 2mM DIC, measured from February-April during 2003 and 2004.

Source of Variation	*SS*	*df*	*MS*	*F*	*P-value*	*F crit*
Month	1387408	2	693704.2	18.13098	<0.05	3.31583
Year	14755.66	1	14755.66	0.385661	0.539279	4.170877
Interaction	133751.7	2	66875.85	1.747899	0.19141	3.31583
Within	1147821	30	38260.71			
Total	2683737	35				

Table 6.6 2-way ANOVA for rates of photosynthesis in *P. palmata* at 8mM DIC, measured from February-April during 2003 and 2004.

Source of Variation	*SS*	*df*	*MS*	*F*	*P-value*	*F crit*
Month	4385826	2	2192913	19.92681	<0.05	3.31583
Year	303166.1	1	303166.1	2.754844	0.107379	4.170877
Interaction	348412.8	2	174206.4	1.582998	0.222036	3.31583
Within	3301452	30	110048.4			
Total	8338856	35				

The temperature of the water from which *P. palmata* was collected was measured each month, and samples of springwater taken from the site of collection was analysed for nitrate content and salinity. These measurements are shown in Figure 6.5, as well as the mean fresh weight of 9mm discs of thalli used in experiments.

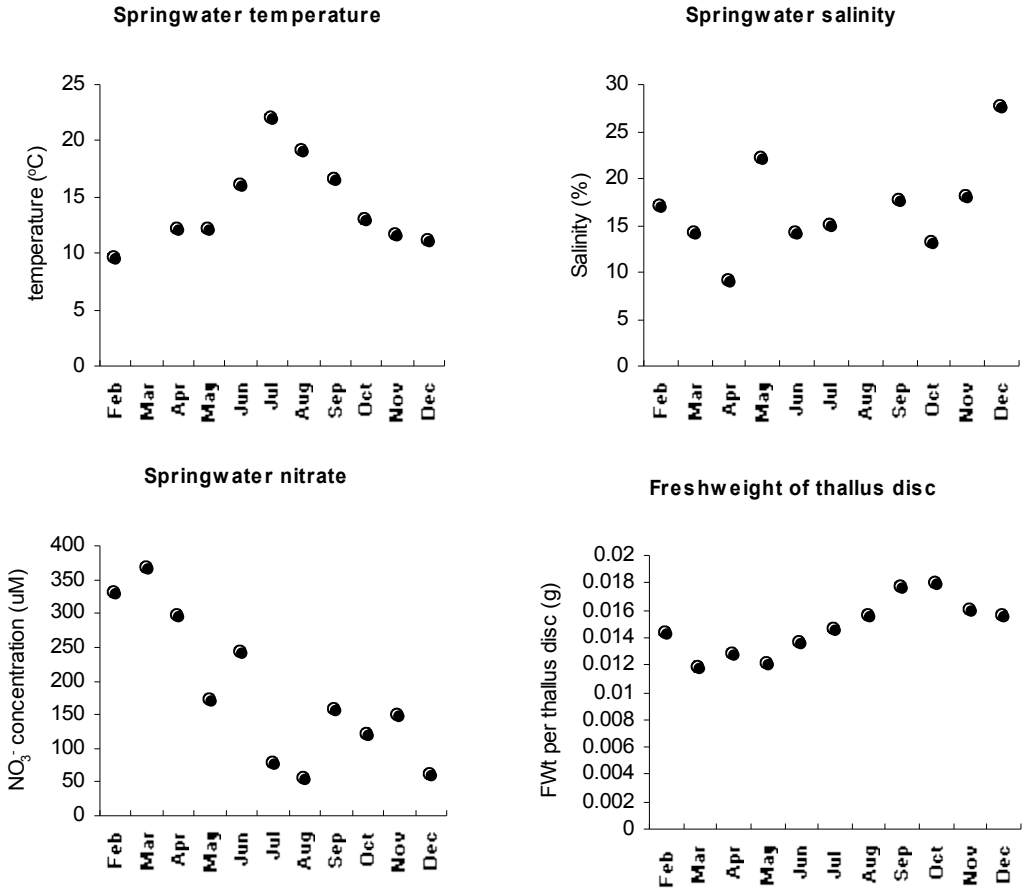

Figure 6.5 Measurements of temperature (°C), salinity (‰), and nitrate concentrations (µmol) concentrations of water collected directly from springs at St. Margaret's Bay, and the mean fresh weight of 9mm discs of thalli used in experiments.

The nitrate content of the springwater varied during the year between 50 µmol and 370 µmol. but appeared to gradually decline from February until December. The highest concentration of 366.7 uM was measured in March and the lowest of 55 uM in August.

The mean fresh weights of the 9 mm discs of thalli used in experiments, were greatest during Winter, and smallest during Summer. Plants collected during

early Spring were smaller and possessed thinner thalli, indicating the onset of new growth, whereas in Winter, they became visibly thicker.

It was anticipated that DIC concentrations could have been determined in the springwater over the time in which *P. palmata* was monitored, by using the Gran titration method (as described in Chapter 2). Unfortunately this was not possible, since the DIC had precipitated in samples that had been stored at –20ºC, and part of each sample had been removed to measure salinity and nitrate concentrations (thus, the original sample volume could not be determined). However, the springwater samples from February, April and August 2003 had been measured on the day they were collected, and were 3.9 mM, 4 mM, and 4.1 mM respectively.

6.5 Discussion

P. palmata growing at St. Margaret's Bay showed substantial seasonal variations in net photosynthesis, DIC stimulation, and bicarbonate transporter activity. In high shore plants, a spring peak in light-saturated photosynthesis occurred in March, then photosynthesis decreased rapidly during spring and summer. Lowest rates were measured in August, which were only about a third of the maximum yearly rate, and a second, smaller peak measured in October was followed by a rapid decline in November and December. A spring peak was also measured in March 2004.

Salinity of the springwater collected from where *P. palmata* was harvested, varied between about 8-28ppt, indicating that it had mixed with seawater. There was some evidence that its DIC content was about double that found in seawater, and its nitrate content varied between about 50 μM and 400 μM. Nitrate concentrations were highest between February and April, and lowest in July, August and December.

The reason for the distinct peaks in photosynthesis is not clear from the data shown in this study. However, it appears that they coincided with the equinoctial tides during 2003, and in the spring equinoctial tide in 2004. During this time:-

1 Because of a fast increase in day length in the weeks approaching the spring equinox, and since plants were submersed in shallow waters, the incident irradiance on the thallus would have been high compared to previous months.
2 Plants will be submersed for longer in the springwater/seawater mixture, therefore would have been exposed for longer to the high concentrations of carbon and nitrate measured in the springwater.

Thus, as a result of the high light and nutrient availability during spring and autumn, photosynthesis and growth may have been stimulated as they are in phytoplankton.

DIC addition stimulation of photosynthesis occurred throughout the year, but was greatest in thalli collected during March and October, suggesting that

during these times, thalli were most limited by DIC. The decline in photosynthetic rates following the spring and autumn peaks indicate that DIC became less limiting during this time.

If it is assumed that the DIC content of the springwater was approximately 4 mM throughout the year, according to the nitrate measurements, this means that the C:N ratios during the March and October peaks were approximately 10:1 and 21:1 respectively. During August, when thalli were least photosynthetically active, the C:N ratio was approximately 80:1. Given that the accepted average for the C:N:P ratio in marine plants that are not nutrient-limited is 106:16:1, which describes a C:N ratio of 6.625:1 (Redfield, 1958), this suggests that thalli submerged in springwater are not limited by carbon at any time of year. However, since exposure to springwater is maximal during the equinoctial tides, and declines during summer, it is possible that carbon is more limiting during spring and autumn compared to summer and winter months. Because thalli in summer spend more time covered in the turbid chalky seawater, it is also possible that despite an increase in the incident irradiance on the sea surface, they receive less light compared to spring and autumn. Dring (1987) has shown that the intertidal habitat receives less light in summer than in spring because the high tide is more likely to occur during the day. Therefore, in high shore plants, photosynthesis and growth may be determined more by the availability of nutrients than by light.

This idea is supported by measurements of photosynthesis in low shore plants which received less exposure to the springwater, and although photosynthesis increased from February to April, no distinct March peak was shown. Also,

photosynthetic rates were substantially less than in high shore plants until July, at which point exposure of the high shore plants to springwater would also have decreased. By August, the height of the low tide had increased to such an extent that it became difficult to harvest low shore plants, therefore it was not possible to compare autumn and winter photosynthesis in low and high shore plants.

It is established that macroalgae are capable of accumulating and storing nutrients in thalli when the seawater concentrations are high during autumn and winter, so that they can be used to support growth when the seawater concentrations become limiting during summer. Seasonal variations in the thallus content of N and P in two northern Spanish populations of *P. palmata* have been examined by Martinez & Rico (2002). They suggested that these elements are stored mainly as phycoerythrin, and accumulated during autumn and winter months when growth became light-limited, and the seawater N and P concentrations increased. The onset of spring growth led to a decline in the thallus N and P content, and by late summer, when both seawater and thallus concentrations of these elements was very low, growth was suppressed, suggesting nutrient limitation had occurred. In *Laminaria longicruris*, it was shown that an increase in seawater nitrate results in the accumulation of nitrate in thalli which is up to 28,000 greater than the maximum seawater concentration. Net photosynthesis in this species is maximal during mid summer, and an accumulation of the laminarin polysaccharide content in tissues suggests that excess photosynthate is being stored. A decrease in photosynthesis during autumn and winter is followed by a rapid decrease in

laminarin content, indicating that it is used to support growth when light is limiting and temperatures are low (Chapman & Cragie, 1978; 1977).

Since the experiments in this chapter were not designed with set hypotheses, and instead were used to determine how photosynthesis and bicarbonate transporter activity were influenced by seasonality, they do not support any of the far-reaching conclusions described above. However, they provide important information which could be used to indicate the direction of future work. For example, although it is not possible to establish if exposure to the springwater influences photosynthesis and bicarbonate transporter activity in *P.palmata*, the experiments in this chapter suggest that it may increase photosynthesis if exposure is long enough to allow sufficient amounts of C and N to be taken up by thalli, and if the incident irradiance is high. In future experiments it would be interesting to examine the relationship between length of exposure to the springwater, and the N and C content in thalli. According to the previous studies of *P. palmata* and *L. longicruris*, increased exposure to the nutrient-rich springwater during the equinoctial tides at St. Margaret's Bay would result in tissue accumulations of nutrients, which decline as exposure to the springwater decreases during summer and winter. However, unlike *L. longicruris*, which showed maximal photosynthesis in mid-summer, a decline in photosynthesis is observed from March onwards. It is possible, however, that in *P. palmata*, growth during winter is supported by photosynthate accumulated during the autumn peak in photosynthesis.

Chapter 7

Discussion

The present study has shown that at the ambient DIC concentration in seawater, *Palmaria palmata* uses an AE1-like mechanism to procure bicarbonate as a source of DIC for photosynthesis. Previous studies of bicarbonate transporters in marine algae have relied almost exclusively on inhibitor evidence, and are vulnerable to the criticism that inhibitors may be non-specific. Only Sharkia *et al* (1994) have provided molecular evidence for the presence of this mechanism in *Ulva* sp. An important aim in the present study, therefore, was to provide both biochemical and molecular evidence for the presence of this mechanism in *P. palmata*.

By using the large amount of genetical research surrounding mammalian AE1, the polymerase chain reaction was successfully used to clone functional regions of bicarbonate transporter genes in *P. palmata* and *E. huxleyi*. These were shown to be highly homologous to an AE1 gene cloned from *Rattus norvegicus*, which not only reinforces the inhibitor evidence of bicarbonate transporters in algae, it also represents the first description of the AE1 gene outside the animal kingdom.

Now that the gene sequences are known, there is the potential for algal bicarbonate transporters to be examined in algae with various molecular techniques. Specific fluorescent DNA probes can be designed, for example, which bind to bicarbonate transporter gene sequences, and could be used to screen for the presence and activity of AE1 in natural populations of algae, and algae in culture. Also, the expression of bicarbonate transporters in response to environmental factors, such as concentrations of DIC and other essential

nutrients, and changes in temperature and light supply, could be determined with real-time PCR, which allows gene expression to be quantified.

In future experiments, such techniques could be used to investigate the inhibitor experiments in the present study, such as the experiments where DIDS was used to demonstrate that AE1 activity in *P. palmata* was suppressed at low DIC and increased at elevated DIC, whereas in *C. crispus* the normally-absent AE1 mechanism was induced at elevated DIC. Although these experiments indicate there is a relationship between DIC concentration and AE1 activity in these species, they do not determine whether DIC was influencing a mechanism that regulates the activity of the AE1 protein in the cell membrane, or if it was regulating the rate of transcription of the AE1 gene in the cell nucleus. This could be examined, however, if real-time PCR is used alongside AE1 inhibitors to monitor the rate of transcription of the AE1 gene in response to DIC concentration. For example, if AE1 activity increased in response to elevated DIC but did not cause an increase in transcription of the AE1 gene, this would suggest that transcription is not used as a regulatory factor in response to DIC concentration.

In previous studies, algal bicarbonate transporters have only been investigated in their role as DIC uptake mechanisms, perhaps because the principal function of AE1 in animals is to mediate HCO_3^- transport in erythrocytes. Yet AE1 in animals is involved in several other processes, such as regulating pH, osmotic balance, and chloride concentration in several types of animal cell (Sterling 2002). It can also transport anions other than HCO_3^-, such as NO_3^- and PO_4^-

(Cabantchik 1991). Since the present study has shown that the bicarbonate transporters in *P. palmata* and *E. huxleyi* are both genetically similar to AE1 in rats, it is possible that they perform numerous functions in algae as they do in animals.

If the algal mechanism is capable of transporting NO_3^- and PO_4^- as well as HCO_3^-, for example, it may be involved in N and P acquisition. Consequently, the presence of the mechanism would have important ecological consequences, by reducing the nutritional and energetic cost of using three separate mechanisms. Algae growing in oligotrophic waters that possess AE1 may therefore have a competitive advantage over algae that procure DIC with external CA exclusively, and use additional mechanisms to procure N and P. It can be argued, however, that high concentrations of NO_3^- and/or PO_4^- would competitively inhibit HCO_3^- uptake. Thus, AE1-users growing in eutrophic waters would be inefficient at acquiring DIC, unless the ambient HCO_3^- was also high.

The historical decline of DIC in seawater is likely to have affected the expression of DIC acquisition mechanisms in algae (Giordano *et al* 2005), and *P. palmata* may have responded by increasing the activity of its bicarbonate transporter mechanism. In contrast, the external CA mechanism may have been downregulated to an extent that it is now no longer active at ambient DIC, and instead acts as a supplementary mechanism of DIC uptake at low DIC.

In a wider context and in the longer term, the forecast acidification of seawater

associated with the rising levels of atmospheric CO_2 will cause an increase in HCO_3^- concentration. According to experiments in this study with *C. crispus*, this may induce bicarbonate transporters in algae that currently use extracellular CA. To establish this, it would be necessary to repeat this experiment using a wider range of DIC concentrations, which are more similar to the concentrations predicted for future oceans, and to examine many more species. An increase in DIC may confer a competitive advantage to species which possess the bicarbonate transporter mechanism, and to those with the ability to induce it, so that they will replace species that rely on extracellular CA.

Previous studies have established that HCO_3^- binds to the acceptor and donor sides of Q_A, and it has also been shown that photosythetic electron transport in isolated thylakoid membranes of *Chlorella* sp. is DIC-dependent.. In the present study, it was hypothesised that DIC addition stimulates PSII activity in algae, and would therefore increase the rate of photosynthetic electron transport at both saturating and subsaturating light. As a result, the relationship between light and DIC supply would be the same as that described by Bose (1924) rather than the more widely-accepted Blackman model (1903).

Experiments in this study show that, at saturating light, DIC addition to buffered natural seawater increases photosynthetic electron transport rate (ETR) in three species of macroalgae: *P. palmata*, *Alaria esculenta*, and *L. digitata*, and in the latter species DIC significantly also increases photosynthesis at subsaturating light, although this effect was very small. DIC stimulation of ETR at subsaturating light also occurred in *P. palmata* when measured at below-

ambient and above-ambient DIC concentrations, but again, only a small increase was shown.

These findings suggest that, depending on species, the interaction between DIC and light in marine macroalgae can be true to either Blackman's or Bose's model. This has not been shown in previous studies, perhaps because photosynthesis is seldom examined in marine algae at elevated DIC concentrations, and also because the increase in stimulation may be too small to easily detect. Since the predicted increase in ambient DIC in seawater is much smaller than the DIC additions used in these experiments, it is unlikely that photosynthesis at subsaturating irradiances will increase in macroalgae growing in the marine environment.

Conclusions.

The present study has shown that *P. palmata* possesses two mechanisms for acquiring DIC for photosynthesis – a bicarbonate transporter genetically similar to mammalian AE1, which is used as the sole mechanism of DIC uptake at the ambient DIC concentration in seawater, and an extracellular carbonic anhydrase which is active at low DIC. Extracellular CA can be induced in thalli incubated in ASW containing 0-0.25mM added DIC when an N-source is present. AE1 is present at both below-ambient and above-ambient DIC concentrations, and unlike CA, its activity is not regulated by DIC availability in *P. palmata*, but it is induced by DIC addition in the CA-user *Chondrus crispus*. AE1 activity in *P. palmata* varies with season, and is most active in spring, and least active during late summer. Like AE1 activity, rates of photosynthesis

peaks during spring, and shows a decline from spring to summer, followed by a second peak in autumn. Study of the interaction between light and DIC in P. palmata demonstrated that photosynthesis is limited by DIC at saturating irradiances, and measurements of induced chlorophyll fluorescence showed that DIC addition to natural seawater does not increase photosynthetic ETR at subsaturating light in this species and in *Alaria esculenta*. However, an increase in ETR was measured at subsaturating light between 1mM and 8mM DIC. In *Laminaria digitata*, stimulation of light-limited photosynthesis was measured when 6mM DIC was added to buffered natural seawater.

References

Alber, B.E., and J.G. Ferry (1996). Characterization of heterologously produced carbonic anhydrase from *methanosarcina thermophila*. *Journal of Bacteriology:* **178:** 3270-3274

Allen, J.F. (2004). Cytochome b & f: structure for signalling and vectorial metabolism. *Trends in Plant Science*: **9: 3**: 130-137

Alper, S.L. (1991). The Band 3-related anion exchanger family. *Annual Reviews of Physiology*. **53**: 549–564.

Alper, S.L., R.R. Kopito, S. Libresco, and H.F. Lodish (1988). Cloning and characterisation of a murine Band 3- related CDNA from kidney and a lymphoid cell line. *Journal of Biological Chemistry*: **263**: 17092- 17099

Ananyev GM, L. Zoltsman, C. Vasko, and G.C. Dismukes. (2001). The inorganic biochemistry of photosynthetic oxygen evolution/water oxidation. *Biochimica & Biophysica Acta* **1503**:52–68

Andria, J.R., J.L. Perez-Llorens, and J.J. Vergara. (1999). Mechanisms of inorganic carbon acquisition in *Gracilaria gaditana* nom. prov. (Rhodophyta). *Planta.* **208**: 564-573

Andria, J.R., J.L. Perez-Llorens, J.J. Vergara. (2001). Acclimation responses of *Gracilaria* sp (Rhodophyta) and *Enteromorpha intestinalis* (Chlorophyta) to

changes in the external inorganic carbon concentration. *Botanica Marina*. **44**: 361-370

Atkins, P., J. de Paula, and W.H. Freeman (2001). Physical Chemistry. 7th Edition: 1072 pp.

Axelsson, L., C. Larsson and H. Ryberg (1999). Affinity, capacity and oxygen sensitivity of two different mechanisms for bicarbonate utilisation in *Ulva lactuca* L. (Chlorophyta). *Plant, Cell and Environment.***22**: 969-978

Axelsson, L., H. Ryberg and S. Beer (1995). Two modes of bicarbonate utilisation in the marine green macroalga *Ulva lactuca. Plant, Cell and Environment.* **18**: 439- 445

Badger M.R., D. Hanson, and G.D. Price. (2002). Evolution and diversity of CO2 concentrating mechanisms in cyanobacteria. *Functional Plant Biology*. **29**:161–73

Badger M.R., and G.D. Price. (2003). CO2 concentrating mechanisms in cyanobacteria: molecular components, their diversity and evolution. *Journal of Experimental Botany*. **54**:609–22

Barrow, C., and F. Shahidi (2007). Marine nutraceuticals and functional foods. *CRC*: 1st edition: pp 512.

Bassham, JA., Benron, AA., Calvin, M. (1950). The path of carbon in photosynthesis. VIII. The role of malic acid. J*ournal of Biological Chemistry* **185:** 781-787

Beardall, J., and M. Giordano (2002). Ecological implications of microalgal and cyanobacterial CCMs and their regulation. *Functional Plant Biology.* **29**: 335-347

Beardall, J., P. Heraud, S. Roberts, K. Shelly and S. Stojkovic (2002). Effects of UV-B radiation on inorganic carbon acquisition by the marine microalga *Dunaliella tertiolecta* (Chlorophyceae). *Phycologia.* **41**: 268-272

Beardall, J., and J. A. Raven (2004). The potential effects of global climate change on microalgal photosynthesis, growth and ecology. *Phycologia.* **43**: 31-45

Beardall, J., S. Roberts, and J. Millhouse (1991). Effects of nitrogen limitation on inorganic carbon uptake and specific activity of ribulose-1, 5-P2 carboxylase in green microalgae. *Canadian Journal of Botany.* **69**: 1146-1150

Beer, S. (1995). Photosynthetic utilization of inorganic carbon in *Ulva*. *Scientia Marina*. **60:** 125-128

Berg, J., J. Tymoczko and L. Stryer (2002). Biochemistry (Fifth Edition). W.H. Freeman and Company

Blackman, F. F. (1905). Optima and Limiting Factors. *Annals of Botany.* **19**: 281-298.

Blackman, F.F., and S. Mahaei (1905). A quantitative study of carbon dioxide assimilation and leaf temperature in natural illumination. *Proceedings of the Royal Society*: **B volume 1xxvi**: 402-460

Bose, J. C. (1924). The Physiology of Photosynthesis*. Longmans, Green & Co., London.*

Bracey, M.H., J. Christiansen, P. Tovar, S.P. Cramer, and S.G. Bartlet (1994). Spinach carbonic anhydrase: investigation of the zinc-binding ligands by site-directed mutagenesis. *Biochemistry*: **33**: 13126-13131

Bradfield, J.R.G (1947). Plant carbonic anhydrase. *Nature*: **159**: 467-468

Brenchley A. L., J. A. Raven, A. M. Johnston. (1997). Resource acquisition in two intertidal fucoid seaweeds, *Fucus serratus* and *Himanthalia elongata*: seasonal variation and effects of reproductive development. *Marine Biology* **129:** 367-375

Broecker, W. and T. H. Peng (1982). Tracers in the sea. *Lamont-Doherty Geological Observation,* New York: Columbia University.

Brosius-III, F.C., S.L Alper, A.M. Garcia, and H.F. Lodish. (1989). The major kidney Band 3 gene transcript predicts an aminoterminal truncated Band 3 polypeptide. *Journal of Biological Chemistry*. **264**: 7784–7787.

Bruce, L.. J., M. M. Kay, C. Laurence, M. J. Tanner. (1993). Band 3 HT, a human red-cell variant associated with acanthocytosis and increased anion transport, carries the mutation Pro-868-->Leu in the membrane domain of band 3. *Biochemistry Journal*. **293**: 317-320

Cabantchik, Z. I., and G. Greger (1992). Chemical probes for anion transporters of mammalian cell membranes. *American Journal of Physiology.* **262**: C803- 827

Cabantchik and Rothstein (1974). Membrane proteins related to anion permeability of human red blood cells. I. Localization of disulfonic stilbene binding sites in proteins involved in permeation. *The Journal of Membrane Biology*: **15**: 207-226

Caldeira, K., and M.E. Wickett (2003). Anthropogenic Carbon and Ocean pH. *Nature*: **425**

Chapman, A. R. O., and J. S. Craigie (1977). Seasonal growth in *Laminaria longicruris:* relations with dissolved inorganic nutrients and internal reserves of nitrogen. *Marine Biology.* **40**: 197-205.

Ch'En, FF- T., F.C. Villafuerte, P. Swietach, P.M. Cobden and R.D. Vaughan-Jones (2008). 50 859, a N-cyanosulphonamide inhibitor of sodium-bicarbonate cotransport in the heart. *British Journal of Pharmacology*: **153**: 972-982

Chernova, M. N., L. Jiang, M. Crest, M. Hand, D. H. Vandorpe, K. Strange, S. L. Alper. (1997). Electrogenic sulfate/chloride exchange in *Xenopus* oocytes mediated by murine AE1 E699Q. *Journal of General Physiology*. **109**:345-60.

Cockburn, A. F., J. A. Seawright, (1988). Techniques for mitochondrial and ribosomal DNA analysis of *Anopheline* mosquitoes. *Journal of the American Mosquito Control Association.* **4**: 261-265

Coleman, J.R., J.A. Berry, R.K. Togasaki and A.R. Grossman (1984). Identification of extra cellular carbonic anhydrase of *Chlamydomonas reinhardtil. Plant Physiology:* **76:** 472-477

Colman, B., and C. M. Cook (1985). Photosynthetic characteristics of the marine macrophytic red alga *Rhodymenia palmata*: evidence for bicarbonate transport. In *Inorganic carbon uptake by aquatic photosynthetic organisms.* Eds W. J. Lucas and J. A. Berry. pp. 97-110. Rockville, MD: American Society of Plant Physiologists.

Colman, B., A. Huertas, S. Bhatti and J. S. Dason (2002). The diversity of inorganic carbon acquisition mechanisms in Eukaryotic microalgae. *Functional Plant Biology.* **29**: 261-270

Cook C. M., T. Lanaras, B. Colman. (1986) Evidence for bicarbonate transport in species of red and brown macrophytic algae*. Journal of Experimental Botany*. **180:** 977-984

Cordat, E., and J.R. Casey, (2009) Bicarbonate transport in cell physiology and disease. *Biochemistry Journal.* **417:** 423–439

Davison, I. R., and G. A. Pearson (1996). Stress tolerance in intertidal seaweeds. *Journal of Phycology.* **32**: 197-211

Dawczynski, C., R. Schubert and G. Jahreis (2007). Amino acids, fatty acids and dietry fibre in edible seaweed products. *Food Chemistry* **103: issue 3**: 891-899

Dickson, A. G. (1981). An exact definition of total alkalinity and a procedure for the estimation of alkalinity and total inorganic carbon from titration. *Deep-Sea Research.* **28**: 609-623

Dismukes, G. C., V. V. Klimov, S. V. Baranov, Yu. N. Kozlov, J. DasGupta and A. Tyryshkin (2001). The origin of atmospheric oxygen on Earth: the innovation of oxygenic photosynthesis. *Proceedings of the National Academy of Sciences, USA*. **98**: 2170-2175

Dong, L. F., B. Thake, and P. Heathcote (1991). The role of carbonic anhydrase in carbon acquisition in three species of seaweeds. *Oebalia.* **17**: 49-64

Dong, L. F. (1993). Inorganic carbon acquisition in marine macroalgae. PhD thesis, *University of London*

Douglas, S.E., A.W.D. Larkum and J.A. Raven (2003). Photosynthesis in algae. Springer: pp479

Drew E. A. (1983). Light. In Earll R., Erwin D. G. (eds). Sublittoral Ecology. The Ecology of the Shallow Sublittoral Benthos (pp. 10-57). *Oxford: Clarendon Press*

Dring, M. J. (1982). The Biology of Marine Plants (1st edition). *Edward Arnold (Publishers) Limited*. pp. 199

Dring, M.J. (1987). Light climate in intertidal and subtidal zones in relation to photosynthesis and growth of benthic algae: a theoretical model. In R.M.M. Crawford (ed.), Plant Life in Aquatic and Amphibious Habitats (pp 23-34). Oxford: Blackwell Scientific.

Dunbar, B.S. (1994). Protein blotting: A practical approach (The practical approach series 140). USA: Oxford University Press: pp 272

Esminger I., C. Hagen, W. Braure. (2000). Strategies providing success in a cariable habitat II. Ecophysiology of photosynthesis of *Cladophroa glomenta*. *Plant, Cell and Environment* **23**: 1129-1136

Falkowski, P. G., and J. A. Raven (1997). Aquatic Photosynthesis. *Malden, MA: Blackwell Science.*

Fan, H-T., S. Morishima, H. Kida and Y. Okada (2001). Phloretin differentially inhibits volume-sensitive and cyclic AMP- activated, but not Ca- activated, Cl- channels. *British Journal of Pharmacology*: **133**: 1096-1106

Field, C., M. J. Behrenfeld, J. T. Randerson, and P. Falkowski (1998). Primary production of the biosphere: integrating terrestrial and oceanic components. *Science.* **281**: 237-240

Fisher, Z., J.A. Hernandez Prada, C. Tu, D. Duda, C. Yoshioka, H. An, L.. Govindasamy, D.N Silverman, R. McKenna (2005). *Biochemistry***: 44**: 1097-1105

Fogg, G. E., B. Thake. (1987). Algal Cultures and Phytoplankton Ecology. *University of Wisconsin Press*. pp. 269

Frohlich, O. and R.B. Gunn (1986). Erythrocyte anion transport: the kinetics of a single-site obligatory exchange system. *Biochimica & Biophysica Acta:* **864**: 169-194

Fujiwara, S., H. Fukuzawa, A. Tachiki and S. Miyachi (1990). Structure and differential expression of two genes encoding carbonic anhydrase in *Chlamydomonas reinhardtii. Proceedings of the National Academy of Sciences of the USA.* **87**: 9779-9783

Fukuzawa, H., K. Miura, K. Ishizaki, K.-I. Kucho, T. Saito (2001). *Ccm1,* a regulatory gene controlling the induction of a carbon concentrating mechanism in *Chlamydomonas reinhardtii* by sensing CO_2 availability. *Proceedings of the National Academy of Sciences of the USA.* **98**: 5347-5352

Fukuzawa, H., S. Fujiwara, A. Tachiki and S. Miyachi (1990). Nucleotide sequences of two genes CAH1 and CAH2 which encode carbonic anhydrase polypeptides in *Chlamydomonas reinhardtil. Nucleic Acid Research***: 18: 21**: 6441-2

Gatusso, J. P., R. W. Buddemeier. (2000). Ocean biogeochemistry: calcification and CO_2. *Nature*. **407:** 311-313

Geider R.J., E.H. Delucia, P.G. Falkowski, A.C. Finzi, J.P. Grime, J. Grace, T.M. Kana, J. La Roche, S.P. Long, B.A. Osborne, T. Platt, I.C. Prentice, J.A. Raven, W.H. Schlesinger, V. Smetacek, V. Stuart, S. Sathyendranath, R.B. Thomas, T.C. Vogelmann, P. Williams, and F.I. Woodward. (2001). Primary productivity of planet earth: biological determinants and physical constraints in terrestrial and aquatic habitats. *Global Change Biology*. **7:** 849-882

Giordano, M., J. Beardall and J. A. Raven (2005) CO_2 concentrating mechanisms in algae: mechanisms, environmental modulation, and evolution. *Annual Review of Physiology* **56:** 99-131

Giordano, M., and S. C. Maberly (1989). Distribution of carbonic anhydrase in British marine algae. *Oecologia.* **81**: 534-539

Giordano, M., A. Norici, M. Forssen, M. Eriksson, and J. A. Raven (2003). An anaplerotic role for mitochondrial carbonic anhydrase in *Chlamydomonas reinhardtii. Plant Physiology.* **132**: 2126-2134

Gran, G. (1952). Determination of the equivalence point in potentiometric titration, part II. *Analyst.* **77**: 661-671

Granbom, M., and M. Pedersen (1999). Carbon acquisition strategies of the red alga *Eucheuma denticulatum. Hydrobiologia.* **398/399: 349-354**

Greene R. W., V. A. Gerard. (1990). Effects of high-frequency light fluctuations on growth and photoacclimation of the red alga *Chondrus crispus*. *Marine Biology*. 105: 337-34493: 12245-1225-

Groves, J. D., P. Falson, M. le Maire, M.J. Tanner. (1996). Functional cell surface expression of the anion transport domain of human red cell band 3 (AE1) in the yeast *Saccharomyces cerevisiae*. *Proceedings of the National Academy of Science USA.* **93**: 12245-12250

Guiry, M.D., and G. Blunden (1991). Seaweed resources in Europe: uses and potential. Pp. xi, 432. Chichester, West Sussex, England; New York: John Wiley and Sons

Hagen Rødde, R.S., K.M. Vårum, B.A. Larsen, and S.M. Myklestad (2004). Seasonal and geographical variation in the chemical composition of the red alga *Palmaria palmata* (L.) Kuntze. *Botanica Marina*: **47: issue 2**: 125-133

Hanes, CS (1932). Studies on plant amylases: The effect of starch concentration upon the velocity of hydrolysis by the amylase of germinated barley. *Biochemical Journal* **26**: 1406–1421.

Henley, WJ (1993). Measurement and interpretation of photosynthetic light-response curves in algae in the context of photoinhibition and diel changes. *Journal of Phycology* **29**: 729-739

Harrison, M.L., C.C. Isaacson, D.L. Burg, R.L. Geahlen, and P.S. Low. (1994). Phosphorylation of human erythrocyte band 3 by endogenous P72syk. *Journal of Biological Chemistry.* **269**: 955–959.

Harrison, P. J., R. E. Waters and F. J. R. Taylor (1980). A broad spectrum artificial seawater medium for coastal and open ocean phytoplankton. *Journal of Phycology.* **16**: 28-35

Herfort, L., B. Thake and J. Roberts (2002). Acquisition and use of bicarbonate by *Emiliania huxleyi. New Phytologist.* **156**: 427-436

Hewett- Emmett, D., and R.E. Tashian (1996). Functional diversity, conversion, and convergence in the evolution of the alpha-, beta-, and gamma-carbonic anhydrase gene families. *Molecular Phylogenetic Evolution*: **5**: 50-77

Hill, R., and F. Bendall (1960). Function of the two cytochome components in chloroplasts- a working hypothesis. *Nature*: **186**: 136-137

Hofstee, B.H.J. (1959). Non-Inverted Versus Inverted Plots in Enzyme Kinetics. *Nature* **184**: 1296–1298

Holbrook, G. P., S. Beer, W. E. Spencer, J. B. Reiskind, J. S. Davis and G. Bowes (1988). Photosynthesis in marine macroalgae: evidence for carbon limitation. *Canadian Journal of Botany.* **66**: 577-582

Inoue, K., Fujii, T., Yokoyama, E., Matsuura, K., Hiyama, T., Sakurai, H. (1989). The photoinhibition site of Photosystem I in isolated chloroplasts under extremely reducing conditions. *Plant Cell Physiology.* **30**: 65-71

Irvine, L.M., W. F. Farnham. (1983). Seaweeds of the British Isles. Volume 1 Rhodophyta part 2A Cryptonemiales (sensu stricto), *Palmariales*, *Rhodymeniales* ed. by L.M. Irvine (ed.) *Lavoisier.* pp. 228

Israel, A., S. Katz, Z. Dubinsky, J. E. Merrill and M. Friedlander (1999). Photosynthetic inorganic carbon utilisation and growth of *Porphyra linearis* (Rhodophyta). *Journal of Applied Phycology.* **11**: 447-453

Israel, A., M. Hophey. (2002). Growth, photosynthetic activities, and Rubisco activities and amounts of marine macroalgae grown under current and elevated seawater CO_2 concentrations. *Global Change Biology* **8:** 831-840

Jennings, M. L. (1995). Rapid electrogenic sulfate-chloride exchange mediated by chemically modified band 3 in human erythrocytes. *Journal of General Physiology* **105**:21–47

Jennings, M.L. (1989). Structure and function of the red blood cell anion transport protein. *Annual Reviews of Biophysics and Biophysical Chemistry* : **18**: pp 397-430

Jensen, F.B. (2004). Red blood cell pH, the Bohr effect, and other oxygenation-linked phenomena in blood, oxygen and carbon dioxide transport. *Acta Physiologica Scandinavica*: **182: 3**: 215-227

Jerlov N. G. (1976). Marine Optics. *Amsterdam: Elsevier* pp. 231

Johnston A.M. (1991). The acquisition of inorganic carbon by marine macroalgae. *Canadian Journal of Botany.* **69**:1123–32

Johnston, A. M., S. C. Maberly, and J. A. Raven (1992). The acquisition of inorganic carbon by four red macroalgae from different habitats. *Oecologia.* **92**: 317-326

Kaplan, A., M. Ronen-Tarazi, H. Zer, R. Schwarz, D. Tchernov, D.J. Bonfil, D. Schatz, A. Vardi, M. Hassidim, and L. Reinhold. (1998). The inorganic carbon-concentrating mechanism in cyanobacteria: induction and ecological significance. *Canadian Journal of Botany.* **76**: 917- 924

Kennish, M.J. (2000). Practical Handbook of Marine Science.3rd Edition: Pp 896: CRC

Kimber, M.S., and E.F. Pai (2000). The active site architecture of *Pisum satirum* β- carbonic anhydrase is a mirror image of that of α- carbonic anhydrase. *EMBO Journal*: **19**: 1407-1418

King, R. J., and W. Schramm (1976). Photosynthetic rates of benthic marine algae in relation to light intensity and seasonal variations. *Marine Biology*. **37**: 215-222

King, R. J., and W. Schramm (1976). Determination of photosynthetic rates for the marine algae *Fucus vesiculosus* and *Laminaria digitata*. *Marine Biology* **37**: 209-213

Kirk, J.T.O. (1994). Light and photosynthesis in aquatic ecosystems.

Cambridge: Cambridge University Press: pp 410

Kollert- Jons, A., S. Wagner, S. Hubner, H. Appelhams and D. Drenckhahn (1993). Anion exchanger one in human kidney and oncocytoma differs from erytwoid AE1 in its NHz terminus. *American Journal of Physiology and Renal Physiology*: **265: 6**: 813-821

Kopito R.R., and H.F. Lodish. (1985). Primary structure and transmembrane orientation of the murine anion exchange protein. *Nature*. **316(6025)**: 234–238.

Kubler, J. E., and J. A. Raven (1995). The interaction between inorganic carbon supply and light supply in *Palmaria palmata* (Rhodophyta). *Journal of Phycology* **31**: 369-375

Kudrycki, K.E., P.R. Newman and G.E. Shull (1990). CDNA cloning and tissue distribution of MRNAs for two proteins that are related to the Band 3 Cl-/ H00$_3$- exchanger. *Journal of Biological Chemistry:* **265**: 462-471

Kudrycki, K.E., and G.E. Shull. (1989). Primary structure of the rat kidney Band 3 anion exchange protein deduced from cDNA. *Journal of Biological Chemistry.* **264**: 8185–8192.

Kuntze, O (1981). *Revisogenerum plantarum.* Pars 2. pp 375-1011. Leipzig, London, Milano, New York, Paris: Arthur Felix, Dulau and Co.

Lane, T., M.A. Saito, G.N. George, I.J. Pickering, R.C. Prince and F.F.M. Morel (2005). A cadmium enzyme from a marine diatom. *Nature*: 2005: **435**: 42

Larsson, C., and L. Axelsson, (1999). Bicarbonate uptake and utilisation in marine macroalgae. *European Journal of Phycology.* **34**: 79-86

Larsson, C., L. Axelsson, H. Ryberg and S. Beer (1997). Photosynthetic carbon utilisation by *Enteromorpha intestinalis* (Chlorophyta) from a Swedish rockpool. *European Journal of Phycology.* **32**: 49-54

Lindskog, S., (1997). Structure and mechanism of carbonic anhydrase. *Pharmacology and Therapeutics*: **74: 1**: 1-20

Lineweaver, H and D. Burk. (1934). The Determination of Enzyme Dissociation Constants. *Journal of the American Chemical Society* **56**: 658–666

Lobban S., P. J. Harrrison. (1997). Seaweed Ecology and Physiology *Cambridge University Press* pp. 365

Maberly, S. C. (1990). Exogenous sources of inorganic carbon for photosynthesis by marine macroalgae. *Journal of Phycology*. **26**: 439-49

Mann, T., and D. Keilin (1940). Sulphanilamide as a specific inhibitor of carbonic anhydrase. *Nature*: **146**: 164-165

Martinez, B., and J.M. Rico (2008). Changes in nutrient content of *Palmaria palmata* in response to variable light and upwelling in Northern Spain. *Journal of. Phycology.* **44 issue 1**: 50-59

Martinez B., J. M. Rico. (2004). Inorganic nitrogen and phosphorus uptake kinetics in Palmaria palmata (Rhodophyta). *Journal of Phycology* **40**: 642-650

Martinez, B. and J.M. Rico (2002). Seasonal variation of P content and major N pools in *Palmaria palmata* (Rhodophytal). *Journal of Phycology*: **38: 6**: 1082-1089

Martinez, B., R.M. Viejo, J.M. Rico, R.H. Rodde, V.A. Faes, J. Oliveros and D. Alvarez (2006). Open sea cultivation of *Palmaria palmata* (Rhodophyta) on the Northern Spanish coast. *Aquaculture* **vol. 254 1-4**: 376-387

Matos, J., S. Costa, A. Rodrigues, R. Pereira, and I. Sousa Pinto (2005). Experimental integrated aquaculture of fish and red seaweeds in Northern Portugal. *Aquaculture* **252, issue 1**: 31-42

Matsuda, Y., and B. Colman (1996). Active uptake of inorganic carbon by *Chlorella saccharophila* is not repressed by growth in high CO_2. *Journal of Experimental Botany.* **47**: 1951-1956

Meldrum, N.U., and F.J.W. Roughton (1933). Carbonic anhydrase . its preparation and properties. *Journal of Physiology (London):* **80**: 113-132

Mercado, J. M., F. J. L. Gordillo, F. L. Figueroa and F. X. Niell (1998). External carbonic anhydrase and affinity for inorganic carbon in intertidal macroalgae. *Journal of Experimental Marine Biology and Ecology.* **221**: 209-220

Mercado, J. M., and F. X. Niell (1999). Carbonic anhydrase activity and use of HCO_3^- in *Bostrychia scorpioides* (Ceramiales, Rhodophyceae). *European Journal of Phycology.* **34**: 13-19

Mercado, J. M., F. X. Niell, M. C. Gil-Rodriguez (2001). Photosynthesis might be limited by light, not inorganic carbon availability, in three intertidal Gelidiales species. *New Phytologist.* **149**: 431-439

Merrett, M. J., N. A. Nimer, and L. F. Dong (1996). The utilisation of bicarbonate ions by the marine microalga *Nannochloropsis oculata* (Droop) Hibberd. *Plant, Cell and Environment.* **19**: 478-484

Miao, X. L., Q. Y. Wu. (2002). Inorganic carbon utilization in some marine phytoplankton species. *Acta Botanica Sinica.* **44**: 395-399

Michaelis, L., and M. Menten (1913). Die Kinetik der Invertinwirkung, Biochem. Z. **49**:333–369.

Mitra, M., Mason, CB., Xiao, Y., Ynalvez, RA., Lato, SM., Moroney, JV. (2005). The carbonic anhydrase gene families of Chlamydomonas reinhardtii. *Canadian Journal of Botany* **83(7)**: 780-795

Mitsuhashi, S., and S. Miyachi (1996). Amino acid sequence homology between N- and C- terminal halves of a carbonic anhydrase in *Porphyridium purpureum,* as deduced from the cloned cDNA. *The Journal of Biological Chemistry.* **271**: 28703-28709

Mitsuhashi, S., T. Mizushima, E. Yamashita, M. Yarnarnoto, T. Kurnasaka, H. Moriyarna, T. Ueki, S. Miyachi, T. Tsukihara. (2000). X-ray structure on beta-carbonic anhydrase from the red alga*, Porphyridium purpureum*, reveals a novel catalytic site for CO_2 hydration. *Journal of Biological Chemistry.* **275:** 5521-5526

Morel F.M.M., E.H. Cox, A.M.L Kraepiel, T.W Lane, A.J Milligan, et al. (2002). Acquisition of inorganic carbon by the marine diatom *Thalassiosira weissflogii. Functional Plant Biology.* **29**:301–8

Moroney, J. V., S. G. Bartlett, and G. Samuelsson. (2001). Carbonic anhydrase in plants and algae. *Plant, Cell and Environment.* 24: 141-153

Nimer, N. A., M. D. Iglesias-Rodriguez and M. J. Merrett (1997). Bicarbonate utilisation by marine phytoplankton species. *Journal of Phycology.* **33**: 625-631

Nimer, N. A., M. Warren and M. J. Merrett (1998). The regulation of photosynthetic rate and activation of extracellular carbonic anhydrase under CO_2 limiting conditions in the marine diatom *Skeletonema costatum. Plant, Cell and Environment.* **21**: 805-812

Nimer, N., M. X. Ling, C. Brownlee, M. J. Merrett. (1999) Inorganic carbon limitation, exofacial carbonic anhydrase activity and plasma membrane redox activity in marine phytoplankton species. *Journal of Phycology.* **35**: 1200-1205.

Orr, J.C., V.J. Fabry, O. Aumont, L. Bopp, S.C. Doney, R.A. Feely, A. Gnanadesikan, N. Gruber, A. Ishida, F. Joos, R.M. Key, K. Lindsay, E. Maier-Reimer, R. Matear, P. Monfray, A. Mouchet, R.G. Najjar, G. Plattner, K. Rodgers, C.L. Sabine, J.L. Sarmiento, R. Schlitzer, R.D Slater, I.J. Totterdell, M. Weirig, Y. Yamanaka and A. Yool (2005). Anthropogenic ocean acidification over the twenty-first century and its impact on calcifying organisms. *Nature*: **437**: 681-688

Palmqvist, K., S. Sjoberg, and G. Samuelsson (1988). Induction of inorganic carbon accumulation in the unicellular algae *Scenedesmus obliquus* and *Chlamydomonas reinhardtii. Plant Physiology.* **87**: 437-442

Pang, S.J., and K. Lüning (2006). Tank cultivation of the red alga *Palmaria palmata*: year-round induction of tetrasporangia, tetraspone release in darkness and mass cultivation of vegetative thalli. Aquaculture **vol. 252, issue 4,** 20-30.

Papageorgiou, G.C., and Govindjee (Eds.). (2004). Chlorophyll Fluorescence. Springer: pp 818

Park, H., P.J. McGinn, and F.M.M. Morel (2008). Expression of cadmium carbonic anhydrase of diatoms in seawater. *Aquatic Microbrial Ecology*: **51: 2**:

183-193

Passow, H. (1986). Molecular aspects of Band 3 mediated anion transport across the red blood cell membrane. *Review of Physiological Biochemistry and Pharmacology*: **103**: 61-223

Perez-Llorens, J. L., F. G. Brun, J. Andria, and J. J. Vergara (2004). Seasonal and tidal variability of environmental carbon related physico-chemical variables and inorganic C acquisition in *Gracilariopsis longissima* and *Enteromorpha intestinalis* from Los Torunos salt marsh (Cadiz Bay, Spain). *Journal of Experimental Marine Biology and Ecology*. **304**: 183-201

Pinet, P.R. (1996). Invitation to oceanography. St. Paul: West Publishing Company: 126, 134-135

Provan, J., Wattier, R. A., and Maggs, C.A. (2005). Phylogeographic analysis of the red seaweed *Palmaria palmata* reveals a Pleistocene marine glacial refugium in English Channel. *Molecular Ecology.* **14:** 793-803.

Pytkowicz, R.M., E. Atlas and C.H. Culberson. (1977). O*ceanography and Marine Biology, Annual Reviews*. **15**: 11- 45

Rabinowitch E. (1951). Photosynthesis and related processes, 2(1). *New York: Interscience.*

Raven JA. (1997). Putting the C in phycology. *European Journal of Phycology*. 32:319–33

Raven, J. A. and P. G. Falkowski (1999). Oceanic sinks for CO_2. *Plant, Cell and Environment.* **22**: 275-278

Raven, J. A., A. Osborne, A. M. Johnston. (1985). Uptake of CO_2 by aquatic vegetation. *Plant, Cell and Environment.* **8**: 417-425

Redfield, A.C. (1958). The biological control of chemical factors in the environment. *American Scientist.* **46**: 205-221

Riebesell, U., D. A. Wolf-Gladrow, and V. Smetacek (1993). Carbon dioxide limitation of marine phytoplankton growth rates. *Nature.* **361**: 249-251.

Reinfelder JR, A.J. Milligan and F.M.M Morel. (2004). The role of C4 photosynthesis in carbon accumulation and fixation in a marine diatom. *Plant Physiology.* **135**:2106–11

Reiskind JB, and G. Bowes.(1991). The role of phosphoenol pyruvate carboxykinase in a marine macroalga with C4-like photosynthetic characteristics. *Proceedings of the National Academy of Science USA* **88:**2883–87

Riley, G.A. (1957). Phytoplankton of the North Central Sargasso Sea, 1950-1952. *Limnology & Oceanography*. **2**: 252-270

Riley, J.P., and R. Chester (1971). Introduction to *Marine Chemistry.* London: *Academic Press.*465 pp.

Rogalski, A.A., T.L. Steck, and A. Waseem. (1989). Association of glyceraldehyde-3-phosphate dehydrogenase with the plasma membrane of the intact human red blood cell. *Journal of Biological Chemistry.* **264**: 6438–6446.

Rybicki, A.C., J.J.H. Qui, S. Musto, N.L. Rosen, R.L. Nagel, and R.S. Schwartz. (1993). Human erythrocyte protein 4.2 deficiency associates with hemolytic anemia and a homozygous40 glutamic acid → lysine substitution in the cytoplasmic domain of band 3 (band 3montefiore). *Blood*, **181**: 2155–2165.

Salhany, J. M., R. L. Sloan, K. S. Cordes. (2003). The carboxyl side chain of glutamate 681 interacts with a chloride binding modifier site that allosterically modulates the dimeric conformational state of band 3 (AE1). Implications for the mechanism of anion/proton cotransport. *Biochemistry.* **42**:1589-602.

Salhany, J.M., R.L. Sloan, and L.M. Schopfer (1996). Characterization of the stilbenedisulphonate binding site on band 3 Memphis variant II (Pro-854-->Leu). *Biochemistry Journal*: **317 part 2:** 509-514

Sasaki, T., R. Togasaki and Y. Shiraiwa. (1997). Carbonic anhydrase is induced prior to arylsulfatase under the simultaneous deprivation of inorganic carbon and sulphate in *Chlamydomonas reinhardtii* (Volvocales, Chlorophyta). *Phycological Research*. **45**: 207- 211

Sawaya, M.R., G.C. Cannon, S. Heinhorst, S. Tanaka, E.B. Williams, T.O. Yeates and C.A. Kerfeld (2006). The structure of β- carbonic anhydrase from the carboxysonal shell reveals a distinct subclass with one active site for the price of two. *The Journal of Biological Chemistry*: **281: 11**: 7546-7555

Schreiber, U., W. Bilger and C. Neubauer (1994). Chlorophyll fluorescence as a nonintrusive indicator for rapid assessment of in vivo photosynthesis. *Ecological Studies.* **100**: 49-70

Sekino, K., Kobayashi, H., Shiraiwa, Y. (1996). Role of coccoliths in the utilization of inorganic carbon by a marine unicellular coccolithophorid *Emiliania huxleyi*: a survey using intact cells and protoplasts. *Plant and Cell Physiology* **37(2)**: 123-127

Sharkia, R., S. Beer and Z. I. Cabantchik (1994). A membrane-located polypeptide of *Ulva* sp. which may be involved in HCO_3^- uptake is recognised by antibodies raised against the human red-blood cell anion-exchange protein. *Planta.* **194**: 247-249

Shiraiwa, Y., and S. Miyachi (1985). Effects of temperature and CO_2 concentration on induction of carbonic anhydrase and changes in efficiency of photosynthesis in *Chlorella vulgaris* 11h. *Plant and Cell Physiology.* **26**: 543-559

Simkiss, K., Wilbur, KM. (1989). Biomineralization: cell biology and mineral deposition. *Academic Press* San Diego, CA.

Sly, W.S. and P.Y. Hu (1995). Human carbonic anhydrases and carbonic anhydrase deficiencies. *Annual Review of Biochemistry*: **64**: 375- 401

Smith, R. G., and R. G. S. Bidwell (1987). Carbonic anhydrase-dependent inorganic carbon uptake by the red macroalga *Chondrus crispus. Plant Physiology.* **83**: 735-738

Smith, R. G., and R. G. S. Bidwell (1989). Mechanism of photosynthetic carbon dioxide uptake by the red macroalga, *Chondrus crispus. Plant Physiology.* **89**: 93-9

Smith, K.S., C. Jahubzick, T.S. Whittam and J.G. Ferry (1999). Carbonic anhydrase is an ancient enzyme widespread in prokaryotes. *Proceedings of the National Academy of Science of the USA*: **96: 26:** 15184- 15189

So, AK-C., G.S. Espie, E.B. Williams, J.M. Shively, S. Heinhorst, and G..C. Cannon (2004). A novel evolutionary lineage of carbonic anhydrase (ε class) is a component of the carboxysome shell. *Journal of Bacteriology*: **186: 3**: 623-630

Soto, A.R., H. Zheng, D. Shoemaker, J. Rodriguez, B.A. Read, and T.M. Wahlund. (2006). Identification and Preliminary Characterization of Two cDNAs Encoding Unique Carbonic Anhydrases from the Marine Alga Emiliania huxleyi. *Applied Environmental Microbiology.* **72(8):** 5500- 5511

Steck, T.L., B. Ramos, and E. Strapazon (1976). Proto-olytic dissection of Band 3, the predominant transmembrane polypeptide of the human erythrouyte membrane. *Biochemistry*: **15**: 1153-1161

Stemler, A.J. (2005). The bicarbonate effect, oxygen evolution, and the shadow of Otto Warburg. *Advances in Photosynthesis and Respiration*: **20: 5**: 391-397

Sterling, D., B.V. Alvarez and J.R. Casey (2002). The extra cellular component of a transport metabolon: extra cellular loop four of the human AE1 Cl^-/HCO_3^- exchanger binds carbonic anhydrase IV. *Journal of Biological Chemistry*: **277**: 25239-25246

Sterling, D., and J. R. Casey (2002). Bicarbonate transport proteins. *Biochemistry and Cell Biology.* **80**: 483-497

Sterling, D., R. A. F. Reithmeier, J. R. Casey (2001). A transport metabolon: functional interaction of carbonic anhydrase II and chloride/ bicarbonate exchangers. *The Journal of Biological Chemistry*. **276**: 47886-47894

Strickland, J. D. H., and T. R. Parsons (1972). *A Practical Handbook of Seawater Analysis,* 2nd ed. Fish. Res. Bd. Canada Bull. 167, 310 pp. [4.7.1, 5.2, 6.3]

Stryer, L. (1995). Biochemistry, 4th Edition. *W.H. Freeman & Company*. pp. 1064

Stumm, W., and J. J. Morgan (1996). Aquatic chemistry, 3rd edition. *New York, USA: Wiley, J. and Sons*

Sultemeyer, D. (1998). Carbonic anhydrase in eukaryotic algae: characterisation, regulation and possible functions during photosynthesis. *Canadian Journal of Botany.* **76**: 962-972

Tanner, M. J., P. G. Martin and S. High (1988). *Biochemistry Journal.* **256**: 703-712

Tcherkez, G.G., G.D. Farquhar, and T.J. Andrews (2006). Despite low catalysis and confused substrate specificity, all ribulose bisphosphate carboxylases may be nearly perfectly optimized. *Proceedings of the National Academy of Science of the USA*: **103**: 19

Tiwari, A., P. Kumar, S. Singh and S.A. Ansari (2005). Carbonic anhydrase in relation to higher plants. *Photosynthetica***: 43: 1**: 1-11

van der Meer, J. P., E. R. Todd (1980). The life history of *Palmaria palmata.* A new type for the Rhodophyta. *Canadian Journal of Botany.* **58**: 1250-1256

Vézina, A.F., and O. Hoegh-Guldberg (2008). Effects of acidification on marine ecosystems. *Marine Ecology Progress Series*: **373**: 199-201

Wächtershäuser, G. (1989). The case for an autotrophic origin. *Origins of Life and Evolution of Biospheres*: **19: 3-5**: 423-424

Warburg, O. (1919). Über die Geschwindigkeit der photochemischen Kohlensäurezersetzung in lebenden Zellan. *Biochemische Zeitschrift* **100:** 230-270

Warburg, O., Krippahl, G. (1958). Hill-Reaktionen. *Zeitschift für Naturforschung* 13: 509-514

Whorf, T.P., and C.D. Keeling (2005). *Atmospheric carbon dioxide records from sites in the 510 air sampling network trends.* A compendium of data on global change. Carbon dioxide Information Analysis Centre: Oak Ridge National Laboratories, US Department of Energy, Oak Ridge, Penn USA. Period of record: 1958-2004.

Wu, H., D. Zou and K. Gao (2008). Impacts of increased atmospheric carbon dioxide concentration on photosynthesis and growth of micro and macro-algae. *Science in China Series C: Life Sciences*: **Volume 51: Number 12**: 1144-1150

Xu, Y., L. Feng, P.D. Jeffrey, Y. Shi, and F.M.M. Morel (2008). Structure and metal exchange in the cadmium carbonic anhydrase of marine diatoms. *Nature*: **452**: 56-61

Zeebe, R., and J.P. Gattuso (Ed.) (2006). *Marine Carbonate Chemistry*, Encyclopaedia of Earth: J. Cutler (Ed.). Cleveland, Washington DC

Zhang, D., A. Kyatkin, J.T. Bolin, and P.S. Low. (2000). Crystallographic structure and functional interpretation of the cytoplasmic domain of erythrocyte membrane band 3. *Blood.* **96**: 2925–2933.

Zhu, Q., D.W.K. Lee, and J.R. Casey (2003). Novel topology in C-terminal region of the human plasma membrane anion exchanger AE1. *The journal of Biological Chemistry*: 3112-3120

Zolotarev, A.S., M.N. Chernova, D. Yannowkakos and S.L. Alper (1996). Proteolytic cleavage sites of native AE2 anion exchanges in gastric mucosal membranes. *Biochemistry*: **35**: 10367-10376

Zouni, A., H. T. Witt, J. Kern, P. Fromme, N. Krauss, W. Saenger, P. Orth. (2001). Crystal structure of photosystem II from *Synechococcus elongatus* at 3.8 A resolution. *Nature* **409:** 739-743.

Zou, D., J. Xia, Y. Yang (2004). Photosynthetic use of exogenouinorganic carbon in the *agarophyte gracilania lemaneifornuis* (Rhodophyta). *Aquaculture*: **237: issue 1-4**: 421-431